GEOARCHAEOLOGICAL APPROACH TO RESOLVING THE ORIGINS OF BISON BONE BEDS AT BONFIRE SHELTER, 41VV218, VAL VERDE COUNTY, TEXAS

by

Ashley Eyeington, B.A.

A thesis submitted to the Graduate Council of
Texas State University in partial fulfillment
of the requirements for the degree of
Master of Arts
with a Major in Anthropology
December 2022

Committee Members:

James David Kilby, Chair

Stephen L. Black

Charles Fredrick

FAIR USE AND AUTHOR'S PERMISSION STATEMENT

Fair Use

Duplication Permission

ACKNOWLEDGEMENTS

This thesis would not have been possible without the support of my family, friends, and colleagues. First, I would like to thank the Skiles family for their stewardship and accommodations for the entire ASWT project. Next, thank you to my family for their unending patience and support while awaiting the completion of my “paper”. I had to miss out on many events to make time for classes, then for analyses, and finally for writing. I love you all and I cannot wait to spend more time with you again.

Next, I would like to thank my fantastic cohort, professors, and fellow students who volunteered for the AWST project. I could not have made it through this journey without all of you. Joy Tatem and James Ramsey were especially instrumental in lifting me up throughout graduate school and the subsequent field data collection. Thank you both for tagging along! Another shout out to those amazing friends who helped me move literal tons of dirt and rock from one room to another, then one lab to another, and then from the lab to my apartment (Nora Berry, Zach Jamieson, Janaka Greene, and so many others!). To all the volunteers and undergraduate students who worked out at Bonfire Shelter with us: Chris Ringstaff, Marvin Gohlke, Vicky and Jerod Roberts, John Hedges, Rich McAuliffe, Darla Messina, Eden Meadows, and Aaron Brown. And of course, I couldn’t forget to thank Dr. Hamilton for all his guidance and humor in the field. It was fantastic getting to know and work with you all!

I would also like to thank my committee for supporting me all the way to the end, though it felt endless. Dr. David Kilby, thank you for your patience and support. I truly appreciate all your guidance, being able to complete a thesis on Bonfire Shelter with a focus on geoarchaeology has been a rewarding experience. Dr. Stephen Black, it was a pleasure, and I am honored to have been able to work with you on such an amazing project. Dr. Charles Frederick, I truly could not have finished this project without your continued guidance and thorough explanations.

Finally, I would like to thank my friends and colleagues at SWCA. Ken Lawrence, I would not be where I am today without all your support. Thank you for pushing me. Tina Nielsen, thank you for being a great friend and for not only being a sounding board but a technical editor for my thesis. I couldn't have done it without all of you!

TABLE OF CONTENTS

Page

LIST OF TABLES

Table **Page**

LIST OF FIGURES

Figure **Page**

I. INTRODUCTION

A common research interest in Paleoindian archaeology focuses on the phenomenon of large mammal hunting and more specifically bison drive events. Such hunting methods require group cooperation, an understanding of the local landscape, and knowledge of bison herd behavior (Bement and Buehler 1994; Carlson and Bement 2013; Frison 1991a; 2004; Wyckoff and Dalquest 1997; Zedeño et al. 2014). Research on sites representing such events can aid in furthering our understanding of subsistence, tool technology, and group dynamics and intergroup relationships.

Bonfire Shelter (41VV218) is located in Val Verde County, Texas and consists of a multicomponent prehistoric rockshelter site. It is one of two known bison drive sites in Texas and hosts three identified bone beds. Bone Bed 1 (BB1) is the deepest and oldest bone bed found in the center of the shelter and has been dated to at least 14,600 calBP, though no cultural material has yet been found in association with this deposit (Dibble and Lorrain 1968; Bement 1986; Farrell 2020; Kilby et al. 2020). Bone Bed 2 (BB2) is the middle bone bed and has been dated to around 12,025 calBP. If the Paleoindian-age bison bone bed was deposited as a result of a bison drive, it would make Bonfire Shelter the location of the oldest bison drive event in North America. There has been much debate as to the origin of the bone bed (i.e., as a drive event or result of secondary processing) and as to the number of cultural events represented (Dibble and Lorrain 1968; Dibble 1970; Bement 1986, 2007; Binford 1978; Bousman et al. 2004; Byerly et al. 2005, 2007; Holliday 1997; Kilby et al. 2020; Meltzer et al. 2007; Prewitt 2007; Turpin 2004). The uppermost bone bed is Bone Bed 3 (BB3) which has been dated to roughly

2,500 calBP and is considered to represent a Late Archaic bison drive event (Dibble and Lorrain 1968; Byerly et al. 2005:620; Kilby et al. 2020).

At first glance, it is easy to see why Bonfire Shelter would be an ideal location for a bison drive event. The canyon rim rises slightly up just before the edge, making it difficult to see over the precipice. At the southern end of the shelter there is a notch in the canyon rim which acts as a natural funnel bringing rocks, dirt, and debris into the shelter (Figure 1.1). Below this notch a talus cone of rock, dirt and bison bone has accumulated (Figure 1.2). It is in this cone that Bone Bed 3 and a majority of Bone Bed 2 are found, though Bone Bed 2 has been found to extend into the shelter interior.

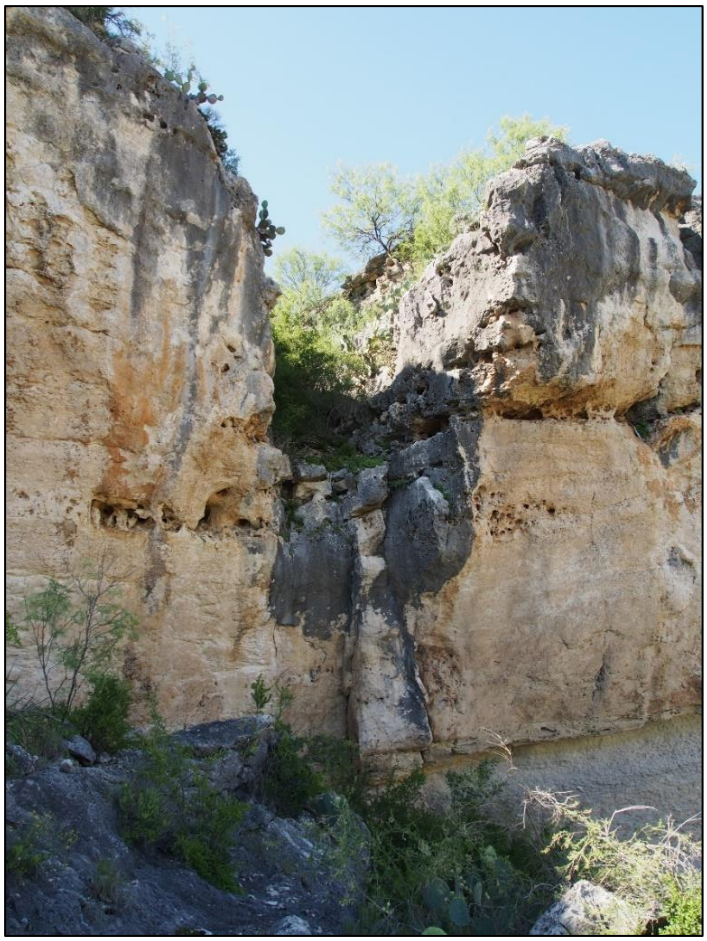

Figure 1.1. Overview of the notch in the canyon rim immediately above the talus cone (photo courtesy of Dr. David Kilby).

Figure 1.2. Overview of Bonfire Shelter showing the talus cone below the notch, view south (Photo courtesy of Dr. David Kilby).

The purpose of my thesis research is to conduct geoarchaeological analyses to address the ongoing debate of Bone Bed 2's origin with a focus on the deposits in the talus cone (Figure 1.3). The first excavations at Bonfire Shelter under David S. Dibble in the 1960s recorded three distinct stratigraphic units within Bone Bed 2 suggesting that they represented three individual depositional events (Dibble and Lorrain 1968). Documentation of the profile and designations of the strata within appear to be the extent of the work reported from that time. Later researchers have challenged this interpretation, but with an emphasis using faunal analysis (Bement 2007; Binford 1978a; Byerly et al. 2005, 2007a, 2007b; Prewitt 2007). Up to this point, no in-depth research has been done

on the stratigraphic context and depositional formation of the talus cone and subsequent Bone Bed 2 within. This thesis is presented as the first attempt to outline the formation and depositional history of the talus cone, and to address the questions about Bone Bed 2's formation and quantity of events from this perspective.

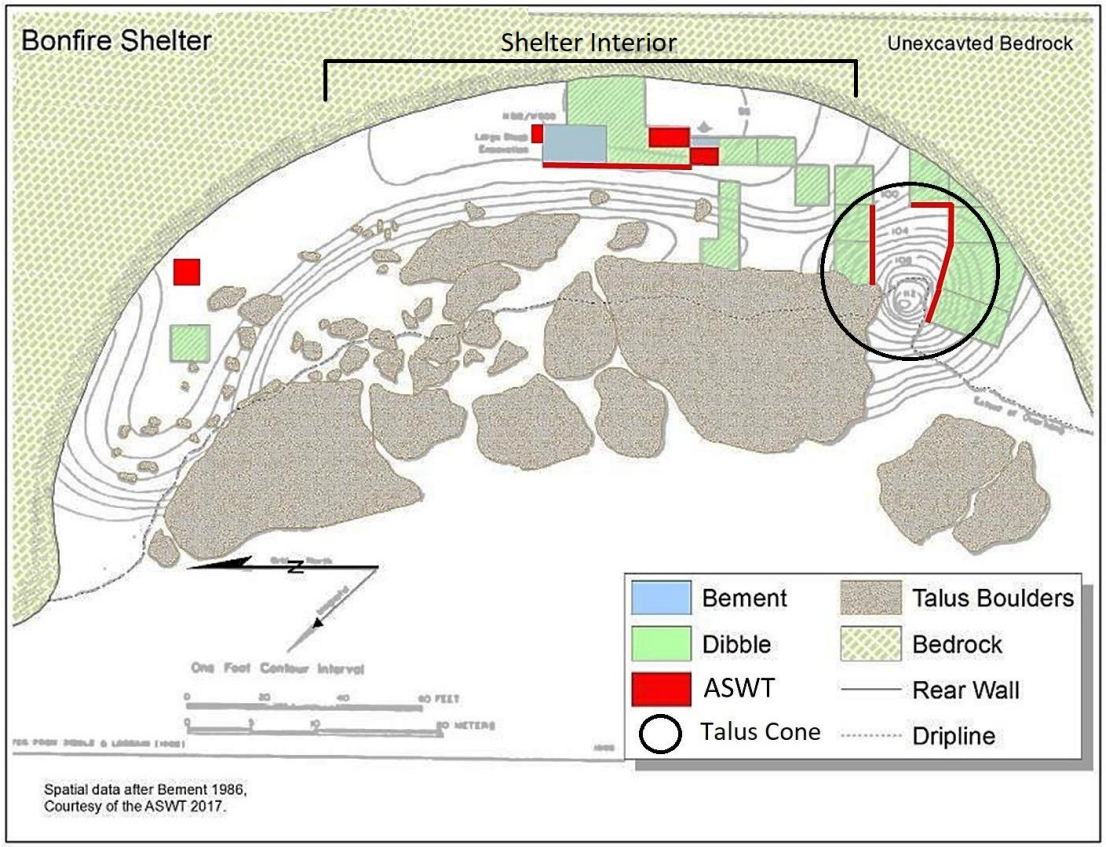

Figure 1.3. Overview of Bonfire Shelter showing previous excavations (modified from Kilby et al. 2020).

II. ENVIRONMENTAL BACKGROUND

Bonfire Shelter (41VV218) is located in Val Verde County, Texas, along the United States and Mexico border. It is located within a 1.5-kilometer-long limestone canyon known locally as Mile Canyon or Eagle Nest Canyon (Figure 2.1). The site is situated within a unique physiological, ecological, and geological position which has played a large part in the historical use of the site. This chapter briefly discusses the environmental landscape of the region with an emphasis on Bonfire Shelter and Eagle Nest Canyon.

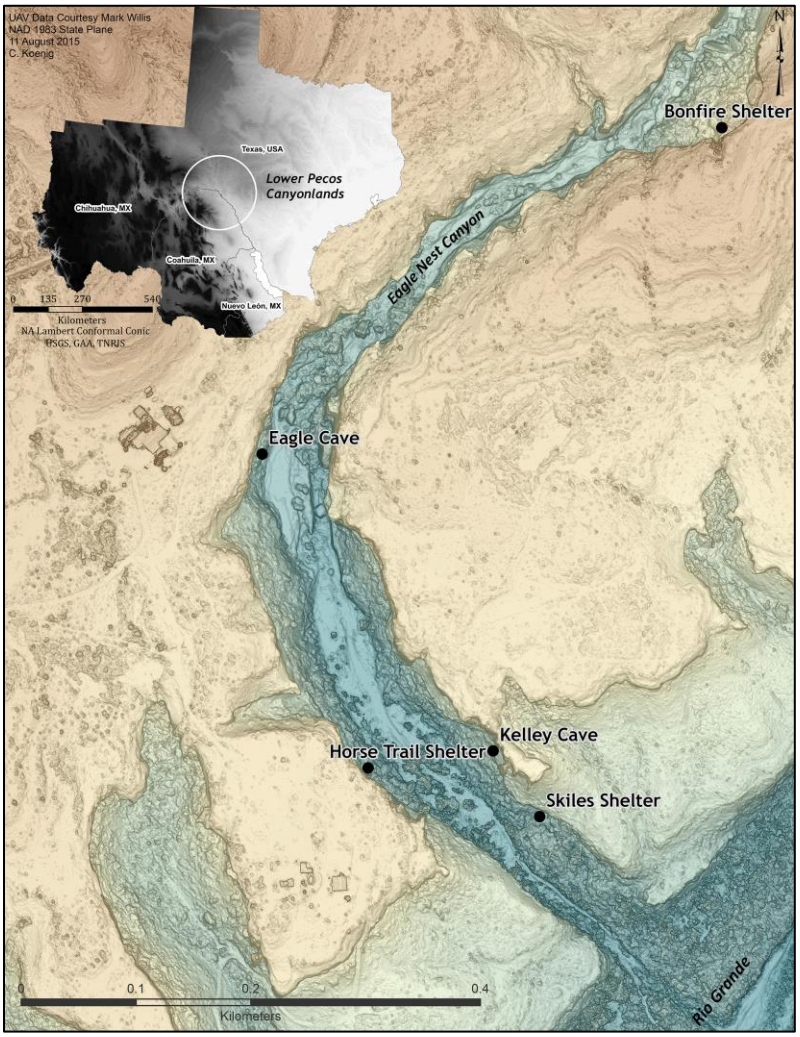

Figure 2.1. Map of Eagle Nest Canyon with the location of Bonfire Shelter and adjacent sites (from Koenig et al. 2017).

Physiographic Region

A physiographic province is a division based on geomorphology, including landforms and their underlying geologic makeup (National Park Service [NPS] 2019). Each province represents a unique geologic history of deposition and erosion that generated the rocks, soils, vegetation, and climate of the region (Wermund 2019). Bonfire Shelter and Eagle Nest Canyon are within the southernmost portion of the Great Plains province.

The Great Plains province consists of a large level to gently undulating plateau with an average elevation of 3,000 feet (Wermund 2019). Multiple prominent rivers and drainages, including the Canadian River, Red River, Prairie Dog Town Fork of the Red River, and Pecos River, intersect the province creating deep incisions and divided uplands while playas are found within the flat plains and plateaus. Within Texas, the Great Plains has been divided into multiple subregions including the Southern High Plains, the Edwards Plateau, and the Central Texas Uplift (Wermund 2019). Bonfire Shelter is located within the Southern High Plains and at the western end of the Edwards Plateau, as defined by Wermund.

The Edwards Plateau is currently dominated by savannahs which include mixed grasses and herbaceous plants with groves of oak (*Quercus* spp.), juniper (*Juniperus ashei*), and mesquite (*Prosopis* sp.). It's shallow limestone bedrock overlain by thin, rocky soil is largely used as pastureland (Bush and Hanselka 2017; Wermund 2019). The Southern High Plains is very large and variable but is generally characterized as grasslands with shrub vegetation such as brasil (*Condalia, hookeri*) and huisache (*Vachellia farnesiana*) (Bush and Hanselka 2017). As its name suggests, the Southern

High Plains is a large grassland plateau consisting of deep eolian soils. In Val Verde County, the Pecos River and other major drainages have eroded the escarpment creating a dynamic landscape of canyons. Being situated among these diverse environments, Bonfire Shelter is at an ideal location for the procurement of multiple valuable resources including variable flora, faunal, and geologic materials.

Chihuahuan Desert Ecoregion

Ecoregions are ecologically and geographically defined regions consisting of distinct flora and fauna assemblages. Bonfire Shelter is situated within the Chihuahua Desert level III ecoregion as defined by Omernik and Griffith (2014). The Chihuahuan Desert is the southernmost desert in North America. It lies within the American Southwest, specifically Arizona, New Mexico, and Texas, extending south into Mexico. The region covers an area of over 200,000 km^2 and it is home to a diverse environmental and cultural history (Omernik and Griffith 2014).

From a broad view, vegetation within the Chihuahuan Desert consists of desert grassland and arid shrubland with pinyon pine (*Pinus remota*), juniper (*Juniperus* spp.), and oak woodlands only occurring in high elevations or along waterways. Common flora across the region includes creosote (*Larrea tridentata*), lechuguilla (*Agave lechuguilla*), sotol (*Dasylirion texanum*), ocotillo (*Fouquieria splendens*), and yucca (*Yucca torreyi*) (Bush and Hanselka 2017; Omernik and Griffin 2014).

The Chihuahuan Desert has relatively few major river drainages (e.g., the Rio Grande, Devils River, Pecos River, Rio Conchos, etc.) and water is predominantly internally drained into playa lakes. Riparian zones include a rich array of flora such as the common reed (*Phragmitesaustralis*), Texas persimmon (*Diospyros texana*), little walnut

(*Juglans macrocarpa*), hackberry (*Celtis* sp.), onion (*Allium* sp.), and willow (*Salix* sp.) (Bush and Hanselka 2017:23-24; Omernik and Griffin 2014). Due to the paucity of water in this region, all sources were and still are considered a valuable resource.

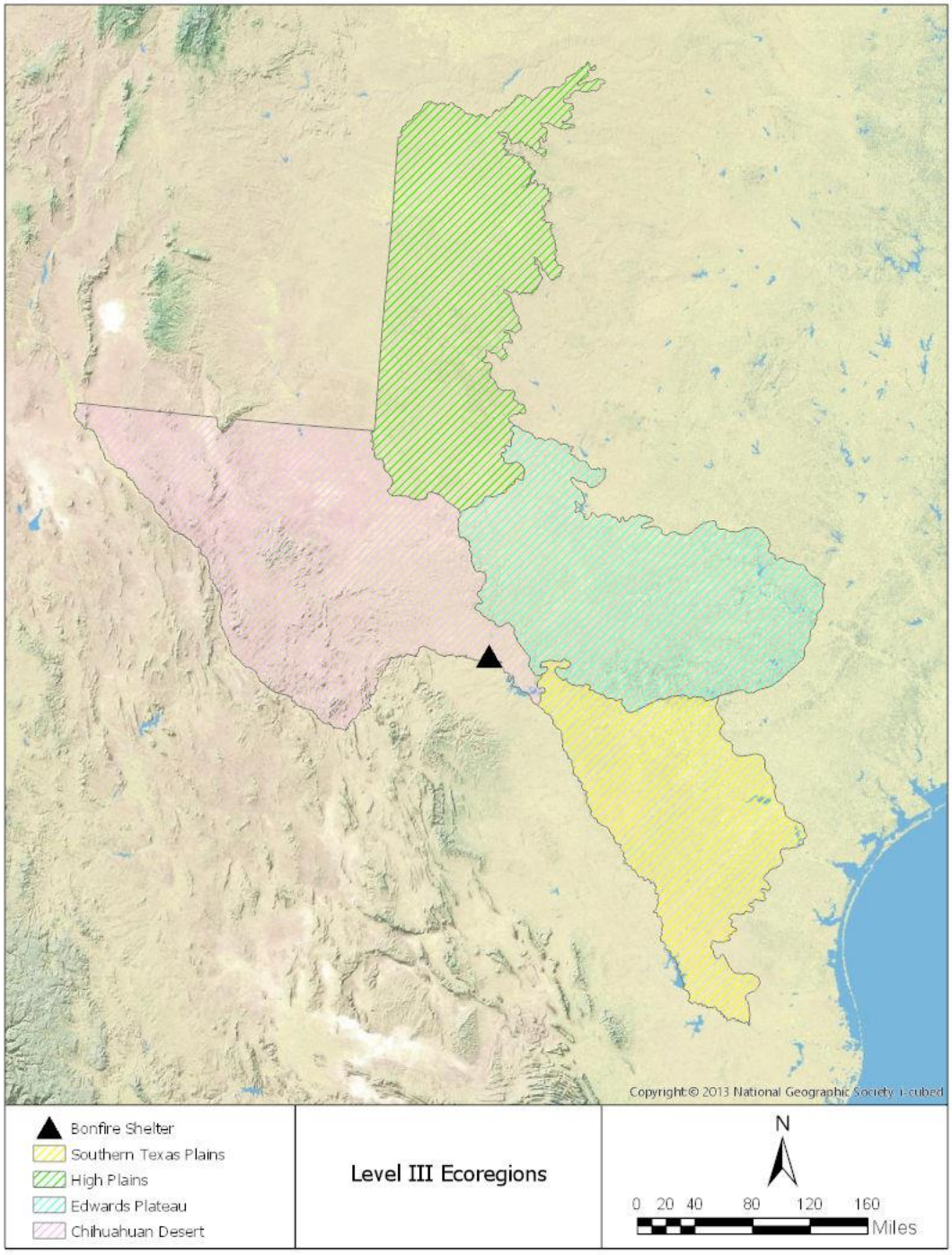

Figure 2.2. Texas level III ecoregions and location of Bonfire Shelter (Base Map: ESRI ArcGIS Online, accessed April 2020).

Bonfire Shelter is located along the eastern extent of the Chihuahuan Desert region near the confluence of the Rio Grande and Pecos River. It is also near the convergence of the Chihuahuan Desert, Edwards Plateau, and Southern Texas Plains ecoregions (Figure 2.2). This places the sites within Eagle Nest Canyon, including Bonfire Shelter, at a prime location with access to a diverse array of valuable floral and faunal resources.

Paleoenvironmental Conditions

Paleoenvironmental research has been ongoing in Texas and the Southwest for as long as archaeological research has (Bousman and Brown 1998). At Blackwater Draw, researchers in the 1930s developed one of the first successful paleoenvironmental reconstructions in the Southern Plains through the use of palynology, paleontology, botany, and geology (Antevs 1935; Cotter 1937, 1938; Howard 1935a, 1935b; Stock and Bode 1937). Since then, regional studies have focused on central Texas (e.g., Potzger and Tharp 1943, 1947), west Texas and in particular the Paleoindian period (e.g., Sellards 1938, 1952, 1955; Sellards and Evans 1960; Sellards et al. 1947), and the High Plains (e.g., Holiday 1995, 1997; Wendorf and Hester 1975). One of the most complete reconstructions to note was Vaughan Bryant's palynological study of both Late Pleistocene and Holocene paleoenvironments of Texas conducted by (Bryant 1969, 1977a). He surmised that more mesic environments transitioned to more xeric conditions around 10,000 B.P. The transition was proposed to have been gradual with fully modern vegetation being established around 3000 B.P.

Due to the arid environmental conditions in the Lower Pecos and the presence of many rockshelters, preservation of perishable materials is much higher than other

regions. This has allowed researchers to focus their efforts on reconstructing the paleoenvironmental record of southwest Texas from the often-lost organic record. These reconstructions have largely relied on pollen and macrobotanical, faunal, coprolite, and sedimentary records from archaeological sites such as Devil's Mouth (41VV188), Arenosa Shelter (41VV99), and Bonfire Shelter (41VV218) (e.g., Bryant and Holloway 1985; Dering 1979; Dibble and Lorrain 1968; Johnson 1964; Patton and Dibble 1982; Stock 1983; Williams-Dean 1978) as well as landscape studies of terrace formations along the Pecos (e.g., Kochel 1988; Patton and Dibble 1982).

The Late Glacial period, around 14,000 to 10,000 B.P., consisted of a transitional period characterized by a climatic transition which caused broad mosaic scrub grasslands to overtake the once dominate pinyon-juniper woodlands of the Lower Pecos (Bryant and Holloway 1985:50–56). In general, pollen, macrobotanical, and faunal samples from the region have all concurred with the trend that the Pleistocene was cooler and wetter than the Holocene. The deposits at Bonfire Shelter have reflected this trend with pollen samples showing a decrease in pine and an increase in grass. Additionally, it has been proposed that the Pecos River itself saw a reduction in discharge at this time due to reduced groundwater moisture. Warmer summer temperatures have also been proposed as the reason that pluvial lakes in the region became seasonal (Bryant and Holloway 1985; Rachel et al. 2021; Lucas et al. 2005; Turpin 2004).

The Holocene, from 10,000 B.P. to the present, has become increasingly xeric. While there were no dramatic environmental changes around 10,000 B.P., a subtle change can be noted on a broad regional scale across the entire period (Bryant and Holloway 1985:56). In the Lower Pecos this meant warmer and dryer conditions with

vegetation transitioning from forests and parklands to semi-arid grasslands and desert scrub. This has been confirmed by a decrease in fossilized pine pollen corresponding to an increase in herbaceous plants and grasses from various sites in the region including Devil's Mouth (Bryant and Larson 1968), Eagle Cave (McAndrews and Larson 1966), Bonfire Shelter (Hevly 1966; Bryant 1969), and Hinds Cave (Bryant 1977b). Additionally, subsistence studies in the region have noted that humans were exploiting agave, yucca, sotol, and other modern desert vegetation as early 8500 B.P. (Dering 1979, 1999; Williams-Dean 1978).

The warming trend continued until around 4400 B.P. when there was a period of cooler and wetter conditions (Bryant and Holloway 1985; Dibble and Lorrain 1968). Both Bonfire Shelter and Devil's Mouth have fossil pollen records indicating an increase in pine and decrease in grass during this time (Bryant and Larson 1968). This cooler period also corresponds with Bone Bed 3 the Archaic-age bison bone bed at Bonfire Shelter, and it has been hypothesized that bison returned to the region due to the more mesic conditions (Dibble and Lorrain 1968). After this episode, the region continued to see fluctuations but generally resumed its warming trends with conditions becoming increasingly more xeric until modern times.

Based on palynological, faunal, macroflora, and sediment analyses of samples from Bonfire Shelter and other sites in the region, Eagle Nest Canyon underwent multiple cycles of colder and warmer temperatures (Bryant 1969; Bryant and Holloway 1985; Dering 1979; Dibble and Lorrain 1968; Patton and Dibble 1982; Robinson 1997). Around 14,500 years ago the earth was in one of these warming periods. During this transition to an interglacial phase, something occurred which propelled conditions back to a glacial-

like state. This is known globally as the Younger Dryas (YD) which occurred within Texas and the LPC around 13,000 years ago and continued until around 11,500 years ago when current Holocene interglacial conditions commenced (Alley 2000; Seersholm et al. 2020). Our understanding of the YD centers on research of ice cores from Greenland, and as such, there is still much uncertainty as to what conditions of this time looked like in the United States. Generally, conditions would have been cooler with an increase in seasonality, but summers would still have been warm (Seersholm et al. 2020).

Recent research at Hall's Cave and Eagle Cave has provided a window into the environmental conditions of the YD and resulting subsistence availability for Pleistocene groups (Cordova and Johnson 2019; Koenig et al. 2021; Seersholm et al. 2020). In Hall's Cave, a significant change was noted in the types of flora and faunal remains associated with Pleistocene and Holocene deposits. Researchers found that during the abrupt shift to cooler and drier conditions during the YD, there was a reduction in the number and diversity of both flora and faunal species (Cordova and Johnson 2019; Seersholm et al. 2020).

Additionally, sedimentological, paleontological and isotopic research has indicated that for the past 5,000 years, the Edwards Plateau has had 30 cm or less of soil mantle overlaying limestone bedrock (Cooke et al. 2003:3). As far back as 12,000 years ago, limestone bedrock is proposed to have been increasingly exposed per sedimentological analysis of cave and shelter deposits (Cooke et al. 2003; Toomey 1993) and up to 1.5 meters of soil lost to erosion. This degradation of soil would have impacted not only the available local flora and faunal population but vastly impacted the evolution of the landscape. With less soil and more exposed bedrock, deposition into Eagle Nest

canyon as well as Bonfire Shelter would have been restricted. This coupled with the unique morphology of Bonfire Shelter and its protective ring of canyon collapse, suggests that the talus' bone beds main source of deposition would come from the notch rather than eolian processes. This suggests that available sediments decrease through time and as such, the deeper Pleistocene strata had more available sediments than the younger Holocene strata.

Late Pleistocene Subsistence

As can be seen from paleoenvironmental studies in the region, the flora and fauna available to Paleoindian occupants of Bonfire Shelter would be different from today. Pollen samples from Bonfire Shelter Bone Bed 3 yielded abundant pine (*Pinus*) pollen (a wind-blown taxon whose presence may be overstated in pollen records), as well as oak (*Quercus*), walnut (*Juglans*), daisy family (Asteraceae), and assorted grass pollens (Bryant 1969). The oldest excavated deposits at Eagle Cave are of Late Pleistocene age and produced mesquite wood charcoal, indicating the presence of this tree in the vicinity by about 13,000 B.P. (Bush and Hanselka 2017:24). Recent macrobotanical studies on a Paleoindian feature in Eagle Nest Cave found evidence of predominantly mesquite (*Prosopis sp.*) and juniper (*Juniperus sp.*) fuelwood along with various possible carbonized and uncarbonized food remains (mesquite (*Prosopis sp.*), hackberry (*Celtis sp*.), prickly pear (*Opuntia sp.)*, grass (*cf. Setaria sp.*), agave (Liliaceae), and sotol (Liliaceae)) (Koenig et al. 2021).

Modern vegetation patterns provide a glimpse of the plant resources available to ancient people, but their landscapes would have included more groundcover vegetation and tender grasses and herbs favored by grazers. In addition, the climate would have

allowed more plants with higher moisture requirements (e.g., C3 grasses, trees) to grow, especially in earlier times (Bush and Hanselka 2017:25).

Many of the faunal species found in archeological deposits live in the canyons or inhabit the adjacent rocky upland slopes and rolling plains. Remains of mammals from the uplands and fish from the deep river pools only occur together as evidence of prehistoric food choices, decorative arts, and tool kits in the human habitation sites of the Lower Pecos Canyonlands (Jurgens 2005; Jurgens 2017:31). These faunal species include Alligator gar (*Lepisosteus cf. spatula*), catfish (*Ictalurus* sp.), bass (*Morone* sp.). mallard (*Anas platyrhynchus*) and various other duck species, turkey (*Meleagris gallapavo*), quail (*Colinus virginianus*), deer (*Odocoileus* sp.), sheep (*Ovis* sp.), bison (*Bison bison* and Bison antiquus), jackrabbit (*Lepus californicus*), cottontail (*Sylvilagus sp.*), and others. Of particular interest to the Paleoindian occupations of Bonfire Shelter is the use of large mammals such as bison. These animals were not only hunted for meat, but the byproducts of their remains were incorporated into the technological systems as has been found in Eagle Cave where a fragmented informal bone butchering tool was found in Feature 14 (Jurgens 2017; Koenig et al. 2021).

Geological Background

Geologically the region surrounding Bonfire Shelter is composed of a combination of igneous and sedimentary deposits ranging from Precambrian to Tertiary in age (Bureau of Economic Geology [BEG] 1977). Due to its location adjacent to the Rocky Mountains, the Great Plains bedrock geology is overlain by alluvial deposits from east flowing drainages and windblown sand and silts. Within the vicinity of Eagle Nest Canyon are three Cretaceous-age geologic units: Devils River Limestone, Buda

Limestone, and Boquillas Flags (Figure 2.3) (BEG 1977; Frederick 2017; Harbor 2011; Wermund 2019).

The region is known for the deep canyons that have formed within the Devil's River Limestone (Frederick 2017). This Cretaceous-age formation is characterized as being light gray to yellowish gray limestone to mudstone rich in fossils and chert. In nearby Langtry, Texas, the formation is approximately 260 m thick with only the upper 60 m of the deposits being exposed within the canyon (Frederick 2017).

Eagle Nest Canyon, also known as Mile Canyon, is a box canyon that has been carved out of the Devil's River Limestone Formation. The formation of the canyon is still uncertain but current hypotheses include the proposition that it is a collapsed karst system (Frederick 2017; George Veni, personal communications). The canyon's walls range from 20 to 30 m in height (Frederick 2017). Within Eagle Nest Canyon, multiple rockshelters have formed along the canyon walls providing ideal habitation settings for early groups of the region (Hall and Black 2010). Bonfire Shelter is one of these features. The deposits found within the shelter are largely aggregations of colluvial deposition from the Devil's River formation. Eroded sediments from the Buda formations have also contributed substantially to the depositional history of the canyon and Bonfire Shelter.

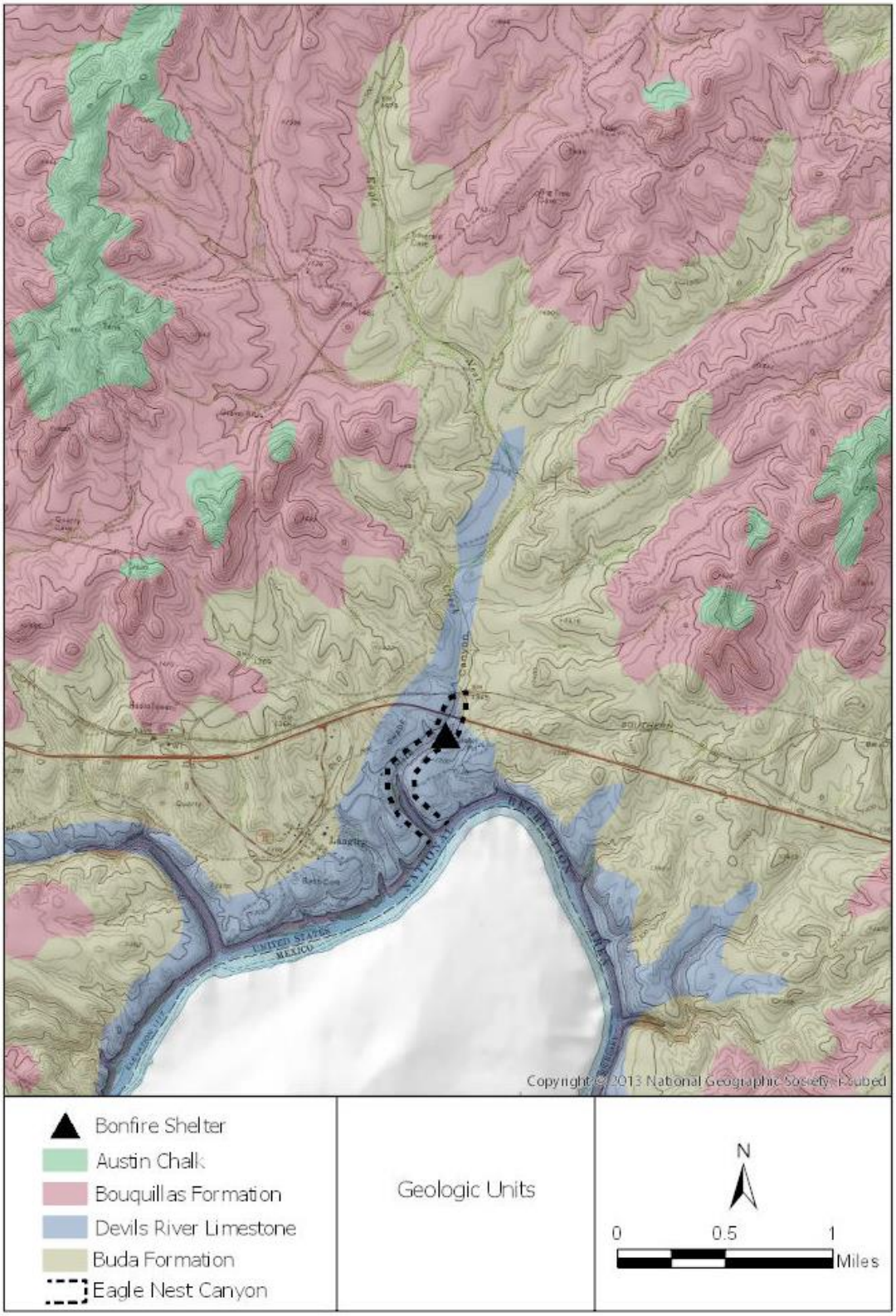

Figure 2.3. Geologic units in proximity to Bonfire Shelter and Eagle Nest Canyon (Base Map: ESRI ArcGIS Online, accessed April 2020).

Eagle Nest Canyon and Bonfire Shelter

The soils found near Bonfire Shelter include the Lozier-Shumla association and the Langtry soil series (NRCS 2019). The Lozier-Shumla association is found immediately above the shelter on the uplands and is being eroded into the shelter through a notch in the canyon rim. Lozier series soils consist of a pale brown (10YR 6/3) carbonate rich loamy-skeletal soil derived from loamy residuum mixed with colluvium from the local bedrock (NRCS 2019). The Shumla series is a shallow yellowish brown (10YR 5/4) loam to a petrocalcic horizon formed in calcareous loamy alluvium over limestone (NRCS 2019). The Langtry series is found to the east on the high terraces that overlook Eagle Nest Canyon. This series is also likely eroding downslope and into the notch above Bonfire Shelter. These soils consist of shallow dark grayish brown (10YR 4/2) very cobbly silty loam formed over Cretaceous age limestone (NRCS 2019).

Geomorphology of Bonfire Shelter

Rockshelters are often defined as shallow voids or ledges which occur underneath an overhang. More simply put, they have wider overhangs than they are deep (Goldberg and Macphail 2013:169). Rockshelters are complicated and eclectic in nature with a multitude of factors influencing not only their formation, but their development, and ultimate collapse (Farrand 2001; Rapp and Hill 2006; Waters 1992). These factors include, but are not limited to, the local lithology, weathering patterns, hydrological conditions, and the outside depositional environment (Waters 1992:245).

As mentioned, the formation of Eagle Nest Canyon is not known for certain, but it has been suggested to be a collapsed cave passage (Frederick 2017; Veni, personal communication). It now exists as an ephemeral, though dynamic, wash that feeds into the

Rio Grande. Such alluvial forces may have contributed to the carving out of all the shelters within the canyon (Frederick 2017). As with typical limestone cave and rockshelter formation, the exposed canyon walls weathered and the softer exposed rock within the center of the walls eroded quicker creating an undercut below the canyon rim (Rapp and Hill 2006). Continued weathering cut further into the canyon wall and created a deep overhang which provides coverage and protection from the elements and predators.

Sedimentation within rockshelters can also come from a number of sources through various depositional processes (Donahue and Adovasio 1990; Farrand 2001; Goldberg and Macphail 2006; Laville 1976; Rapp and Hill 2006; Schiffer 1987; Waters 1992). For Bonfire Shelter, the most likely processes contributing to the development of the talus cone are colluvial and alluvial. Colluvial events have deposited endogenous materials from the rockshelters walls and ceilings while alluvial deposition includes the exogenic materials being brought over the notch in the canyon rim. Aeolian deposition may also be occurring, but due to the closed-in nature of Bonfire Shelter, deposits of this nature would be minimal.

Colluvial environments, such as the talus cone, are complex systems in which various factors contribute including wind exposure, gravity, alluvial runoff, and the degree of slope. The talus cone is most subjected to the natural post depositional processes of mass wasting, or graviturbation, and alluvial runoff (Rapp and Hill 2006; Schiffer 1987; Waters 1992). No environment is the same, and neither is any colluvial slope. This high variability is why each slope must be understood individually (Farrand

2001:42). Additionally, consideration must also be given to what active processes are happening now and how those may have been different in the past.

III. ARCHAEOLOGICAL BACKGROUND

Lower Pecos Cultural Region

Bonfire Shelter lies in the Lower Pecos archeological region of Texas as defined by Turpin (2004). It is also known as the Lower Pecos Canyonlands (LPC) (Black and Dering 2008). The unique situation of resource-rich uplands, shelter-rich canyons, and nearby water sources make Eagle Nest Canyon an attractive habitation setting. The region is distinguished by an over 13,000-year occupational history of early peoples who utilized the natural landscape of the uplands, canyons, rockshelters, and caves within the region (Black and Dering 2008; Turpin 1994, 2004). As a result of this rich history, in January 2021, the Lower Pecos Canyonland Archaeological District was designated as a National Historic Landmark (NPS 2021).

Prior to addressing the regional chronology, a brief history of regional investigations is provided here, in part to note the extensive amount of evidence collected from the region. The archeological significance of the Lower Pecos archeological region was realized in the 1930s with research effort continuing in earnest today (e.g., Bement 1989; Black 2013; Dering 2002; Hall and Black 2010; Turpin 2004). The earliest investigations in the region were conducted in the 1930s by out-of-state archeologists (Black 2013) largely under contracts with museums such as with the Smithsonian Institute and the Museum of the American Indian (Sayles 1935; Setzler 1932). This sparked the interest of Texas-based organizations (e.g., Witte Memorial Museum and University of Texas) who began by focusing on rockshelters within the Pecos and Devil's River canyons (e.g., Davenport 1938; Martin 1933; Pearce and Jackson 1933). These

early projects were typically museum sponsored with the purpose of acquiring cultural material for collections.

It was not until the 1950s and 1960s during the Amistad Reservoir Salvage Project that formal systematic surveys of the canyons, rockshelters, and uplands were conducted. The focus of these projects shifted from collection to research, with questions about cultural chronology and landscape use driving many of the surveys (e.g., Black 2013; Dibble and Lorrain 1968; Graham and Davis 1958; Ross 1965;). The research conducted in the 1950s and 1960s still largely focused on the more obvious sites, rockshelters, and the major canyons and their tributaries with many factors including time, resources, and access restricting a true unbiased sampling of the region (Black 2013; Dering 2002:3.15; Graham and Davis 1958:9; Koenig 2012:23).

Following the 1960s, research within the LPC generally shifted from a regional scale to site focused research questions. University sponsors were still, and continue to be prevalent in the region with various research goals such as expanding understanding of subsistence and diet (e.g., Basham 2015; Black and Thoms 2014; Dering 1979, 2002; Saunders 1986; Williams-Dean 1978), investigations into the regional Pleistocene deposits (Bement 1986; Dibble and Lorrain 1968; Kilby et al. 2021), and surveys to better understand settlement patterns and the distribution of rock art across the Lower Pecos (e.g., Boyd et al. 2012; Koenig 2012; Turpin 1982).

Through all the years of research, the dry rockshelter and cave sites remain to be one of the hallmarks of the region's archeology. This is in large part due to the well preserved and often remarkable art and the high level of preservation of otherwise perishable

materials that are generally lost in more mesic settings. Accordingly, the prehistoric material assemblage is perhaps the most comprehensive in the state.

Eagle Nest Canyon and Beyond

Various significant projects have been conducted in the Lower Pecos region and in proximity to Bonfire Shelter. Two major projects of note include the Amistad International Dam and Reservoir project under the Texas Archaeological Salvage Project and the Ancient Southwest Texas (ASWT) Project through Texas State University. The Amistad Reservoir project resulted in the documentation of over 300 archaeological sites including various rockshelters such as Arenosa Shelter (Dibble 1967), Fate Bell shelter in Seminole Canyon State Park (Parson 1956), Eagle Cave (Ross 1965), and Bonfire Shelter (Dibble and Lorrain 1968). Surveys and excavations conducted during this project resulted in major contributions to the cultural chronology and paleoenvironment of the Lower Pecos region.

Texas State University began research in the Lower Pecos under the ASWT Project in 2009 (Black, personal communication). The purpose of the ongoing research project has been to further the understanding of the archaeological record in the Lower Pecos and to publish research results to encourage further work in the region. Research has been focused around the Pecos and Devils Rivers as well as Eagle Nest Canyon with excavations conducted in various shelters, along the canyon rim, and on the surrounding uplands (Basham 2015; Castañeda 2015; Farrell 2020; Koenig 2012; Nielsen 2017; Pagano 2019; Ramsey 2020; Rodriguez 2015).

Within Eagle Nest Canyon are six rockshelters with prehistoric cultural deposits: Kelly Cave (41VV164), Skiles Shelter (41VV165), Horse Trail Shelter (41VV166),

Eagle Cave (41VV167), Bonfire Shelter (41VV218), and Mile Spring Shelter (41VV2163). The ASWT began work in Bonfire Shelter in 2016 and efforts continue to this day (Black 2017; Kilby et al. 2020).

Lower Pecos Regional History

The extensive investigations conducted in the LPC have provided a long record of cultural history extending from the Late Pleistocene into the Historic period. The table below (Table 3.1) summarizes the major cultural periods as outlined by Turpin (2004). Subsequent sections will go into further detail on the Paleoindian and Archaic periods, the associated cultural remains from Bonfire, and then concludes with an in-depth discussion of the previous and current investigations focused on those deposits. All dates in the following sections are in calBP unless otherwise noted.

Table 3.1. Summary of the Major Cultural Periods in the Lower Pecos Region.

Major Period	Radiocarbon Years (B.P.)
Paleoindian	>2,000 to 9800
Late Paleoindian	9400 to 9000
Early Archaic	9000 to 6000
Middle Archaic	6000 to 3000
Late Archaic	3000 to 1000
Late Prehistoric	1000 to 350

*Table adapted from Turpin (2004:268).

Paleoindian Period

The Paleoindian period (i.e., 14,500–8800 B.P.) spans the Late Pleistocene/Holocene transition, which occurs after the Younger Dryas (ca. 12,800 to 11,300 B.P.). It is a time of relatively rapid climatic, floral, and faunal changes (Turpin

2004:268–269). Turpin (2004) recognizes the Aurora (14,500–11,900 B.P.) and subsequent Bonfire (10,700–9800 B.P.) subperiods represented most notably in Cueva Quebrada (Lundelius 1984) and Bonfire Shelter (Bement 1986; Dibble and Lorrain 1968; Kilby et al. 2020) where cultural deposits are associated with the remains of extinct Rancholabrean species such as camel (*Camelops hesternus),* mammoth (*Mammuthus* sp.), horse (*Equus francisci*), and bison (*Bison antiquus*). The earliest subperiods are the hallmark of the traditionally understood Plains Paleoindian adaptation, a subsistence strategy focused on large game. This subsistence strategy is most evident at Bonfire Shelter, where Bone Bed 2 is proposed to have formed during a bison drive event dated to between 11,500–12,000 B.P. (Bement 1986; Dibble 1968; Dibble and Lorrain 1968; Kilby et el. 2020).

The late Paleoindian Oriente subperiod, (9400–8800 B.P.), represents the gradual transition away from big game hunting to an Archaic lifestyle as the climate shifted towards a more xeric setting (Turpin 2004:269). The change to a more xeric environment at the end of the Paleoindian period and beginning of the Holocene has been seen in pollen data from the region (Bryant and Holloway 1985; Dering 1979; Patton and Dibble 1982; Robinson 1997). Much of the evidence for the paleoenvironmental changes derive from studies conducted in 1970s and 1980s, when a theoretical shift towards an ecological approach made the Lower Pecos an appealing research area because of excellent preservation conditions for floral and faunal remains (Black 2013). Notable among the studies, researchers from Texas A&M University carried out a paleoenvironmental assessments at Hinds Cave (Shafer and Bryant 1977), and archeologists from the University of Texas at San Antonio worked at Baker Cave

(Chadderdon 1983). This environmental transition appears to correlate with an increase in cultural material types as well as a widening subsistence base as seen from floral and faunal remains (Black 2013; Dibble 1967; Hester 1983; Johnson 1964; Sorrow 1968). These changes have been suggested to indicate population growth within the region.

Within Bonfire Shelter, Paleoindian components have been recognized through material remains as well as stratigraphic sequences and radiocarbon dating. Temporally recognized material remains include Folsom and Plainview points identified within Bone Bed 2 (Dibble and Lorrain 1968). These projectile points are morphologically similar except that the Folsom point exhibits a distinctive flute while the Plainview point does not. Both cultural traditions were hunter-gatherer based and adapted for occupation of the southern Plains, but the Folsom material culture has been found to largely postdate the Plainview cultural tradition (Holliday et al. 2017).

The Folsom culture has been dated to roughly 12,900–12,000 calBP and is understood to be a hunter-gather adaption occurring exclusively in the Plains (Bousman, Baker, and Kerr 2004; Buchanan et al. 2021; Kornfeld, Frison, and Larson 2016). It is named for the Folsom site in New Mexico which hosted the first Folsom projectile points. Conversely, the Plainview tradition has been dated to roughly ca. 12,100–11,300 calBP and is understood to be a cultural adapted only to the southern high Plains (Bousman, Baker, and Kerr 2004; Holliday 1997; Holliday et al. 2017; Kornfeld, Frison, and Larson 2016). Based on both cultures tool kits, tool morphology, distribution of known sites, and common occurrence of bison remains at known sites, it is assumed that large game was their primary means of subsistence (Holliday et al. 2017).

The occurrence of both material cultures within Bone Bed 2 raises questions on the temporal association of the bone bed as well as questions on group subsistence

strategies. Does Bone Bed 2 represent multiple events spanning two separate cultural group occupations or were these nomadic hunters coming together and cooperating to take down big game kills? These questions have sparked a lively debate which will be discussed in more detail in the next section of this chapter.

Beyond the temporally diagnostic tools, the lithic assemblage at Bonfire Shelter is key to understanding the activities which occurred at the site. Excavated materials at this time include projectile points, bifaces, and scrapers; tools believed to be associated with hunting and butchering activities. Very little evidence of lithic debitage (i.e., flakes from tool production or resharpening) has been found, which seems to suggest that activities within the excavated portion of the site include hunting and butchering activities (Bement 1986; Dibble and Lorrain 1968).

Archaic Period

In the LPC, the Archaic period ranges from 9,000 1,000 BP (Turpin 2004). This period is most well known as the beginning of plant baking via earth oven technology in the LP (Black and Thoms 2014; Bryant 1968; Dering 2007; Turpin 1994 and 2004; Shafer 1986). The Early Archaic saw an increase in arid conditions which was thought to encourage settlement along the major rivers within rockshelters. It also encouraged an adaptation in subsistence due to a reliance on desert succulents needing special processing in earth oven facilities (Turpin 2004).

Bone Bed 3 is stratigraphically located 1-m above Bone Bed 2 and consists of an accumulation of bison bone (*Bison bison*). Bone Bed 3 has been relatively dated to the Late Archaic period based on the occurrence of bison (*Bison bison*) remains as well as

the identification of Castroville and Montell projectile point types (c. 2,500–2,000 BP) within the bone bed.

Previous Work at Bonfire Shelter

Bonfire Shelter was first identified as having archaeological potential in 1958 when a young man by the name of Michael Collins went exploring in the canyon (Black 2001). Armed with only a shovel, bucket, and passion for archaeology, Collins began digging in the then known Ice Box Cave only to uncover large, burned bones seemingly too sizeable to be cattle. After collecting a mandible from the shelter, Collins took the bone to a family friend, Glen Evans, who was able to confirm the bone belonged to a bison (Black 2001). Thus, began a lifelong love of archaeology for the young Michael Collins who went on to be pinnacle in the field of Texas archaeology.

The Skiles family, owners of the ranch and canyon, became dedicated archaeological stewards actively working to support the study and preserve of Bonfire Shelter and the other sites on their land. For example, during the Texas Archaeological Salvage Project for the construction of the Amistad International Dam and Reservoir, the late Guy Skiles (former owner of the canyon) reached out to the University of Texas and invited archaeologists out to investigate Ice Box Cave. Mark L. Parsons led the study in 1962 and noted a large number of burned bones (Black 2001; THC 2019). Surface collection and subsurface test pits were excavated at the site resulting in the identification of a fiber layer and a Montell projectile point. Parsons determined the site was Middle Archaic in age with possibly older unexcavated occupation layers. Parsons recommended further excavations to determine the extent and significance of the site (Black 2001; THC 2019).

Dibble and Lorrain (1963–1964)

The first formal excavations at Bonfire Shelter were conducted from 1963 to 1964 by David S. Dibble (Dibble and Lorrain 1968). These investigations were conducted as part of the Texas Archeological Salvage Project for the Amistad Reservoir by the University of Texas at Austin. Excavations were focused in two areas, within the shelter interior and on the southern portion of the site around the slope of the talus cone formed below a notch in the canyon rim (Figure 1.1). During the 1960s investigations, three bone beds and an organic fiber layer were identified (Figure 3.1). These were reported as separated by various strata consisting of Archaic-age features or sterile sediment. All dates presented below are uncalibrated radiocarbon dates.

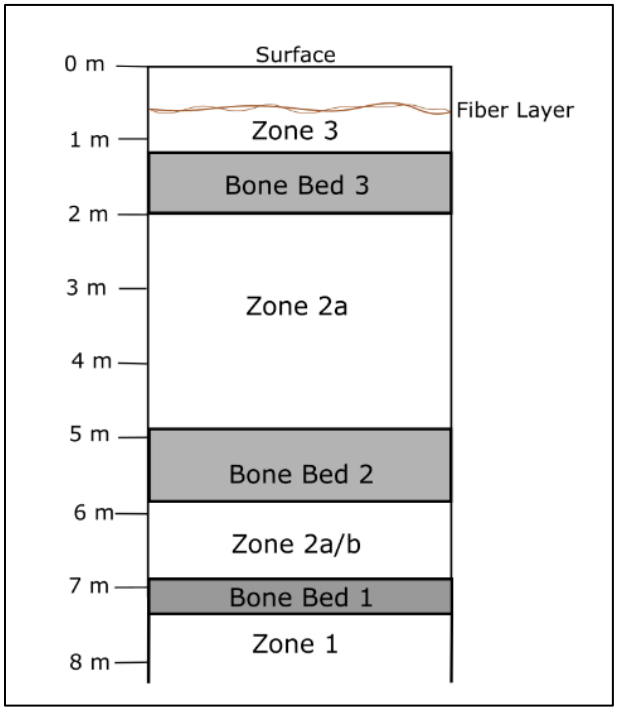

Figure 3.1. General profile overview of zones identified by Dibble (modified from Dibble and Lorrain 1968:50).

Bone Bed 1 was identified within the shelter interior. It consists of a series of horizontally bedded layers of Pleistocene faunal remains including Pleistocene bison (*Bison),* camel *(Camelops),* horse *(Equus*), and mammoth *(Mammuthus).* Though no lithic materials were found in association with Bone Bed 1, Dibble argued that the bone bed was potentially cultural in nature due to the fragmented nature of the bones as well as the occurrence of large roof spalls that could have been used as anvils during processing. He also noted the existence of charcoal flecks in association with the bones and the lack of natural taphonomic processes that might account for these attributes (Dibble and Lorrain 1968:28).

Bone Bed 2 was identified as a layer of faunal remains consisting of Pleistocene bison (*Bison antiquus or Bison occidentalis*). Paleoindian Plainview and Folsom points (N=5) were encountered in Bone Bed 2 (Dibble and Lorrain 1968:33–38) and a single radiocarbon date of 10,230±160 RCYBP was derived from charcoal recovered from Hearth 1, located in the upper portion of Bone Bed 2 (Dibble and Lorrain 1968:33). Along the northern side of the talus cone, Dibble and Lorrain identified three subzones, Components A through C, within Bone Bed 2. From top to bottom, they consist of an upper unburned layer of bone and sandy silt sediment, a thin middle layer of carbon-stained silt and burned bone, and a lower layer of unburned bone and sandy silt similar to the upper layer (Dibble and Lorrain 1968:29).

Bone Bed 3, the uppermost bone bed, was presumed to represent a Late Archaic bison drive event. It consists of a dense accumulation of bison (*Bison bison*) remains (up to 80 centimeters (cm) thick) as well as Castroville, Montell, and Marcos projectile points. The average age of Bone Bed 3, determined by analysis of two charcoal and a

burned bone samples, was determined by Dibble and Lorrain to be 2645±75 RCYBP (Dibble and Lorrain 1968:51).

Dibble and Lorrain's stratigraphic analysis of the shelter identified three major geologic zones in addition to the three identified bone beds (Dibble and Lorrain 1968:24). Zone 1 was described as the lowermost layer consisting of coarse light gray silts of fine-grained texture and lightly weathered limestone spalls that ranged in size from 2.5-cm to 30-cm. This deposit consisted predominantly of limestone spalls with less than five percent of the zone containing silt (Dibble and Lorrain 1968:24). Zone 1 was identified in both the shelter interior and the talus cone (Figure 1.3), but the limestone spalls within the talus deposits appeared to be more weathered (i.e., smaller in size and smoother with an increased amount of silt content) than those in the interior, which Dibble suggests is due to its location below the canyon rim (Dibble and Lorrain 1968:24).

Zone 2 is separated from Zone 1 by Bone Bed 1 within the shelter interior and by Bone Bed 2 within the talus cone. Zone 2 consisted of a thick layer of limestone spalls and silt. Within the talus cone, Zone 2 is described as talus debris which is tan to light gray silt intermixed with various sizes of limestone spalls (Dibble and Lorrain 1968:26). In contrast, Zone 2 within the shelter interior was divided into two subzones.

Zone 2a, the lower of the two, consisted of tan to light brown silt bedding with small and heavily weathered limestone spalls (Dibble and Lorrain 1968:26). This zone was identified to form a bench along the eastern wall of the shelter which extended west to the lowest slope of the talus cone. Zone 2b overlays Zone 2a and grades from unsorted silt and limestone spalls in the south to predominantly fine silts in the northern portion of the shelter (Dibble and Lorrain 1968:26).

Dibble proposed that Zones 2a and 2b formed simultaneously due to the positioning of Bone Bed 2 in relation to the zones (Dibble and Lorrain 1968:29). Within the shelter interior Zone 2a underlies Bone Bed 2, while within the talus cone Bone Bed 2 is found within Zone 2b. This suggests that Zone 2a began to accumulate within the shelter interior while Zone 2b was accumulating on the talus cone. After Bone Bed 2 was deposited, both zones continued to accumulate resulting in Bone Bed 2 overlying and underlying portions of Zone 2a and 2b.

The uppermost Zone 3 was identified in both the shelter interior as well as the talus cone overlaying Bone Bed 3. This zone was described as similar to Zone 2 within the talus cone and consisted of unsorted silt and limestone spalls. Dibble and Lorrain separated Zone 3 from Zone 2 within the talus cone based upon the intervening Bone Bed 3 (Dibble and Lorrain 1968:26). Zone 3 was separated into three subzones within the talus cone due to an intervening fiber layer, Zone 3b, but the upper and lower Zone 3a and 3c were identified as being similar in composition. Within the shelter interior, Zone 3 also exhibited finer texture from south to north similar to Zone 2. The portion of Zone 3 north of the excavation line N98 was almost entirely light brown silt with occasional laminae of very fine white clay (Dibble and Lorrain 1968:26).

Turpin and Bement (1983–1984)

A second round of excavations at Bonfire Shelter was conducted from 1983 to 1984 by Solveig Turpin and Leland Bement (Bement 1986). The excavations were focused within the shelter interior and on evaluating the cultural origin of Bone Bed 1; however, they exposed portions of Bone Bed 2 in the shelter interior in the process. New excavation units were established north of Dibble's main shelter interior units as well as

between the previous excavation units towards the talus cone. Expanding on Dibble's stratigraphic interpretations of Bone Bed 2 and Bone Bed 1, Bement (1986:19–23) created a stratigraphic sequence with nine identified strata (i.e., strata A through I). All dates presented below are uncalibrated radiocarbon dates.

Dibble's original Bone Bed 2 was divided from top to bottom into Component C, B, and A within the talus cone. Likewise, Bement identified three distinct strata within Bone Bed 2 in the shelter interior and used similar alphabetic terminology, but Bement's layers from top to bottom consisted of Stratum A, B, and C (Bement 1986:19–23). Stratum A, which is associated with the uppermost portion of Bone Bed 2, was dated to 10,280±240 RCYBP utilizing loose charcoal recovered from Bement's investigations. This date aligns with Dibble's original date of 10,230±160 RCYBP as well as two subsequent dates (i.e., 9,920±150 RCYBP and 10,100±300 RCYBP) established by Dibble in 1970 from Bone Bed 2/Hearth 1 (Bement 1986:9).

Faunal remains in Bone Bed 2 identified as *Bison antiquus* or *occidentalis* and *Equus* with no unequivocally cultural material encountered during Bement's investigation. Bement argued that Bone Bed 2 does represent a bison jump event due to the previously identified cultural material as well as the presence of a butchering locus in strata B and C (Bement 1986:25–29; Bement 2007).

Stratum D was defined as degraded limestone with limestone spalls. It is characterized as the layer separating Bone Beds 1 and 2 (Bement 1986:20). Bement noted a broad depression marking the lower boundary of the stratum. The only faunal remains associated with Stratum D consisted of a single juvenile gray fox (*Urocyon*

cinereoargenteus) (Bement 1986:32). No radiocarbon analysis was conducted for the stratum.

Bement's strata E, F, and G represent a large, complex deposit of brown silty clay. The division into three strata is arbitrary due to the layers' variable thickness and composition. Bement does not discuss the possible formation processes with the intermittent layer (Bement 1986:20). Stratum E represents the uppermost portion of Bone Bed 1 and included bison, mammoth, horse, and camel (Bement 1986:33). Though no lithic material was encountered with these layers, Bement argues that they are likely cultural in origin. He points to the presence of large limestone blocks in proximity to the bone bed as well as the bone breakage patterns and the occurrence of polish and striations on a spiral-fractured specimen as evidence of human activity (Bement 1986:38).

Bement extended his excavations below Dibble's and identified three additional strata associated with Bone Bed 1. Strata H-1 and H-2 consist of limestone spalls and a fine matrix of limestone powder and Stratum I consist of large limestone boulders with a fine matrix of limestone power. Stratum H-1 contained only horse (*Equus francisci*) and mammoth (*Mammuthus* sp,), with horse making up the bulk of the assemblage (Bement 1986:38). Stratum H-2 consisted of three single elements of antelope (*Capromeryx* sp.). Bement proposed that the faunal remains from these strata were a result of both human and carnivore activity. A charcoal sample collected from a scatter across Stratum H-1 dated to 12,430±490 RCYBP (Bement 1986:54). Stratum I contained the faunal remains of horse and bison. Bement argues for cultural manipulation of faunal remains as evident by the occurrences of large limestone blocks for procurement as well as possible cutmarks on two specimens (Bement 1986:59).

The Bone Bed 2 Debate

After the conclusion of the initial investigations conducted in Bonfire Shelter, a debate arose as to the origin of Bone Bed 2 as well as the number of cultural events represented within it. The two main questions are: 1) Through what cultural processes did the bone beds within the talus cone form? and 2) How many individual cultural events are represented? Table 3.2 below summarizes the various hypotheses and contributing theorist.

The debate began with Dibble's report following excavation and analysis claiming that Bone Bed 2 did represent a bison kill site with up to three individual events (Dibble and Lorrain 1986; Dibble 1970). Others have agreed with Dibble and Lorrain that Bone Bed 2 and their estimated 120 minimum number of individual (MNI) bison represent multiple Paleoindian bison drive events (Bement 1986; Bousman et al. 2004; Holliday 1997; Prewitt 2007; Turpin 2004).

Table 3.2. Summary of the Bone Bed 2 Origins Debate

	Bison Jump	Secondary Butchering
Number of Events	3	1
Material Cultural	Both Plainview and Folsom in comingled assemblage.	Plainview as primary assemblage with contemporary but separate Folsom.
Stratigraphic Evidence	Three separate temporal events represented by the three visible strata.	Single event that has been redeposited through slope erosion.
Supporting Authors	Dibble and Lorrain 1968; Dibble 1970; Bement 1986; Bousman et al. 2004; Holliday 1997; Prewitt 2007; Turpin 2004	Binford 1978; Byerly et al. 2005, 2007; Meltzer et al. 2007

These authors not only cite the bison MNI as support for a drive hypothesis but also the unique stratigraphic sequences encompassing Bone Bed 2. As mentioned above,

in places visible in the profile of the south side of the Talus Cone Bone Bed 2 is made up of three distinct stratigraphic zones which when inspected visually do appear to be individual depositional events (Dibble and Lorrain 1968; Bement 1986).

This theory was first challenged in Binford's *Nunamiut Ethnoarchaeology* (1978:475-476), in which the author compares the frequencies of bison remains to a secondary processing site rather than a kill site/primary processing location. Meaning, that the kill occurred elsewhere and only choice elements were brought into Bonfire Shelter for secondary processing. Research conducted in 2005 by R.M. Byerly and others agreed with Binford and determined that the faunal assemblage of Bone Bed 2 indicated a secondary processing location, not a kill site as previously suggested (Byerly et al. 2005; Dibble and Lorrain 1968). The authors argued that the lack of carnivore activity and the higher occurrence of impact fractures, rather than cut marks, indicated that the human activity centered around secondary marrow extraction (Byerly et al. 2005:515–516). Seasonality was determined using specimen age and tooth eruption patterns; based on these data, the authors determined a single event is represented within Bone Bed 2 rather than three (Byerly et al. 2005:612).

This analysis sparked a public conversation in the 2007 issue of *American Antiquity* between Bement and Byerly (Bement 2007; Byerly et al. 2007). Bement refuted Byerly's methods of determining MNI and claimed cherry picking of results was occurring with an inadequate data set. Byerly in turn responded in defense of his comparative sample collection methods and rebutted that Bement was relying on unproven assumptions, such as Bone Bed 2 being a bison jump. Byerly also called to

attention that the three stratigraphic units of Bone Bed 2 are only visible in a portion of the cone and could have formed postdepositionally.

Other archaeologists have jumped into this arena over the years to tease apart the mystery of Bone Bed 2 and its origins (Bousman et al. 2004; Holliday 1997; Prewitt 2007; Meltzer et al. 2007). What both sides agreed on is that further research is needed to address questions about the formation of the cultural and natural deposits of Bonfire Shelter. The goal of this thesis is to resolve the debate about the origins of Bone Bed 2.

Significance of Bone Bed 2

Successfully executing a bison drive requires a high level of planning and organization. For one, it involves group cooperation among the hunters. Paleoindian group sizes were most likely small as their subsistence strategies required high mobility (Amick 1996). In a large-scale hunting event, of 50 animals or more, multiple groups were probably involved as their subsistence strategy shifted to a low mobility or focused activity (Amick 1996; Bement 2016; Carlson and Bement 2013; Frison 1991b, 2004; Kilby et al. 2020; Zedeño et al. 2014).

Bison drives also require a detailed knowledge of the local landscape and understanding of bison herd behavior (Wyckoff and Dalquest 1997; Carlson and Bement 2013; Frison 1991a; 2004; Zedeño et al. 2014). As bison herd movement in the Southern Plains was tied to the seasonal occurrence of water sources, Paleoindians had to predict this migration (Baker 2017; Kelly 2013). This suggests that multiple groups of hunters were meeting seasonally based on herd behavior patterns to plan, organize, and achieve the drive event. For groups to merge into a cohesive team, certain social conditions likely

needed to be met, such as having a structured hierarchy and division of labor (Carlson and Bement 2013; Kilby et al. 2020).

This cooperation among groups is of particular interest regarding Bone Bed 2. As discussed above, both Plainview and Folsom lithic technologies have been found within the bone bed. These groups are understood to be separate culturally and temporally, though they may overlap briefly in time (Holliday et al. 2017). Another hypothesis based on their similar lithic technology is that Plainview were successors of Folsom (Holliday, Johnson, and Knudson 2017:288-289). If both groups were involved in bison hunting at Bonfire Shelter several questions arise: Were these groups working together in a large-scale hunting event? Were they there separately but utilizing the same knowledge of bison herd movement and landscape? Or, was there an exchange of information occurring so that the Plainview groups learned about Bonfire Shelter's unique morphology from earlier Folsom people? While this thesis is unlikely to uncover any specific answers to these questions, it may aid in establishing some of the parameters; in particular, the origins of Bone Bed 2 and the number of depositional events represented within it.

Current Investigations

Beginning in 2017, Texas State University under the ASWT Project renewed investigations at Bonfire Shelter under the direction of Dr. David Kilby and Dr. Marcus Hamilton. These investigations are focused on four research goals: 1) to create a detailed chronostratigraphic sequence of the site's deposits; 2) to determine if Bone Bed 2 is the location of a bison drive event as opposed to a secondary processing location and if so, to determine the number of bison drive events associated with the deposits; 3) to establish if Bone Bed 1 was the result of human activity or natural causes; and finally, 4) to preserve

the site for the future through stabilization and backfilling of the open excavation areas (Kilby and Hamilton 2018; Kilby et al. 2020).

Site Stability and Preservation

In 2017, work was begun to prepare and stabilize the site for further investigations. Much of this work was done under a Texas Preservation Trust Fund grant by Dr. Stephen Black, Charles Koenig, and Amanda Castañeda. Approximately 30 cubic meters of wall slump and backfill were removed from the previously investigated units which had been left open from the 1964 excavations. Mesh and geotextile fabric were applied to the talus cone to protect it from further erosion. Along the western and northern portion of the site a check dam, various ditches, and retaining walls were constructed to divert runoff within the shelter interior (Kilby and Hamilton 2018).

Bone Bed 1

Within the shelter interior, the previous excavation trenches and blocks were cleared out and reopened. This exposed all three bone beds as well as a series of intervening cultural and sterile zones (Farrell 2020; Kilby et al. 2020). Detailed stratigraphic documentation of the shelter interior resulted in the identification of 28 strata representing over 15,000 years (Kilby et al. 2020).

New excavations were also opened in the shelter interior to test the lower layers of Bone Bed 1. Sean Farrell conducted excavations in 2017 and 2018 to attempt to establish the origins of Bone Bed 1 in the shelter interior. His thesis focused on using geoarchaeological methods along with analysis of faunal and lithic remains to interpret the formation processes of Bone Bed 1 and determine its potential to be anthropogenic in nature (Farrell 2020). While no evidence of human activity could be found in association

with Bone Bed 1, the resulting sedimentological and chronological results have and will contribute to our understanding of the region's Pleistocene history.

Bone Bed 2

In 2017 and 2018, David Kilby created detailed stratigraphic records of profiles in both the shelter interior and along the talus cone. Along the talus cone, the northern, eastern, and southern profiles were re-exposed and cleaned to allow for fresh documentation of the cones stratigraphic sequence. Profiles in the shelter interior, near the center of the site and associated with both excavations in the 1960s and 1980s, were also cleaned and profiled. Stratigraphic analysis of the shelter interior identified 23 strata including Bement's established strata A through I. Stratigraphic investigations of the talus cone in the southern portion of the site led to the identification of 15 strata. These were connected to the work previously done by Dibble (Table 3.3; Figure 3.2).

In addition to the stratigraphic profiles recorded in 2017, two 50 x 50-cm column samples were excavated on the northern portion of the talus cone to aid in establishing the depositional history of the talus cone. During the excavation of the column samples, three new lithic tools were identified: one Castroville projectile point, one Plainview projectile point, and one biface fragment (Table 3.3). In 2018, the southern and eastern portion of the talus cone was exposed and documented, and three additional column samples were excavated for future analysis. The research and analyses presented in this thesis were conducted subsequent to 2018 and focuses on the five excavated column samples with the purpose of establishing the depositional history of the talus cone and subsequent bone bed within.

Final sampling efforts were completed in 2019. These efforts included fine sediment samples, in 5 cm increments, in columns adjacent to each of the five previous mentioned column samples in the talus cone, as well as zooarchaeological analysis of Bone Bed 2. The fine sediment samples were not utilized in this thesis, due to time constraints, but the zooarchaeological analysis was completed in 2020 (Ramsey 2020).

Table 3.3. Summary of Talus Cone Stratigraphy.

Dibble and Lorrain 1968	Kilby (PS05)*	Description	Artifact Associations	Dating Samples	Notes
Not recorded	1	Slump layer of loose light brownish gray sandy-loam to silty-loam.	None	None	Massive debris deposit sloping east and north away from peak of talus cone. Mixture of debris derived from notch, stabilization material, and disturbed surface material.
Zone 3	2	Poorly sorted limestone spalls and friable pale brown sandy silt.	FN# 60158 Castroville projectile point	None	Natural deposits overlaying Bone Bed 3. Includes some bone that have been eroded out.
Bone Bed 3	3	Layer of bone, small rocks, and friable silt. Layer is predominantly ash and burned bone.	None	None	Upper portion of Dibble's Bone Bed 3 possibly representing the latest stage of the drive event.
Bone Bed 3	4	Layer of bison bones, boulders, small rocks, and friable white ashy powder.	None	None	Lower portion of Dibble's Bone Bed 3 and possibly representing the early stage of drive event.
Bone Bed 3	5	Layer of burned bone and small rocks with blue-gray ashy powder.	None	None	Discontinuous thin layer and lowest portion of Dibble's Bone Bed 3.
Zone 2b	6	Layer of friable brown sandy loam with small rocks. Increased organic content and rootlets.	None	FN# 60123 Charcoal	Thin horizon of Dibble's Zone 2b which has been damaged from burning.
Zone 2b	7	Layer of friable grayish red sandy-loam with small angular rocks.	None	None	Horizon is reduced due to overlying burned layer.
Zone 2b	8	Layer of poorly sorted colluvium and friable brown sandy loam.	None	FN# 60665	Horizon represents accumulation from notch, roof, and outside the shelter.

Dibble and Lorrain 1968	Kilby (PS05)*	Description	Artifact Associations	Dating Samples	Notes
					FN# 60665: Talus Cone Stratum 8b, charcoal, RCYBP 6830±36, mean calBP 7661
Zone 2b	9	Layer of poorly sorted angular colluvium and friable pale brown sandy loam.	None	None	Horizon represents one or more depositional events of roof fall.
Zone 2b	10	Layer of poorly sorted colluvium and friable light yellowish-brown sandy loam.	None	FN# 60119, 60553, 60593, 60594	Horizon is comparable to Kilby's Stratum 8 based on color, texture, and structure. It corresponds to Dibble's lower part of Zone 2b. Grades into Kilby's Stratum 11. FN# 60593: Talus Cone Stratum 10b, walnut charcoal, RCYBP 8579±35, mean calBP 9541 FN# 60594: Talus Cone Stratum10b, juniper charcoal, RCYBP 9026±35, mean calBP 10212
Bone Bed 2	11	Massive colluvial deposits with abundant angular to subangular gravels and cobbles with friable brown sandy loam matrix.	FN# 60126, 60236 biface fragment and nearly complete Plainview projectile point	FN# 60644, 60127, 60128, 60237, 60581, 60582, 60587, 60592, 60467, 60468, 60470, 60475 Bone, 60648, 60643	Upper portion of Dibble's Bone Bed 2 differentiated from above layer by presence of bone and increased rocks. FN# 60648: Talus Cone Stratum 11, charcoal, RCYBP 10115±51, mean calBP 11736 FN# 60643: Talus Cone Stratum 11b, burnt matrix, RCYBP 8843±41, mean calBP 9938

Dibble and Lorrain 1968	Kilby (PS05)*	Description	Artifact Associations	Dating Samples	Notes
Bone Bed 2	12	Massive colluvial deposits with abundant rounded to angular gravels and cobbles with friable gray silty matrix.	None	FN# 60124, 60579, 60580, 60584, 60586, 60588, 60667, 60469, 60471, 60472, 60473 Bone, 60600 Ash, 60052 Charcoal, 60589 Burned matrix, 60600	Horizon has gray ashy silt and burned bone. Possibly represents initial fall deposit with colluvium from the rim. FN# 60600: Talus Cone Stratum 12, ashy sediment, RCYBP 7638±35, mean calBP 8426 FN# 60589: Talus Cone Stratum 12b, charcoal, RCYBP 9831±36, mean calBP 11236
Zone 2b	13	Massive colluvium with jumbled rocks in friable to firm grayish brown sandy silt matrix.	None	None	Horizon is differentiated from above layer predominately due to lack of bison bone.
Zone 2b	14	Layer of firm reddened sandy loam matrix and subangular gravels and cobbles.	None	FN# 60585, 60590, 60595, 60597, 60668 Bone	Colluvial with increased clay content underlaying Bone Bed 2. Possibly represents an increase in sediments being deposited from outside the shelter.
Zone 2b	15	Massive colluvium with small rocks in friable to firm grayish brown sandy silt matrix.	None	FN# 60534 Charcoal	Horizon is comparable to Kilby's Stratum 13 with finer gravels and little matrix. Corresponds to the lower section of Dibble's Zone 2b.

References: Dibble & Lorrain 1968

Note: PS05* Refers to the northern talus cone profile.

Stratum	Description	Dibble and Lorraine 1966
TC-1	Sandy loam; light brownish gray (10YR 6/2), debris derived from notch, stabilization materials, and disturbed surface material.	Zone 3
TC-2	Sandy loam; pale brown (10YR 6/3), poorly sorted limestone gravel in massive matrix.	Zone 3
TC-3	Ashy silt loam; white (10YR 8/1), massive accumulation of bison bone, much of it reduced to calcined powder, burned lithic artifacts.	Bone Bed 3
TC-4	Ashy silt loam; light gray (10YR 7/1), massive accumulation of bison bone, boulders, and smaller rock, all subjected to intense heat.	Bone Bed 3
TC-5	Silty; light bluish gray (Gley 10B 7/1), discontinuous lens of fibrous ashy powder, perhaps representing burned pooled tissue.	Bone Bed 3
TC-6	Sandy loam; brown (10YR 4/3), scorched/oxidized surface underlying Bone Bed 3.	Scorched earth layer
TC-7	Sandy loam; weak red (2.5YR 5/2), reduced/oxidized expressed variably in thin layer, thickens to east.	Zone 2b
TC-8	Sandy loam; brown (10 YR 5/3), massive poorly sorted colluvial gravel and cobbles.	Zone 2b
TC-9	Sandy loam; pale brown (10YR 6/3), poorly sorted colluvium, including large boulder in center of profile.	Zone 2b
TC-10	Sandy loam, light yellowish brown (10YR 6/4), colluvial gravel and cobbles, some rocky lenses.	Zone 2b
TC-11	Sandy loam; pale brown (10YR 6/3), massive colluvium with abundant gravel and cobbles; abundant bison bone, unburned artifacts.	Bone Bed 2
TC-12	Silt loam; light brownish gray (10YR 6/2), massive colluvium wit abundant gravel, cobbles, and boulders; occasional bison bone.	Bone Bed 2
TC-13	Sandy loam; yellowish brown (10YR 5/4), massive colluvium including gravel and cobbles; surface underlying Bone Bed 2.	Zone 2b
TC-14	Loam; brown (7.5YR 5/4), massive colluvium including gravel, reddened due to increased clay content.	Zone 1
TC-15	Sandy loam; yellowish brown (10YR 5/6), massive colluvium including gravel and small cobbles with little fine sediment in between.	Zone 1

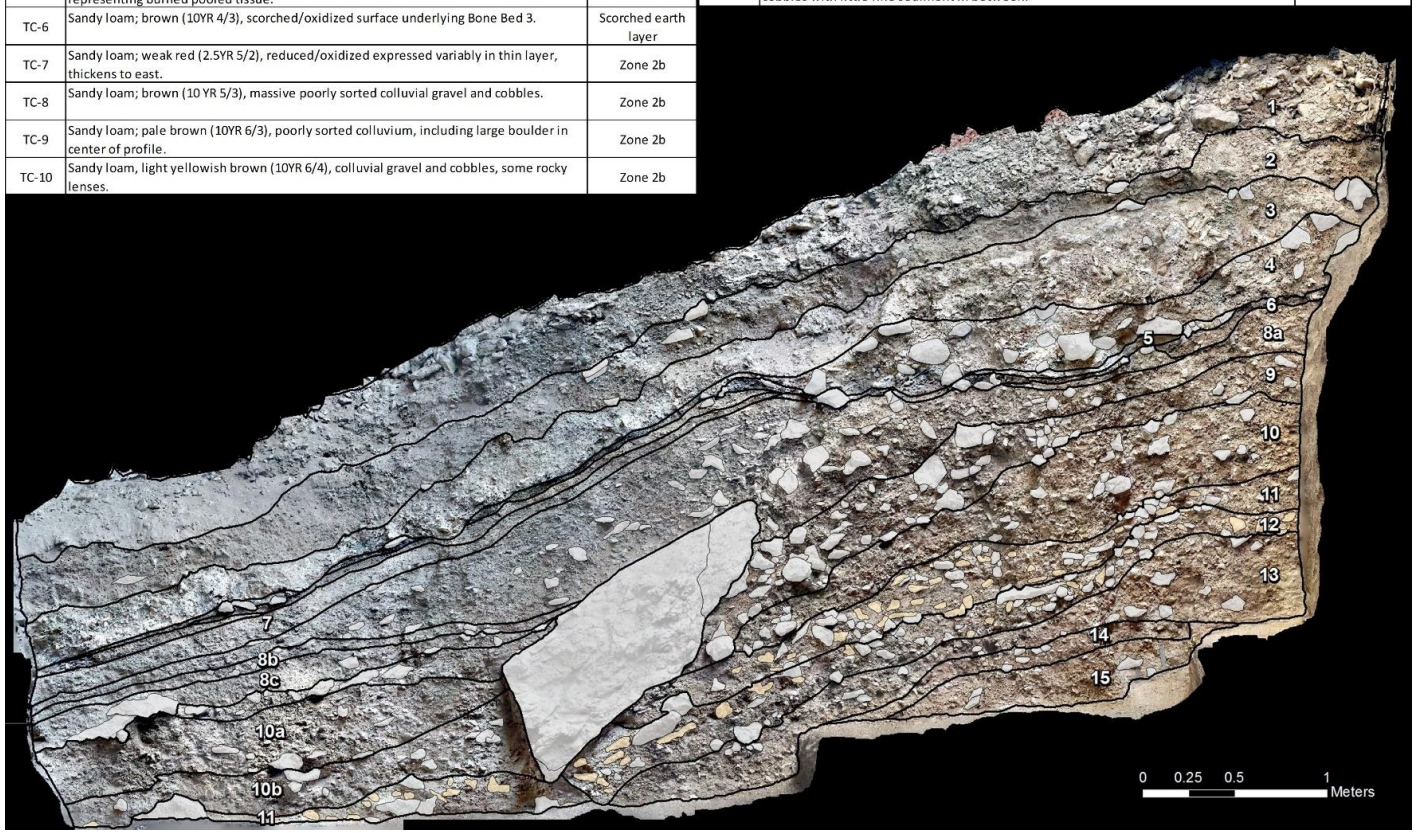

Figure 3.2. Stratigraphic overview of PS05 and talus cone (from Kilby et al. 2020).

Stratigraphic Discussion

Within the talus cone there are three strata associated with Bone Bed 3 (Table 3.3). Stratum 3 is the upper most portion consisting of a massive accumulation of calcified bison bone, small cobbles and pebbles, and silty matrix. Stratum 4 is similar but contains markedly more cobbles, boulders, and very little sediment. Finally, Stratum 5 is a discontinuous thin fibrous and heavily burned layer of small gravels and bone fragments.

In sum, as is currently understood by ASWT, Bone Bed 3 appears to represent a dynamic colluvial depositional episode resulting from a single bison drive from the canyon above. Stratum 4 is the initial fall event consisting of a mass jumble of large clast rocks and bison bones. Stratum 3 is the secondary portion of the fall event which consists of mostly bone and a possible fining upward sequence of gravels and sediment. The underlaying Stratum 5 is the lowest portion of the drive and could be translocated remains of sediment, bone, and organic material from the mass burning event that occurred after deposition. This is the current interpretation of BB3 but might be revised in light of ongoing analyses by ASWT.

Bone Bed 2 is a little more complicated but is found in four strata across the cone: strata 11, 12, 13 and 14 (Table 3.3). Details on each Bone Bed 2 stratum by column is summarized in Chapter 6, but a brief summary is included here. Bone Bed 2 has been historically described as three stratigraphic zones: an unburned layer of bone and sediment (Stratum 11), a densely burned layer of bone and ashy sediment (Stratum 12), and an unburned layer of bone and sediment (strata 13 and 14). Detailed examination of

the talus stratigraphy has broken these strata into various substrata largely depending on their horizontal and vertical location within the cone.

Radiocarbon Dating

As part of ASWT's mission to detailed chronostratigraphic sequence of the site's deposits, additional radiocarbon dates were submitted. Radiocarbon samples have been difficult to come by Bonfire Shelter due to the low preservation quality of bone and limited charcoal remains. Currently, only the upper portion of Bone Bed 2 has been dated (Table 3.4). Four charcoal samples from a stratigraphically, but not directly, associated hearth feature and another charcoal sample within proximity (less than a meter) to a lanceolate point have returned radiocarbon dates between 11,500 to 12,000 calBP (Bement 1986; Dibble and Lorrain 1968; Dibble 1970; Kilby et al. 2020). Radiocarbon results from three charcoal samples within Bone Bed 3 have returned dated between 2,500 to 3,000 cal BP (Dibble and Lorrain 1968; Kilby et al. 2020).

Table 3.4. Summary of Radiocarbon Dates from Bonfire Shelter (to-date).

Sample No.	Provenience	Material	RCYBP	Cal BP (2σ)	Source
TX-151	Fiber Layer, Hearth 7	Charcoal	1,400±130	AD 406-894; AD 925-936	Dibble and Lorrain 1968
TX-194	Fiber Layer, Hearth 6	Charcoal	1,690±80	AD 132-541	Dibble and Lorrain 1968
TX-046	Bone Bed 3	Burned Bone	2,310±210	-	Dibble and Lorrain 1968
TX-047	Bone Bed 3	Burned Bone	2,810±110	-	Dibble and Lorrain 1968
TX-106	Bone Bed 3	Charcoal	2,780±110	2,867	Dibble and Lorrain 1968
TX-131	Bone Bed 3	Charcoal	2,510±100	2,680	Dibble and Lorrain 1968
D-AMS 027372	Bone Bed 3, Stratum Talus Cone 5	Charcoal	2,516±24	2,740-2,494	Kilby et al. 2020
D-AMS 031259	ASWT Feature 1, Stratum Site Interior 15	Charcoal	5,943±47	6,889-6,668	Kilby et al. 2020
D-AMS 031257	ASWT Feature 1, Stratum Site Interior 15	Charcoal	6,034±36	6,979-6,786	Kilby et al. 2020
D-AMS 031258	ASWT Feature 1, Stratum Site Interior 15	Charcoal	5,950±42	6,885-6,675	Kilby et al. 2020
TX-152	Intermediate Zone, Hearth 2	Charcoal	7,240±220	8,066	Dibble and Lorrain 1968
TX-153	Bone Bed 2, Hearth 1	Charcoal	10,230±160	12,006	Dibble and Lorrain 1968
TX-657	Bone Bed 2, Hearth 1	Charcoal	9,920±150	11,516	Dibble 1970
TX-658	Bone Bed 2, Hearth 1	Charcoal	10,100±300	11,805	Dibble 1970
AA-346	Bone Bed 2, Component A	Charcoal	10,280±430	13,002-10,770	Bement 1986
D-AMS 034555	Bone Bed 2, Stratum Talus Cone 11	Charcoal	10,115+51	11,999-11,405	Kilby et al. 2020
AA-334	Bone Bed 1, Stratum H-1	Charcoal	12,460±490	16,184-13,435	Bement 1986
D-AMS 034547	Bone Bed 1, Stratum Site Interior 24	Charcoal	12,112±69	14,145-13,770	Kilby et al. 2020

*Adapted from Ferrell 2020 and Kilby et al. 2020.

IV. RESEARCH QUESTIONS AND HYPOTHESES

As detailed in Chapter 3, past research at Bonfire Shelter has resulted in conflicting interpretations on the origins and composition of Bone Bed 2. The primary purpose of this thesis is to address two research questions on these issues utilizing geoarchaeological methods: (1) are the Bone Bed 2 deposits within the talus cone the result of a bison drive from the canyon rim above, and (2) how many cultural events are represented in Bone Bed 2? Addressing these questions will be facilitated by establishing specifically how the talus cone formed. An understanding of the natural depositional processes of the talus cone is critical to recognizing deviations to those processes as the result of human activity. By establishing how the cone formed naturally, I can test my hypotheses on the formation of the bone beds through cultural means.

Origins of Bone Bed 2

Determining whether Bone Bed 2 is the result of a bison drive is significant in that it will broaden our understanding of Paleoindian site use in Texas and the Southern Plains. Answering this question opens research avenues into Paleoindian subsistence studies. It also highlights questions on what social mechanisms facilitated such strategies (i.e., group size or communal hunting).

If Bone Bed 2 represents a bison jump then Bonfire Shelter would be the oldest and southernmost site with evidence of this hunting technique. Successfully executed, a bison drive hunting event requires knowledge of the landscape, herd behavior, and cooperation between the hunters (Frison 1991a). This determination would bring into question whether other such sites are located within the Southern Plains and, if so, how

were these hunting events conducted? Alternatively, if Bone Bed 2 did not form as a result of a bison drive, was it instead a secondary processing location?

To determine whether Bone Bed 2 formed as a result of a bison drive event or events rather than a secondary processing and butchering location, stratigraphic analysis, particle size analysis (PSA), magnetic susceptibility (MS), total organic content (TOC), carbonate content, and gypsum content of stratum from five column samples were examined (Table 4.1). These column samples were excavated from the northern, eastern, and southern faces of the talus cone, and analyzed strata include the entire exposed profiles (i.e., from above Bone Bed 3 to below Bone Bed 2). This has allowed for comparison within Bone Bed 2, between Bone Bed 2 and Bone Bed 3, and of non-bone bed strata with bone bed strata.

Origin Hypothesis

If Bone Bed 2 is the result of a single bison drive event, then stratigraphic and particle size analyses should show a fining upward sequence within a massive colluvial event. At its most basic morphology the particle size should begin in the highest clast size (boulder) and become smaller in size (cobbles, pebbles, sand, and then silt), as we move up the profile. If bison were being driven over the canyon edge, a mass of boulders and gravels intermixed with bison bone could be expected to represent the main drive event. This main event should then be overlain by fining upward gravels and finally silty sediment which would have fallen as the dust settled, so to speak. While occurring under different conditions (colluvial rather than fluvial), this assumption is based on Stokes Law in which larger sediments take more energy to suspend than smaller sediments, resulting in a well-sorted fining upwards sequence (Waters 1992: 36-40).

Additionally, if there were multiple bison drive events represented within Bone Bed 2, multiple individual fining upward sequences should exist. If the bones are not mixed with large clasts, appear to be in a single layer between depositional events, or are within ongoing depositional intervals, then the bones were likely deposited during a processing event rather than as a drive.

Table 4.1. Expectations for whether Bone Bed 2 formed due to a bison drive or as a secondary processing/butchering location.

Analysis	Jump Drive	Secondary Processing
Stratigraphic	Bones intermixed with sediment and gravel in bone beds. Not restricted to stratigraphic boundaries and not restricted to boundary orientation	Minimal mixing with sediment and gravel. Discreet layer of bone that doesn't cross stratigraphic boundaries and bones that lie parallel to stratigraphic boundaries
Particle Size	Fining upward sequence	Predominately bone with little matrix and no fining upward sequence
Magnetic Susceptibility	Dramatic spike in values occurring in association with each individual event	A smaller, less dramatic spike; only one spike in association with BB2
Organic Content	Dramatic spike in values occurring in association with each individual event	A smaller, less dramatic spike; only one spike in association with BB2
Carbonate Content	Decrease in bone beds due to exogenic deposition from drive event	No difference across bone beds or natural strata due to continuous endogenic deposition
Gypsum Content	Increase in bone beds due to upland sources during drive event	Consistent across natural and bone bed strata

Traditional sedimentological investigation of the profile were conducted to determine the strata's thickness, texture, inclusions, and boundaries. This will help establish a stratigraphic context to the talus cone and the depositional events making up the bone beds. The remaining analyses (i.e., magnetic susceptibility, organic content, carbonate content, and gypsum content) may not vary based on the different cultural

formation processes proposed, but due to the unique conditions occurring within the Bonfire Shelter talus cone, these analyses were run for comparisons between the two bone beds as well as with non-bone bed strata. Overall, these sedimentological analyses will be key when creating a broad depositional picture of the formation of the talus cone. Together with the PSA and stratigraphic analysis, trends should provide support for interpreting whether Bone Bed 2 was deposited as a result of a bison drive or secondary processing.

The MS measurements of the bone bed strata should be higher than non-bone bed strata due to increased organic content (i.e., decomposing bison) and burning. I expected a large spike within Bone Bed 3 and a smaller but still distinct spike in Bone Bed 2. These spikes should be distinguishable from other human activities occurring across the talus cone. This argument could also be made for the organic content. Carbonate content should decrease as more outside parent material (i.e., the Boquillas Formation) is introduced during a drive event while gypsum content would increase as it originates in the uplands.

Number of Events

The number of events represented in Bone Bed 2 is significant because it provides valuable information on the cultural behavior of Paleoindians in not only Texas but in wider North America. If multiple hunting events occurred, it could indicate that the site was selected as an advantageous location and reused repeatedly or even seasonally specifically for bison hunting. This would than raise questions about how cultural groups utilized Bonfire Shelter and the surrounding landscape. On the other hand, if Bone Bed 2

is the result of only one event, it would also bring into question why two distinct lithic technologies, Plainview and Folsom, are found in Bone Bed 2.

To determine whether Bone Bed 2 formed as the result of one or more depositional events, the same analyses mentioned above were utilized: stratigraphic analysis, particle size analysis (PSA), magnetic susceptibility (MS), total organic content (TOC), carbonate content, and gypsum content of stratum from the five column samples (Table 4.2). Currently, Bone Bed 2 within the talus cone is recognized as two distinct strata on the north and east side of the talus cone and three distinct strata on the south side (Dibble and Lorraine 1968). To answer this research question, particular interest was given to comparing the Bone Bed 2 strata, and in comparing them to the Bone Bed 3 strata.

Number of Events Hypothesis

If Bone Bed 2 represents three separate cultural events, then stratigraphic and particle size analyses should result in the determination of multiple depositional events. Stratigraphically, Bone Bed 2 has already been reported as encompassing two to three strata within the talus cone (Dibble and Lorrain 1968). These strata should also be distinguishable based on multiple fining upward sequences of particle size if multiple bison drive events are represented. If Bone Bed 2 only represents one cultural depositional event, the stratigraphic and PSA should be similar to Bone Bed 3 in showing only one fining upward trend, or perhaps no discernable trend if redeposited.

As the sediments making up each of the individual strata within Bone Bed 2 should have similar sources (i.e., colluvium coming from the canyon rim and from the roof of the rockshelter) differences in the mineral and chemical makeup of each

component may aid in distinguishing individual depositional events. As such, additional analyses including MS, TOC, carbonate content, and gypsum content should show consistent differences or spikes in values if they represent multiple cultural events. If only one cultural event is represented only one spike should occur indicating the single cultural depositional event.

Table 4.2. Expectations of whether Bone Bed 2 formed due to one or multiple depositional/cultural events.

Analysis	Single Event	Multiple Events
Stratigraphic	Single distinct stratigraphic layer	Multiple distinct stratigraphic layers
Particle Size	Single fining upward sequence	Multiple fining upward sequences divided
Magnetic Susceptibility	Single distinct spike in values	Multiple spikes in value
Organic Content	Single distinct spike in values	Multiple spikes in value
Carbonate Content	Single distinct spike in values	Multiple spikes in value
Gypsum Content	Single distinct spike in values	Multiple spikes in value

Theoretical Framework of Analyses

Geoarchaeology applies the concepts and methods of various geosciences (e.g., geology, mineralogy, sedimentology, hydrology, and more) to address archaeological research questions (Waters 1992). Not only does geoarchaeology offer a way to better understand the context in which archaeological materials are found but provides a broad-spectrum approach to understanding the relationship between people and their environment (Goldberg and Macphail 2006; Schiffer 1987; Waters 1992). It is essential to the interpretation of the human past particularly in regard to the reconstruction of site formation and landscapes. This is especially true with research focused on Paleoindian sites as they are often deeply buried, well stratified, and are displaced to such a distant time that post depositional processes can heavily impact modern interpretations. Below I

will provide a brief discussion of the theoretical framework behind the geoarchaeological analyses conducted which is followed by the laboratory results for the five column samples.

Particle Size Analysis

Particle size analysis is the study of the mass fraction of different sizes of the mineralogical particles which comprise soils and sediments (Durner et al. 2017; Folk 1980; Gale and Hoare 1991). This metric provides insight into various properties (i.e., physical and chemical) which can be related to the formation and preservation of archaeological sites. Within archaeological studies, particle size analysis is most commonly utilized to determine the environment of deposition as well as the energy of such deposition (Goldberg and Macphail 2006). For this thesis, particle size analysis is key to understanding the depositional history of the talus cone and identifying bison drive events within the dynamic environment.

Due to the skewed nature of grain size populations, descriptive statistics as presented by Folk (1980) were calculated for the Graphic Mean and Graphic Standard Deviation. Folk presents the graphic mean as the available size range of material and the volume of energy inflicted on the material (Folk 1980:4–5). In a depositional environment, particle size tends to fine outward because heavier particles fall out of suspension first while finer particles are carried further until the force of energy diminishes enough to deposit those particles. As such, the mean statistic provides clues to not only the size of materials present but the energy inflicted on those particles during deposition.

The standard deviation of the population, also known as sorting, is a representation of how uniform the particles are in regard to size. The smaller the standard deviation, the better sorted the particles are, and higher standard deviations can represent higher energy environments. How cohesively the population is sorting can reflect various factors including time, parent material, transportation conditions (i.e., energy), and deposition type (Folk 1980:4; Goldberg and Macphail 2006:336-337). For the purposes of this thesis standard deviation will aid in distinguishing more dynamic colluvial events, such as a bison drive, within the talus cone. Additionally, a greater standard deviation may equal greater variation in energy and environmental conditions. Thus, standard deviation may show differences in high energy depositional conditions (drive event) versus lower energy depositional conditions (processing location).

Magnetic Susceptibility

Magnetic minerals are prevalent in the natural environment and are sensitive to environmental changes (Gale and Hoare 1991:201–202; Goldberg and Macphail 2006:350–352). Magnetic Susceptibility analyses of soils have been utilized for archaeological investigations for several decades and have focused on a wide range of investigations including surveys (e.g., Crowther and Barker 1995; Dalan 1996, 2008; Wiewel and Kvamme 2014) as well as archeological site formation and associated depositional processes (Dalan 2006, 2008). In particular, these analyses have assisted in identifying buried or thermally altered soils associated with cultural activities, as well as identifying the horizontal extent of cultural features (e.g., Dalan and Banerjee 1998; Dalan and Bevan 2002; Frederick 2010).

The magnetism, the size and shape of the grains, internal stress, and other factors can initially influence the susceptibility value (Dearing 1999a, 1999b; Gale and Hoare 1991:204). However, of relevance to this thesis, factors including organic content, pedogenesis, thermal alteration, and cultural activities (e.g., ash-charcoal and refuse) can subsequently alter, usually increase, the susceptibility values. The implications of using magnetic susceptibility (MS) for archaeological research is that when examining either vertical or horizontal areas, the susceptibility values can assist in identifying cultural activity areas that may otherwise be blurred at a macro level.

Horizontally, the application of MS analysis has been used to define the limits of cultural features and activity zones within a site area (e.g., Mauldin and Figueroa 2006; Wiewel and Kvamme 2014). Vertically, the MS results have been applied to recognizing and delineating cultural horizons (e.g., Frederick 2010, 2012; Lawrence and Frederick 2012). In the case of the talus cone at Bonfire Shelter, the MS values should spike or increase in relation to the burned bone beds but may also show less obvious cultural horizons within the mass colluvium that are not as easily seen with the naked eye.

Gypsum

As previously discussed, gypsum-rich sediments have been found within Bonfire Shelter as well as other shelters within Eagle Nest Canyon (Farrell 2020; Frederick 2017; Nielsen 2017; Pagano 2019). Gypsum is presumed to be weathering from the Boquillas Flags Formation, also known as Eagle Ford Shale, via the weathering of iron sulfide minerals within water rich in calcium (Bain 1990; Freeman 1961; Frederick 2017:13; Lock and Wawak 2010; Veni 1994). The weathering of gypsum salts into Eagle Nest Canyon is also believed to be a significant contributor to the formation of the canyon

rockshelters (Frederick 2017:18; Veni 1994). As gypsum is reprecipitated within the karstic environment it forms crystals within cracks and contributing to the erosion of shelter and canyon walls.

Gypsum is presumed to have infiltrated the talus cone sediments either through the evaporation of precipitates or through the introduction of gypsum rich upland materials which have eroded down due to colluvial events. While gypsum content is expected across the talus cone, it is assumed here that an increase or spike in gypsum content will correlate to the bone bed stratum and represent the introduction of exogenic materials.

Inorganic and Organic Carbon Content

Determination of the ratio of organic to inorganic carbon content of sediment is used to address various questions in geoarchaeological research such as, resolving the origin of sediments (i.e., identifying parent materials), recognizing changes in past environmental conditions, and as an indication of human activity (Goldberg and Macphail 2006:344). Eagle Nest Canyon and Bonfire Shelter itself have formed from erosion of the Devils River Formation limestone. This limestone has been found to consist of over 97 percent calcium carbonate ($CaCO_3$) making it nearly entirely inorganic carbon (Fredrick 2017). Because the sediment within Bonfire Shelter is assumed to be largely derived of Devil's River Limestone, it can be suggested that it will be largely inorganic in nature. If deviations are found in the ratio of inorganic verses organic carbon across the strata of the talus cone, it could indicate that different formation processes have contributed to the cone.

Additionally, due to the high ratio of inorganic carbon in the parent material of the canyon, organic carbon within Bonfire Shelter has most likely been introduced mainly via human and animal activities. Anthropogenic introduction includes bringing in food stuff, wood for fires, excrement, and other general human activities that leave refuse. Finally, I should note that studies have shown that magnetic susceptibility values can be influenced by the presence of organic carbon (Gale and Hoare 1991:209). As such, the analysis of the percentage of organic matter (and by extension organic carbon) was also conducted to determine if samples with elevated magnetic susceptibility values could be attributed to organic materials.

V. FIELD AND LABORATORY METHODS

The field and laboratory methods utilized for this thesis were modeled from methods established and used throughout the ASWT project at other sites within the canyon (Koenig and Black 2015). Sampling procedures focused on upholding the projects goal to preserve Bonfire Shelter for future research through a minimal impact approach. As such, column samples were collected in select locations along the north, east, and southern face of the talus cone with the goal of obtaining samples for research while leaving the integrity of the talus cone intact. This chapter presents the methods utilized to document, sample, and analyze those samples.

Field Methods

Profile Sections

The stratigraphy of the profiles throughout the site were annotated by David Kilby, who also oversaw all excavations. Each of the profiles were given a unique Profile Section number (PS). Profile Sections are defined as distinct vertical facies which were chosen for documentation, sampling, and mapping. These PSs were documented within the shelter interior as well as the talus cone and were correlated to previous investigations conducted at Bonfire Shelter.

Each stratigraphic unit within the PSs was given an individual Field Number (FN). The FN log consisted of a master registry to document all field collected samples (i.e., stratum, features, artifacts, faunal remains, special samples, etc.) and it provided a cohesive list of all samples and their provenience. Assigning FNs to each stratum within a PS allowed for a consistent tracking method of samples across the site as well as site wide mapping of distinct depositional units.

Column Samples

Sediment samples from the talus cone were collected over the course of three field seasons from 2017 to 2019. In total, five column samples (CS) were excavated to sample the length and breadth of the talus cone (Figures 5.1). In 2017, two column samples (CS01 and CS02) from PS05 were collected on the north side of the talus cone by Charles Koenig, Amanda Castañeda, Janaka Greene, and Marcos Hamilton. The columns were approximately 50 centimeters (cm) by 50 cm in size and extended for the full length of the exposed profile which ranged from roughly 1.5 to 2 meters in length.

Column samples excavated on the southern and eastern face, PS07 and PS08 respectively, of the talus cone (CS06, CS07, and CS08) were excavated in 2018 by Marcus Hamilton and me. These columns were slightly smaller at about 30 cm by 30 cm in size and extended the full length of the exposed profile which ranged from roughly 1.5 to 2 meters. All five bulk column samples were excavated by stratum with collection including all sediment, faunal remains, gravels, and boulders fully exposed within the excavated column sample units. Special samples (i.e., ^{14}C), artifacts, and potentially diagnostic faunal remains were collected and mapped separately for further analysis.

Each column sample stratum was bagged separately and assigned a unique FN separate from the individual stratum FN. The top and base of each stratum within the column sample was spatially recorded with a total data station (TDS) unit. Additionally, overview chalkboard photos and structure from motion (SfM) photogrammetry of the opening and closing of each excavation was conducted (Figure 5.2 and 5.3). SfM photogrammetry is a process in which multiple overlapping photos are taken and then

stitched together with computer software such as Agisoft to create a 3-D model (Koenig et al. 2017).

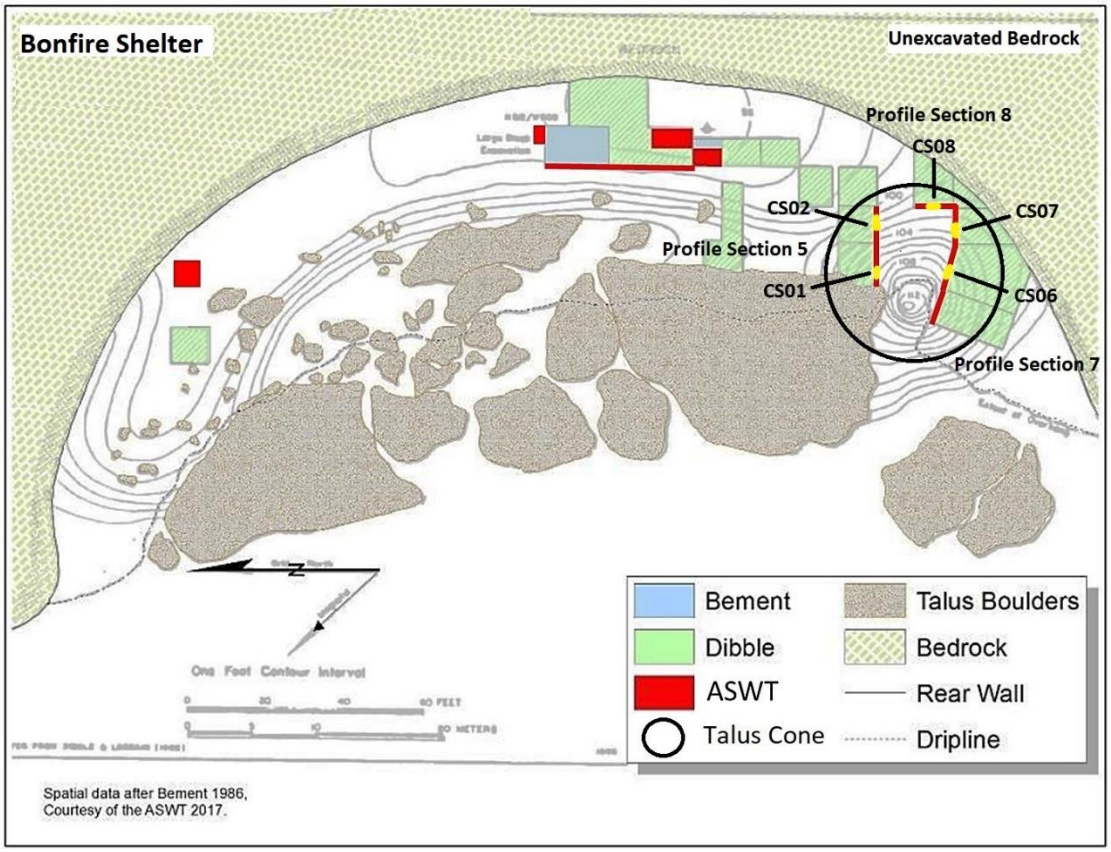

Figure 5.1. Overview of Bonfire Shelter showing the talus cone and five column samples used in analysis.

Particle Size Analysis Columns

During the summer of 2019, an additional five particle size analysis column samples (PSA03 to PSA07) were collected by me with the aid of Ken Lawrence and James Ramsey (Figure 5.1). These PSA columns were roughly 10 cm wide and were collected in 5 cm intervals rather than by stratum. PSA samples were collected in 5 cm increments to further test minute sedimentological changes. Laboratory analysis of these smaller samples may include certain techniques that are sensitive to magnetic contamination. Due to the size of these samples collection was conducted using bamboo, wood, or plastic tools.

Figure 5.2. Closing chalkboard photo of CS07 on the southern face of the talus cone.

The PSAs, when possible, were placed within the preexisting column samples (PSA03, PSA04, and PSA06). When they could not be feasibly excavated within preexisting columns, PSAs were placed immediately adjacent to the original column samples in locations that best represented the stratigraphic sequence (PSA05 and PSA07) (Figures 5.4). Each 5 cm PSA sample was bagged separately, given a unique FN number, and spatially documented with a TDS unit. Chalkboard and SfM photos were taken for each PSA column.

Figure 5.3. Example of SfM for PSA03 on the southern face of the talus cone.

Figure 5.4. Profile Section 8 showing PSA07 (on the left) and CS08 (on the right).

Laboratory Methods

Sample Splitting

Due to the volume of sediment removed during field sampling, the first step of my lab analysis consisted of splitting the bulk column samples into smaller, more usable subsamples. To do this, I used a Gilson Universal Sample Splitter which allowed me to quarter the samples unbiasedly. All bags for each stratum were collected and individually split resulting in a ¼ sample of the entire stratum matrix.

First, the sediment was passed through a 1-inch screen to separate the fraction too coarse to be unbiasedly split by the sample splitter (very coarse pebbles, cobbles, boulders, and faunal remains). All faunal materials were separated by evidence of burning or lack of burning with each subcategory being counted and weighed. The pebbles, cobbles, and boulders were separated by size using the classification specified in Table 5.1, based on the Wentworth classification (1922). Boulders too large for collection were notated on the profile forms in the field. Then each of these size categories were visually sorted by sphericity and roundness into well-rounded, rounded, sub-rounded, sub-angular, angular, and very angular groupings (Krumbein and Sloss 1963; McLane 1995). The gravel samples were then counted, weighed, and recorded per these morphological subcategories (Figure 5.5).

The remaining sediment sample, including gravels and bone less than 1-inch, was then poured into the sample splitter (Figure 5.6). The sample splitter divides each sample into two equal parts. As such, each bucket of sediment was split twice to obtain a ¼ sample. The subsample used for this thesis was always taken from the right side of the sample splitter to remove any unintentional bias.

Each ¼ sample was weighed and re-bagged separately from the bulk ¾ sample. The remaining bulk sample was kept for future research and is currently stored on Texas State Campus. The ¼ samples were moved to the on-campus Center for Archaeological Studies (CAS) lab for further analysis.

Table 5.1. Size sorting of larger than 1-inch (2.54 cm) gravels.

Size Range (cm)	**Wentworth Classification***	**Designation**
0 to 6.4	Pebble	P
6.5 to 10	Cobble	C_1
10 to 15	Cobble	C_2
15 to 25.6	Cobble	C_3
25.7 and above	Boulder	B

* Wentworth 1922

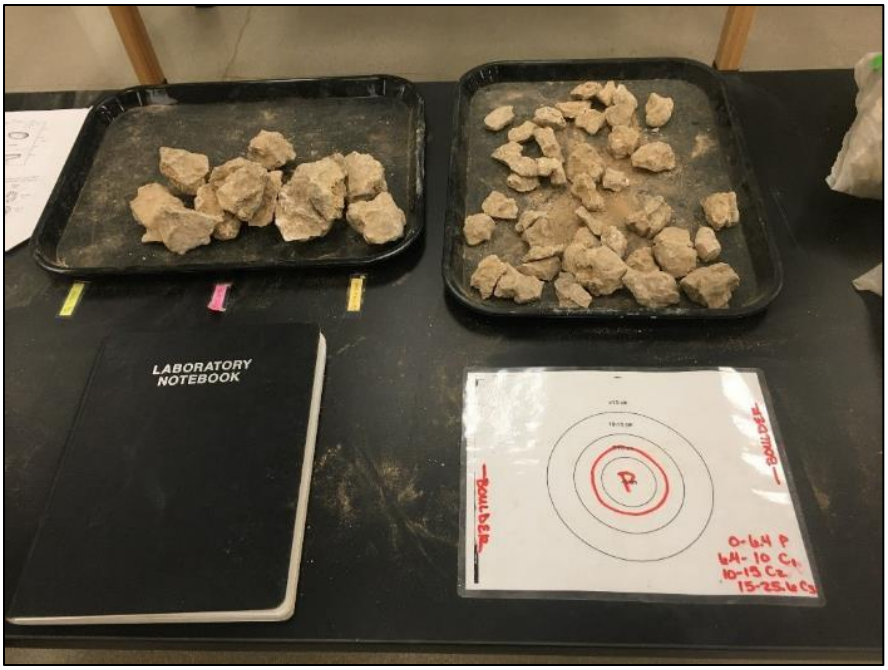

Figure 5.5. Laboratory setup for rock sorting by size and sphericity.

Figure 5.6. Sample splitting setup with splitter on right side of photo.

Coarse Grain Particle Size

Once the ¼ subsamples were moved to the on-campus CAS laboratory, coarse grain particle size analysis was conducted using nested sieves and an electric sieve shaker (Folk 1980; Gale and Hoare 1991). Subsamples were split into roughly 1-to-2-liter units and were sieved through a series of nested geologic screens ranging from -5φ to -1φ (32mm to 2mm) with all sediment <2mm being collected in the bottom pan. The screens were attached to a Ro-Tap sieve shaker and agitated for a total of four minutes with the screens being turned every two minutes to prevent clumping of the sediment on the sides of the screens. Due to the fragile nature of the limestone within the shelter, longer agitation could not be conducted without risk of breakage to the gravels (Farrell 2020:141).

For subsamples with bone fragments included within the sediment, bone fragments larger than 2mm were picked out and weighed separately by size class to the

nearest 1/100th gram. The remaining gravels and sediment from each size class were separated, weighed (nearest 1/100th gram), and recorded to be included in later fine particle size analysis.

The entire <2mm sample for each stratum was weighed and bagged separately. Pebbles, bone, and sediment <2mm could not be separated due to size and were left commingled. From this fine fraction sample, a series of laboratory samples were split out for further analysis including fine grain particle size analysis. In general, enough sediment was collected to run two attempts of each analysis. The laboratory samples are summarized in Table 5.2.

Table 5.2. Summary of laboratory samples.

Proposed Analysis	**Mass (g) of Laboratory Sample**
Hydrometer: Fine Grain Particle Size	120 g
Magnetic Susceptibility	25 g
Gypsum Content	20 g
Carbon Content	50 g
Total Organic Content (Keck)	50 g

Hydrometer and Sieve: Fine Grain Particle Size Analysis

Sediments from the talus cone consist of a wide range of sizes from boulders to fine silts and clays. As the finest sediments (e.g., silts and clays) cannot accurately be measured through sieve techniques, a 50g sample of the <2mm sediment was analyzed using a PARIO METER Environment soil particle analyzer. This analyzer includes a digital meter which takes measurements of pressure variation to determine the rate at which silt particles settle from suspension (Durner, Iden, and von Unold 2017).

The theory behind this method was established by Durner, Iden, and von Unold (2017) and uses Stokes' law; in which, spherical particles will settle in suspension as a known velocity that is determined by various factors (i.e., viscosity, diameter of the

particles, and density differences between the particles and water). By using this meter, I could determine the amount of silt within the sample and then compare that fraction to the totals of the coarser fractions of sand, pebbles, cobbles, and boulders to create a complete particle distribution curve for each stratigraphic level of the talus cone.

All 47 laboratory samples from the bulk column samples were run using this method at the CAS laboratory at Texas State University. Before analysis could be conducted, each sample had to be soaked in 1-liter of distilled water for 24-hours (Figure 5.7) (Farrell 2020). This process was repeated four times to ensure the removal of all the dissolvable gypsum in each sample to prevent flocculation caused by the mineral's presence. Additional pre-treatment included the use of a deflocculant ($(NaPO_3)_6$) to break apart the fine silty sediments. After the deflocculant was added, the samples were agitated for 5 minutes using a dispersion mixer. The samples were then placed in graduated cylinders which were filled with 1000mL of distilled water.

Figure 5.7. Fine grain particle size analysis samples soaking in distilled water to dissolve gypsum.

The samples were once again agitated for 1-minute to ensure all sediment particles were in suspension and then the PARIO meter was placed in the cylinder. I was able to run five PARIO samples at a time (Figure 5.8). The meters plugged into the USB ports of a laptop which ran the computer software necessary for data collection. All samples were run for 8 hours, as recommended by Durner, Iden, and von Unold (2017).

While the samples were running in the PARIO, the sand fraction was sieved using traditional nested screen methods as discussed in the coarse grain particle size section above (Folk 1980; Gale and Hoare 1991). While wet screening of the direct PARIO samples was recommended by Durner, Iden, and von Unold (2017), I dry sieved a separate 50g sample due to time and laboratory limitations. The percent of sand was then incorporated into the PARIO results to calculate final silt and clay ratios.

Figure 5.8. Fine grain particle size analysis being conducted with the PARIO meters.

Magnetic Susceptibility

Magnetic Susceptibility (MS) has been used in identifying buried or thermally altered soils associated with cultural activities, as well as identifying the horizontal extent of cultural features (e.g., Dalan and Banerjee 1998; Dalan and Bevan 2002; Frederick 2010; Jones and Leffler 2003). This is because several factors including organic content, pedogenesis, thermal alteration, and cultural activities (e.g., ash-charcoal and refuse) can cause an increase in the susceptibility values. As such, MS was run for each sample to try and determine if any of these conditions were being met with thermal alteration and cultural activity being of most interest.

The measurement of magnetic susceptibility χ (Chi) is a quantification of the 'magnetisability' of the material (Dalan 2008; Dalan and Banerjee 1998; Dearing 1999b:5; Gale and Hoare 1991:202–204). For the purpose of this thesis, MS samples were collected from each of the bulk stratum samples represented in the five column samples. These samples will represent the vertical distribution of susceptibility across time. Additional samples were collected horizontally along the three profiles of the talus in select stratum (e.g., Stratum 12) to test the horizontal distribution of susceptibility across space. I expected this to be particularly valuable when comparing samples across the cone and at different point of the talus slope.

The select samples were placed in 8-cc inert plastic cubes and were analyzed using a Bartington MS2 meter and MS2B dual frequency sensor to examine both low (χlf) and high (χhf) frequency (470–4700 Hz, respectively) magnetic susceptibility. The cube samples were measured at the high sensitivity setting (i.e., 0.1) compared to the normal sensitivity setting (i.e., 1.0). The high sensitivity setting was necessary since the

frequency dependency of the magnetic susceptibility samples were also calculated (Gale and Hoare 1991:223–224). The values for each cube sample were catalogued twice at both the low and high frequencies to provide an average value using the *Système International* (SI) scale. Each of the χlf, χhf, and the average values were recorded as well as each sample's weight in an Excel table. After every five readings, the Bartington MS2 meter was "zeroed" out to recalibrate the meter and avoid issues associated with drift in the readings.

The cube samples from this analysis were subsequently calculated using the methods outlined by Gale and Hoare (1991:223–226). Briefly, the primary metric for recognizing magnetic susceptibility values of interest is the coefficient of frequency dependency (χfd). This calculation is indicated as:

$$\chi fd = 100\ [(\chi lf - \chi hf)/\ \chi lf]$$

This calculation uses χlf as the 'normal' sensitivity value and contrasts it with the χhf value to reveal significant values of difference in percentages (Dearing 1999a:47, 1999b:17–18; Gale and Hoare 1991:226). Elevated values of χfd can represent concentrations of ultrafine magnetic grains (e.g., maghemite), which are commonly associated with pedogenesis (Dalan 2006:164; 2008:22). A number of factors may cause an increase in χlf values including biological (e.g., bacteria) or inorganic (e.g., natural weathering of iron minerals) processes.

Gypsum Content

Previous researchers in the canyon have realized that the sediment contains very high levels of gypsum (Farrell 2020; Frederick 2017; Nielsen 2017; Pagano 2019). These high levels can influence the results of various analyses and in particular, hydrometer

particle size analysis. Errors occur due to gypsum's high solubility which can impact characteristics such as structure, consistency, and permeability of sediment (Omran 2016:1). As such, gypsum content for each sample was determined to assure proper preparation were made for each analysis.

This was done using the differential water loss method as outlined by Omran (2016). In their methods, a sample of 10 to 20g is weighed and then placed in a crucible and heated in an oven at 70ºC for 45 minutes, at which time the non-gypsum rich water will have been removed and a stable mass is achieved. Once cooled, the sample is weighed. The sample is then returned to the oven to be heated at a temperature of 150ºC for another 45 minutes; then cooled and weighed.

This second heating removes the remaining gypsum and allows for the total gypsum content of the sample to be calculated using the below equation (Omran 2016:4):

$$\boldsymbol{Gypsum}\ \% = \frac{\boldsymbol{W_{70} - W_{150}}}{\boldsymbol{W_{70} - W_d}} \times \mathbf{100} \times \left(\frac{\mathbf{100}}{\mathbf{19.66}}\right) = \frac{\boldsymbol{W_{70} - W_{150}}}{\boldsymbol{W_{70} - W_d}} \times \mathbf{508.65}$$

where $\mathbf{W_{70}}$ = mass of sample + vessel (g) at 70ºC; $\mathbf{W_{150}}$ = mass of sample + vessel (g) at 150ºC; $\mathbf{W_d}$ = vessel mass (g); **19.66** = gypsum recovery factor between 70º C and 150ºC. Gypsum content determination was completed at the SWCA Austin laboratory using a Neycraft Pro6 (model #6-106A) muffle furnace.

Loss-on-Ignition: Inorganic and Organic Carbon Content

There are several methods used to test for inorganic and organic carbon in soils and sediments, but one of the most commonly used analysis is Loss-on-ignition (LOI) (Schulte and Hopkins 1996; Schumacher 2002; Stein 1984; Storer 2005). For the current study the LOI approach was used, which exposes the sample for an extended time at a high temperature to burn off the organic matter and then returns the same sample for

another round of firing to determine inorganic carbon content (Schulte and Hopkins 1996; Schumacher 2002). At its simplest, the LOI is the difference in sample mass quantified by percentage before and after each heating of the sample.

The methods used for the carbon matter analysis at Bonfire Shelter were adapted from Henri et al. (2001) and Soil Survey Staff (2014:314–315). This analysis used a Neycraft Pro 6 (Model 6-160A) programmable muffle furnace (±5˚C accuracy) and an Adam PGW scale (model 153e) with 0.001 g accuracy. Due to the hydroscopic nature of gypsum, the samples used for gypsum content were reused for carbon content. My hope was that by using the samples in which gypsum had already been removed through a differential water loss method the error found by previous researchers would be minimized (Ferrell 2020).

As such, the 10–20g samples used for gypsum content were reweighed (accounting for the crucible). The samples were then placed in the muffle furnace for 2 hours at 500°C, allowed to cool, and weighed. This measurement was used to determine the organic carbon content through the difference of mass from before and after heating. The samples were returned to the furnace for 1 hour at 1000°C, cooled, and weighed again. This measurement was used to determine carbonate content through the combustion of calcium carbonate to carbon dioxide.

$$\boldsymbol{Organic\ Matter}\ \%\ (\boldsymbol{LOI_{500}}) = \frac{\boldsymbol{DW_{105}} - \boldsymbol{DW_{500}}}{\boldsymbol{DW_{105}}} \times \mathbf{100}$$

where $\mathbf{DW_{150}}$ = pre-firing dry weight + vessel (g); $\mathbf{DW_{500}}$ = mass of sample + vessel (g) at 500ºC; $\mathbf{DW_{100}}$ = mass of sample + vessel (g) at 1000ºC; $\mathbf{LOI_{500}}$ = percent of organic matter converted to ash or evolved as CO_2.

$$\boldsymbol{Carbonate\ \%\ (LOI_{1000}) = \frac{DW_{500} - DW_{1000}}{DW_{105}} \times 100}$$

where $\mathbf{DW_{150}}$ = pre-firing dry weight + vessel (g); $\mathbf{DW_{500}}$ = mass of sample + vessel (g) at 500ºC; $\mathbf{DW_{100}}$ = mass of sample + vessel (g) at 1000ºC; $\mathbf{LOI_{1000}}$ **=** percent of CO_2 from calcium carbonate.

As mentioned, the simplicity of LOI does come at a cost and there are a number of factors that can influence or skew the resulting calculations of LOI. These include errors due to the presence of hydrated minerals (i.e., gypsum) or combustible materials that can inflate the mass lost, or simple human or machine error causing inconstancies in firing time or temperature (Herni et al 2001.; Schulte and Hopkins 1996; Rosenmeier 2005). As such, additional methods were used to verify the LOI results.

Chittick: Inorganic Carbon

Once the carbonate content was calculated through LOI methods, unrealistically low values were determined (personal communication Charles Frederick; Appendix A). To resolve the inconsistencies, I also analyzed carbonate content using a Chittick volumetric calcimeter. This method has been found to be more precise and uses highly concentrated acid to digest the sample through a Chittick apparatus. The methods summarized below were adapted from Machette (1986) and analysis was conducted under the supervision of Dr. Charles Frederick.

An 0.85 g sample of finely ground <2.0 mm (0.08 in) sediment was added to an Erlenmeyer flask. With the upper valve open, the reservoir on the Chittick was filled to the -10 mL position and the system closed to create a vacuum loop. Then 10 mL of hydrochloric acid (HCL) was added to the sample and it was agitated for approximately two minutes until the reaction was complete, and no bubbles remained. The room

temperature and local atmospheric pressure were recorded at this time via a Garmin GPS and digital thermometer. Acid was introduced to the sample via a pipette, the bulb was leveled with the reservoir, and volume was recorded in millimeters.

Percentage of calcium carbonate equivalent was calculated using the formula:

$$\boldsymbol{CCE}\ \% = \frac{\mathbf{1.7}}{\boldsymbol{sample\ mass_{(g)}}} \times \left(\boldsymbol{volume\ CO_{2\,(ml)}}\right)[\mathbf{0.0706} + (\mathbf{0.00143} \cdot \mathbf{pressure(mb)}) - (\mathbf{0.00527} \cdot \mathbf{temperature}\ (\mathbf{C_o}))] \cdot \mathbf{0.227}$$

Keck Laboratory: Organic Carbon

Previous researchers in the canyon experienced issues with the determination of organic carbon content through LOI so samples were also sent to the Keck Laboratory (Ferrell 2020; Pagano 2019). Roughly a gram of <2.0 mm (0.08 in) fraction sediment samples were sent to the University of Kansas Keck-NSF Paleoenvironmental and Environmental Stable Isotope Laboratory (KPESIL). The sample was pretreated to remove inorganic carbon and other acid-soluable minerals, burned at temperatures of excess of 1,800°C, and the resulting masses of N_2, CO_2, H_2O, and SO_2 were measured using a Thermal Conductivity Detector and used to calculate the percentage of nitrogen and carbon. In addition to the accurate determination of organic carbon in each stratum, a Stable Isotope Ratio Mass Spectrometer and coupled elemental analyzer measured the carbon and nitrogen isotopic fractionation of that organic material (Appendix A).

Result Digitization

Once laboratory analysis was completed for all samples within the five columns, I created a master results graphic for each column. These graphics included a detailed stratigraphic profile, charts of all six analyses (excluding the unsuccessful LOI attempts for inorganic and organic carbonate), and highlighted sections for each bone bed

represented. These graphics were created by hand using charts made in Microsoft Excel which were then imported in a free and open-source graphic software, Inkscape.

VI. GEOARCHAEOLOGY RESULTS

This chapter presents the geoarchaeological laboratory results for all five column samples from the talus cone. The results of the analyses are presented by column sample with the results from Bone Bed 2 and Bone Bed 3 separated into individual sections. Generally, the results are presented with only a brief interpretation as focus is given to laying out the data for the discussion and interpretations found in Chapter 7.

Column 1

Column sample 1 was excavated on the north side of the talus cone notated as Profile Section 5 (PS05). It is located on the western end of the talus which encompasses the highest and thickest point of the cone and lies against the massive canyon collapse boulders (Figure 6.1). It is also important to note that this face of the talus cone is closest to the center and apex of the cone. As a result, the strata not only slope steeply to the east, down the existing talus slope, but north as well. As this column was the first excavated as part of the ASWT efforts, strata recorded across the cone are correlated to this column. Within this portion of the talus cone, Bone Bed 2 was only initially noted within strata 11 and 12 (Table 6.1; Figure 6.2). Further investigations, particularly on the south side of the talus cone, identified that Bone Bed 2 also occurred within strata 13 and 14. All four strata were considered part of Bone Bed 2 for this discussion.

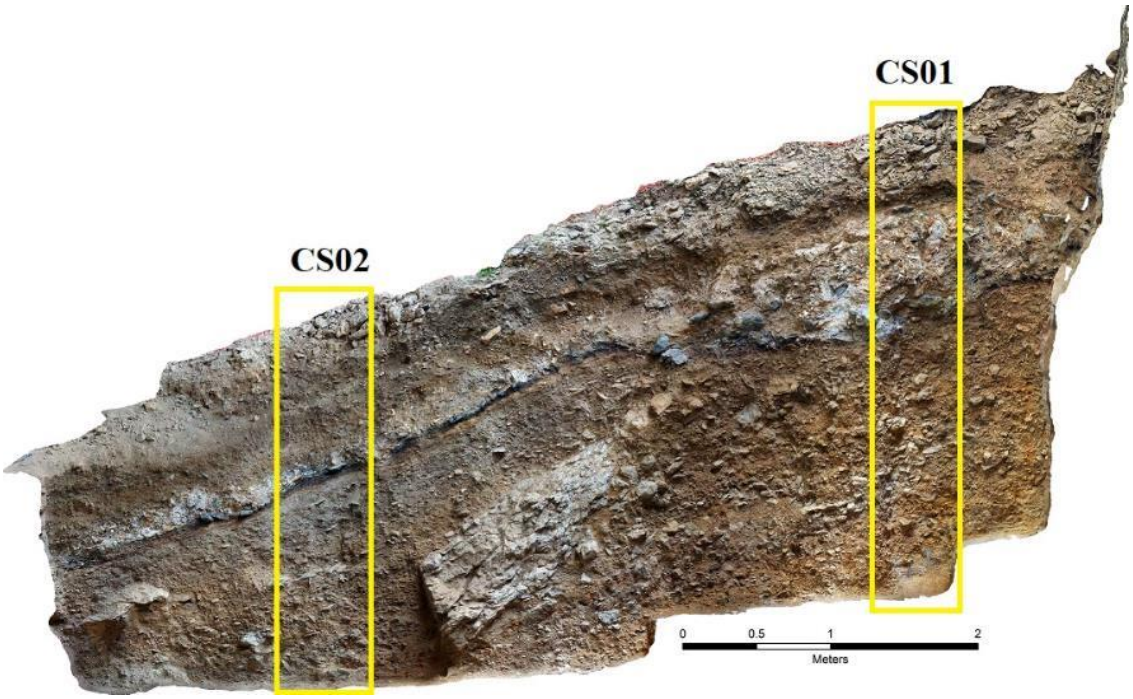

Figure 6.1. Location of CS01 and CS02 within PS05, northern profile of talus cone.

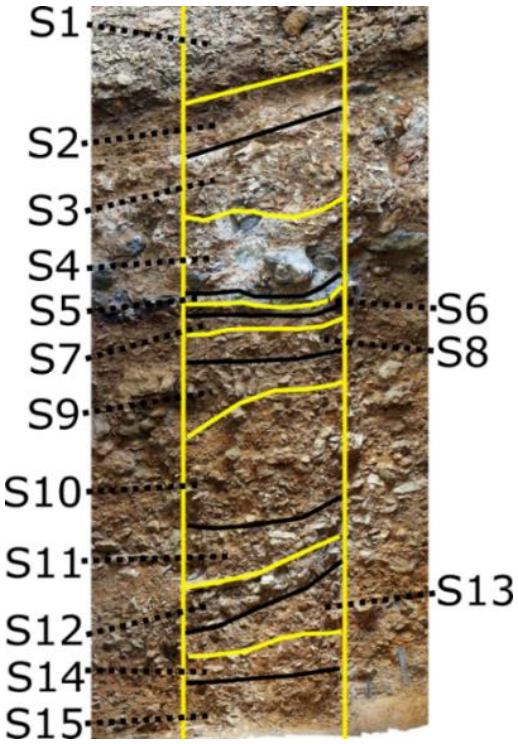

Figure 6.2. CS01 with strata designation.

Table 6.1. Summary of strata within CS01.

ASWT Designation	Dibble Designation	Notes*
S1	Slump	Talus cone slump. Combined debris from notch, stabilization material, and disturbed surface material.
S2	Zone 3	Poorly sorted limestone spalls in sandy silt matrix.
S3	BB3	Massive accumulation of bone (most reduced to calcined powder by burning), small rocks, and silt. Upper BB3 and hypothesized as the end of a fall event.
S4	BB3	Mass of bison bone, boulders, small rocks, and white silty powder (dry: 10YR7/2). Roughly half bone and half burned rocks. Lower BB3 and hypothesized as the start of fall event. Mandible with teeth (FN60171).
S5	BB3	Thin but very dense layer of heavily burned matrix. Layer contains blueish black burned bone and small rocks in a fibrous ash layer.
S6	Zone 2b	Thin zone of scorched, blackened, and oxidized sediment directly underlying BB3. Hypothesized as surface on which the fall event occurred.
S7	Zone 2b	Thin layer of reduced sandy loam with small angular rocks.
S8	Zone 2b	Massive poorly sorted colluvium from the roof, notch, and canyon rim.
S9	Zone 2b	Massive poorly sorted colluvium including a large boulder near the center of the profile.
S10	Zone 2b	Colluvium with angular to subangular gravels and cobbles in coarse sand.
S11	BB2	Massive poorly sorted colluvium with angular to subangular gravels and cobbles in a sandy loam. Bones throughout but concentrated in lower half. Upper BB2. Biface tip (FN60126), rib and long bone (FN60127-60128), and cluster of articulated limb bones (FN60238).
S12	BB2	Massive poorly sorted colluvium with angular to rounded gravels and cobbles in a silty matrix. Bones throughout but concentrated in upper half. Includes ashy as well as burned bone and rocks. Lower BB2.
S13	BB2/Zone 2b	Massive colluvium underlying BB2. Sandy loam matrix with common cobbles and gravels.
S14	BB2/Zone 2b	Reddish zone with subangular gravels and cobbles in sandy loam matrix.
S15	Zone 2b	Dense fine gravels, clast supported with little sandy loam matrix. Similar texture and structure to Stratum 13 with finer sized gravels.

*Derived from profile, column, and personal notes of Dr. Kilby, Dr. Hamilton, and Ashley Eyeington.

Bone Bed 3 Results

Within CS01, Bone Bed 3 appears to represent a single bison drive event. Stratigraphically the zones encompassing Bone Bed 3 are a very poorly sorted (2.0-3.0φ) mix of bone and gravel with little sediment (Figure 6.3; Table 6.2). Sorting of this magnitude suggests a high energy and possible rapid method of deposition (Folk 1980). Additionally, the bones do not appear to parallel or adhere to stratigraphic boundaries. While there is a clear and occasionally abrupt boundary at the base of Bone Bed 3, particularly as you move downslope, I believe this is largely due to the matted Stratum 5 and oxidized burned zone of Stratum 6. The burning that has modified or even created these two strata would have occurred post-depositionally and developed below the bones and gravel at the base of Bone Bed 3.

The fining upwards sequence of particle size and dramatic spike in values of MS, organic carbon content, and gypsum content all fit into the jump drive hypothesis (Figure 6.3; Table 6.2). Though the coarse grain and fine grain analyses could not be combined, they both show a distinct fining upwards trend that begins in Stratum 4 and extends through the top of BB3. This is also seen with the mean particle size which is coarser in Stratum 4 and fines into Stratum 3 (Appendix A). Both the MS and organic content analyses show an increase in values in Stratum 5 (Appendix A). The χlf value in Stratum 5 increases six-fold from the value in Stratum 6 (372.9χlf and 60χlf, respectively). While I was surprised to see such a low value in the heavily oxidized Stratum 6, this does seem to indicate that the bone bed layers have a higher MS. The extremely high values in Strata 4 and 5 (240.2χlf and 372.9χlf) is likely due to intense burning within these layers.

The only analysis that doesn't clearly fit into my hypothesis that Bone Bed 3 is a bison drive event is the CCE. I had expected a decrease rather than the small increase seen in Stratum 4. Overall, the percentage of calcium carbonate remains relatively stable throughout the column, but it does increase from 31 percent in Stratum 5 to 45 percent in Stratum 4 (Appendix A). In sum, Bone Bed 3 within this column clearly points to having originated as a mass colluvial bison drive event (Table 6.2).

Regarding the question of how many depositional events are represented in Bone Bed 3, all analyses point to a single event. While BB3 has been described as two strata, it appears visually as one mass depositional unit. Stratum 4 is the main drive event and includes more gravel and gravels of larger sizes. Stratum 3 includes fewer gravels, smaller gravels, and more sediment, which represents the fining upwards sequence hypothesized to represent a drive event. There is only one fining upward sequence of both gravels and sediment, and all remaining analyses show one single spike or increase indicating only one depositional event occurred (Figure 6.3).

Throughout this experiment, Bone Bed 3 is used as a model for what a single event bison drive would look like. This of course comes with a number of caveats including the fact that Bone Bed 3 is intensively burned throughout and that it is much younger in age. Bone Bed 2 has undergone an additional 10,000 years of post-depositional processes. Despite these factors, it is my hope that by applying the same hypothetical conditions outlined in Chapter 4 for what constitutes a single verses multiple event bison drive to both bone beds – Bone Bed 3 will be shown to provide an accurate prototype of a single bison drive event.

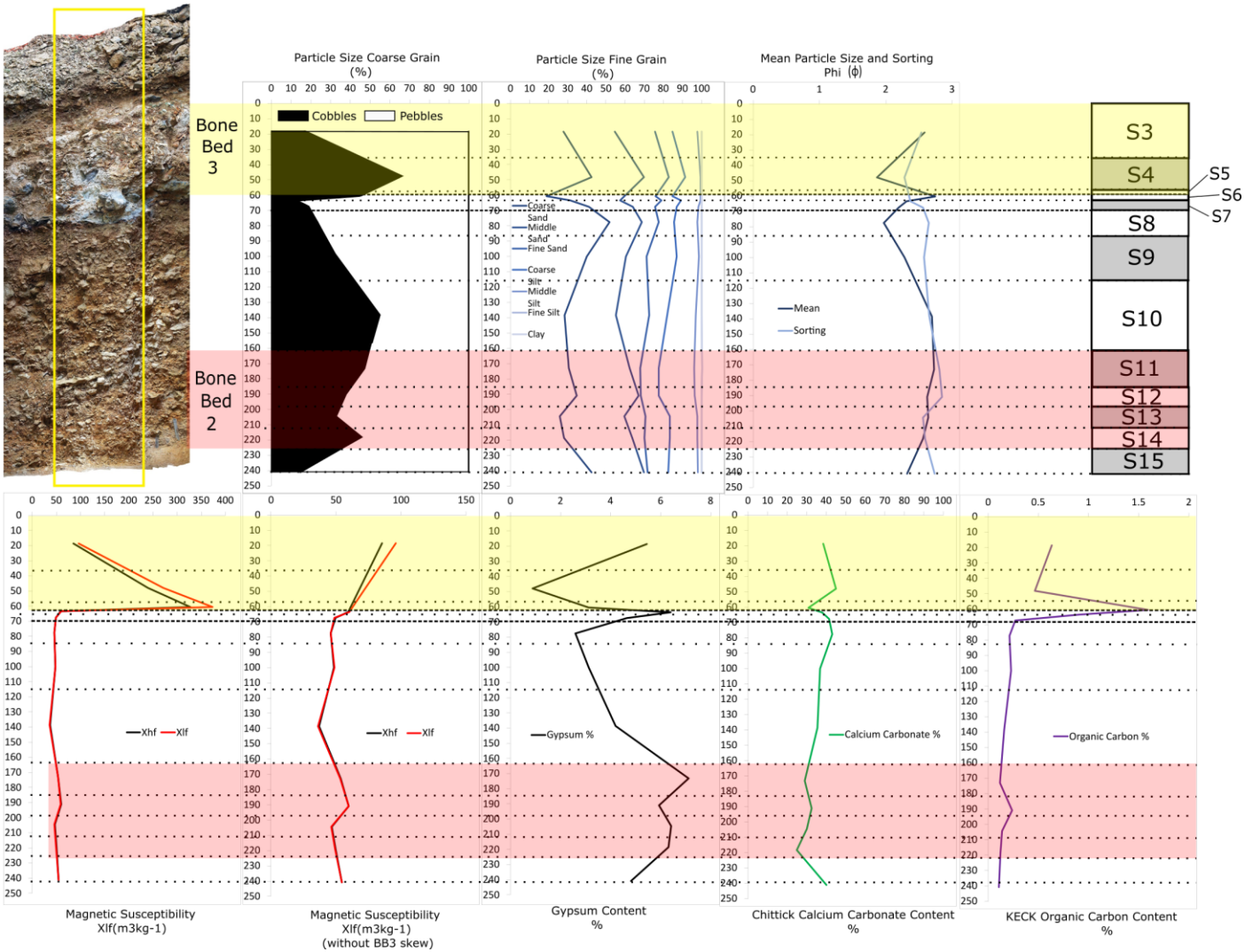

Figure 6.3. Laboratory results for CS01.

Table 6.2. Origin of Bone Bed 3 in CS01.

Analysis	Jump Drive*	Secondary Processing*	Column Sample 1
Stratigraphic	Bones intermixed with sediment and gravel in bone beds.	Minimum mixing with sediment and gravel.	Very poorly (2.0-3.0φ) sorted mix of bone, gravels, and little sediment.
	Not restricted to stratigraphic boundaries and not restricted to boundary orientation.	Discreet layer of bone that doesn't cross stratigraphic boundaries and bones that lie parallel to stratigraphic boundaries.	The bones and gravels do not adhere to or parallel stratigraphic boundaries.
Particle Size	Fining upward sequence.	Predominately bone with little matrix and no fining upward sequence.	There is a very distinct fining upward sequence of both the coarse and fine grain particle size distribution in BB3 beginning in stratum 4 and fining through stratum 3.
Magnetic Susceptibility	Dramatic spike in values occurring in association with each individual event.	A smaller, less dramatic spike; only one spike in association with BB2.	Very dramatic spike in stratum 5 (372 χlf), which consists of a thin layer of burned matrix on which BB3 sits.
Organic Content	Dramatic spike in values occurring in association with each individual event.	A smaller, less dramatic spike; only one spike in association with BB2.	There is a spike (1.59%) in stratum 5, which consists of a thin layer of burned matrix on which BB3 sits.
Carbonate Content	Decrease in bone beds due to exogenic deposition from drive event.	No difference across bone beds or natural strata due to continuous endogenic deposition.	There is a spike in carbonate content within stratum 4 (45%) and a sharp decrease below it in stratum 5 (31%).
Gypsum Content	Increase in bone beds due to upland sources during drive event.	Consistent across natural and bone bed strata.	There is a dramatic spike in stratum 6 (6.39%).

*Analysis results contradicting expectations are grayed out.

Bone Bed 2 Results

The results for Bone Bed 2 are a little more complicated than those presented for Bone Bed 3 but seem most likely to represent a bison drive with one or two events. Stratigraphically the zones encompassing Bone Bed 2 are also a very poorly sorted (2.0-3.0φ) mix of bone, gravel, and sediment (Figure 6.3; Table 6.3). Additionally, the bones do not appear to parallel or adhere to stratigraphic boundaries. While the two bone beds do not look identical, they do share similarities in their structure. Both are a mass of jumbled and mixed colluvial materials which largely encompass large clast sediment and gravel. The bones are comingled with gravel and the lower boundaries of the stratigraphic layers are irregular to wavy and generally clear.

There is a fining upwards sequence in both the gravel clasts as well as the sediment, but they do not occur within the same stratum (Table 6.3; Appendix A). Gravel particle size distribution shows a spike in Stratum 14, a decrease in Stratum 13, and then a gradual increase into Stratum 10. The sediment particle size distribution decreases in size through Strata 13 and 14 before a spike in coarse and medium sand is seen in Stratum 12 (Appendix A).

Could this be two drive events of different magnitude? Or perhaps the two drive events were close in time, which impacted the stability of the shelter walls, ceiling, and/or the notch? The upwards sequences of coarser clast gravels in Strata 12 and 11 could be the result of the notch and shelter ceiling becoming unstable after the first drive event in Stratum 14. In fact, this increase in cobbles continues into Stratum 10 and may be associated with the very large boulder overlaying Bone Bed 2 near the center of the cone (Figure 6.1). There could also be an issue with the cobble samples from Bone Bed

2, as the collection of rocks from the profiles was attempted to be done systematically, but the nature of large cobbles makes it inherently difficult to unbiasedly collect and record them.

The MS, organic, and inorganic carbonate analyses remain stable with only a small spike occurring in Stratum 12 within Bone Bed 2 (Table 6.3; Appendix A). These values are low, but they do align with the increase of coarse and middle size sand seen in the sediment particle size analysis. Perhaps my hypothesis of a lower spike in MS and organic carbon indicating a processing event rather than a bison drive event was too simplified. If we were looking at bone beds of a similar age and composition, this comparison may have held true; but due to time and post depositional factors, a low value spike may still be representative of a drive event.

Within Bone Bed 2 there are two small spikes of gypsum content. This is interesting because within CS01, the percentage of gypsum is the only analysis to suggest multiple spikes (Table 6.3; Appendix A). The lowest spike occurs in strata 13 and 14 which corresponds with the increase in cobble size material. This suggests that the increase in gypsum content could be related to the introduction of outside material during a fall event. The second spike occurs in Stratum 11. This could correlate to either the increase in coarse grain sediments in Stratum 12 or the steady increase of gravels.

Overall, the results for Bone Bed 2 do not clearly indicate whether one or multiple depositional events are represented but seem to indicate that it was deposited as a drive event. Stratigraphic, particle size, and gypsum analyses all suggest multiple events may have occurred, but the remaining analyses do not show multiple increases in values. The

northern profile doesn’t present the most distinct or intact portion of Bone Bed 2 and as such, the remaining columns will be key to final interpretations of Bone Bed 2.

Table 6.3. Origin of Bone Bed 2 in CS01.

Analysis	Jump Drive*	Secondary Processing*	Column Sample 1
Stratigraphic	Bones intermixed with sediment and gravel in bone beds.	Minimum mixing with sediment and gravel.	Very poorly sorted (2.0-3.0φ) mix of bone, gravels, and sediment.
	Not restricted to stratigraphic boundaries and not restricted to boundary orientation.	Discreet layer of bone that doesn't cross stratigraphic boundaries and bones that lie parallel to stratigraphic boundaries.	The bones do not consistently parallel the stratigraphic boundaries. Additionally, there is no distinct or very abrupt lower boundary to the strata within BB2.
Particle Size	Fining upward sequence.	Predominately bone with little matrix and no fining upward sequence.	There is a distinct increase of cobble clast material in stratum 14 followed by a decrease in gravel in stratum 13, and finally, a steady increase of cobble size materials across strata 12 and 11. An increase in coarse and medium sand is also seen in stratum 12.
Magnetic Susceptibility	Dramatic spike in values occurring in association with each individual event.	A smaller, less dramatic spike; only one spike in association with BB2.	A small spike in MS is seen in stratum 12 (59 χlf), but overall, it trends smoothly until BB3.
Organic Content	Dramatic spike in values occurring in association with each individual event.	A smaller, less dramatic spike; only one spike in association with BB2.	A small spike is seen in stratum 12 (.24%), but overall, it trends smoothly until BB3.
Carbonate Content	Decrease in bone beds due to exogenic deposition from drive event.	No difference across bone beds or natural strata due to continuous endogenic deposition.	BB2 sees a small increase in secondary carbonate content within strata 12 and 13 (32.5% and 30% respectively).
Gypsum Content	Increase in bone beds due to upland sources during drive event.	Consistent across natural and bone bed strata.	There are two small spikes in the gypsum content within strata 13/14 (6.4% and 6.3 %) and stratum 11 (7.15%).

* Analysis results contradicting expectations are grayed out.

Column 2

Column sample 2 was excavated on the north side of the talus cone. It is located on the eastern end of the talus which encompasses the lower and thinner point of the cone as it fans out to the back wall of the shelter (Figure 6.1). The strata recorded within CS02 are correlated to the western column, CS01 (Figure 6.4; Table 6.4). Bone Bed 3 is represented as strata 3 and 4 and underlain by the intensely burned Stratum 6a and reduced strata 6b and 7. Within this portion of the talus cone, Bone Bed 2 is only exposed at the very deepest portion of the column within strata 11a and 11b (Figure 6.4; Table 6.4).

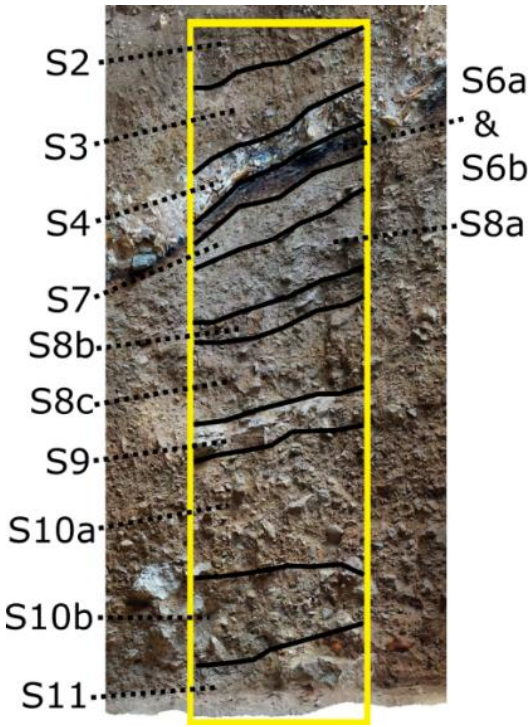

Figure 6.4. CS02 with strata designation.

Stratum 11a is recognized as the same Stratum 11 noted in CS01. Stratum 11b is similar but contains decomposing bone and large rocks with reddish to purple coloration. Lenses of alternating reddish and gray silt were noted within the stratum which were particularly noticeable as pockets between larger colluvium clasts of gravels and cobbles.

This stratum may correlate to strata 12 or 12b as described in the southern profile, PS07. In 2019, the profile wall was extended into the floor of the talus cone to expose strata 13 and 14. Samples taken below S11b include only fine samples, which were not included within this thesis, but may provide further information in the future.

Bone Bed 3 Results

Bone Bed 3 within CS02 looks very different than CS01, but also represents a single bison drive event. This is largely to do with CS02's position at the toe slope of the talus cone as well as the fact that it largely accumulated via erosion down the talus slope (Figure 6.4). Strata 3 and 4 are much thinner and compressed in this portion of the cone. The bones and gravels within Bone Bed 3 do not consistently parallel the lower boundaries of each layer but, they do so much more than CS01. Additionally, the lower boundaries of each stratum are also more abrupt and easily defined than further west in the cone (Table 6.5).

Particle size analysis of CS02 indicates a clear increase in cobbles within Stratum 4, a decrease in Stratum 3, and finally, a steady increase into Stratum 2, a non-bone bed layer (Figure 6.5; Table 6.5; Appendix A). The sediment PSA also shows an increase in mean particle size within Stratum 4 and a rise in the percent of middle sand in Stratum 3. Overall, PSA indicates a single fining upwards sequence in support of a one-time drive event.

The particle size distribution is more difficult to discern due to the position of CS02 within the talus cone. This column is located at the tail slope of the cone and so materials are largely accumulated through erosion from the top of the cone. This means that we are observing a distribution formed from a different depositional process. We still

see the fining upwards sequence because the coarser material from Stratum 4, the main fall event, was still deposited first, and then overlain by the finer particles associated with Stratum 3. It is just not as dramatic as the sequence seen in CS01.

The remaining analyses suggest Bone Bed 3 is a single bison drive event with increases in MS, organic carbon, and gypsum and a decrease in calcium carbonate equivalent (Table 6.5; Appendix A). The trends seen in all four analyses are clearly associated with the lower portion of Bone Bed 3 and occur only once. The one analysis that doesn't wholly support a drive event is the stratigraphy. This I associate with CS02's position within the talus cone and slope erosion. As materials moved downslope, it is likely that bone and rock orientations would parallel and sit on top of Stratum 6 rather than present as the mass jumble seen in CS01. This trend in CS02 may be beneficial in comparing to other columns with sloping portions of Bone Bed 2 (CS07 and CS08), particularly because CS07 has the most distinct and clearly separated multi-strata portion of Bone Bed 2. Are these separate bison drive events or one drive event that has been redeposited down slope?

Table 6.4. Summary of strata within CS02.

ASWT Designation	Dibble Designation	Notes*
S1	Slump	Talus cone slump. Combined debris from notch, stabilization material, and disturbed surface material.
S2	Zone 3	Small colluvium in sandy silt matrix. Burned Castroville point (FN60158).
S3	BB3	Massive accumulation of bone (most reduced to calcined powder by burning), small rocks, and silt. Upper BB3 and hypothesized as the end of a fall event.
S4	BB3	Mass of bison bone, boulders, small rocks, and white silty powder (dry: 10YR7/2). Roughly half bone and half burned rocks. Lower BB3 and hypothesized as the start of fall event. DNA Sample 7 (FN60272).
S6a	Zone 2b	Thin but very dense layer of heavily burned matrix.
S6b	Zone 2b	Thin zone of reduced light brown sediment directly underlying BB3. Hypothesized as surface on which the fall event occurred.
S7	Zone 2b	Reduced sediment with almost greenish color. Silty with many small, rounded pebbles.
S8a	Zone 2b	Massive poorly sorted colluvium from the roof, notch, and canyon rim. Gravels are generally small, thin, and horizontally bedded.
S8b	Zone 2b	Similar to stratum 8a with and increase to medium sized gravels and loamier sediment.
S8c	Zone 2b	Similar to stratum 8a with medium sized gravels and few cobbles in silt. A thin pebble lens was noted encompassing a cobble – removed during sampling.
S9	Zone 2b	Massive poorly sorted colluvium including a large boulder near the center of the profile. Charcoal sample (FN60219).
S10a	Zone 2b	Colluvium with angular to subangular gravels and cobbles in silty matrix. Comparable to S8 but redder in color.
S10b	Zone 2b	Colluvium with angular to subangular gravels and cobbles in loamy matrix.
S11a	BB2	Massive poorly sorted colluvium with angular to subangular gravels and cobbles in a sandy loam. Correlates to S11 in CS01. Plainview point (FN60236) and charcoal sample (FN60237).
S11b	BB2	Reddish to purple decomposing bone and large rocks. Lenses of alternating reddish and gray silt in pockets between large rock clasts. May correlate to stratum 12/12b in PS07. DNA Sample 6 (FN60271).

*Derived from profile, column, and personal notes of Dr. Kilby, Dr. Hamilton, and Ashley Eyeington.

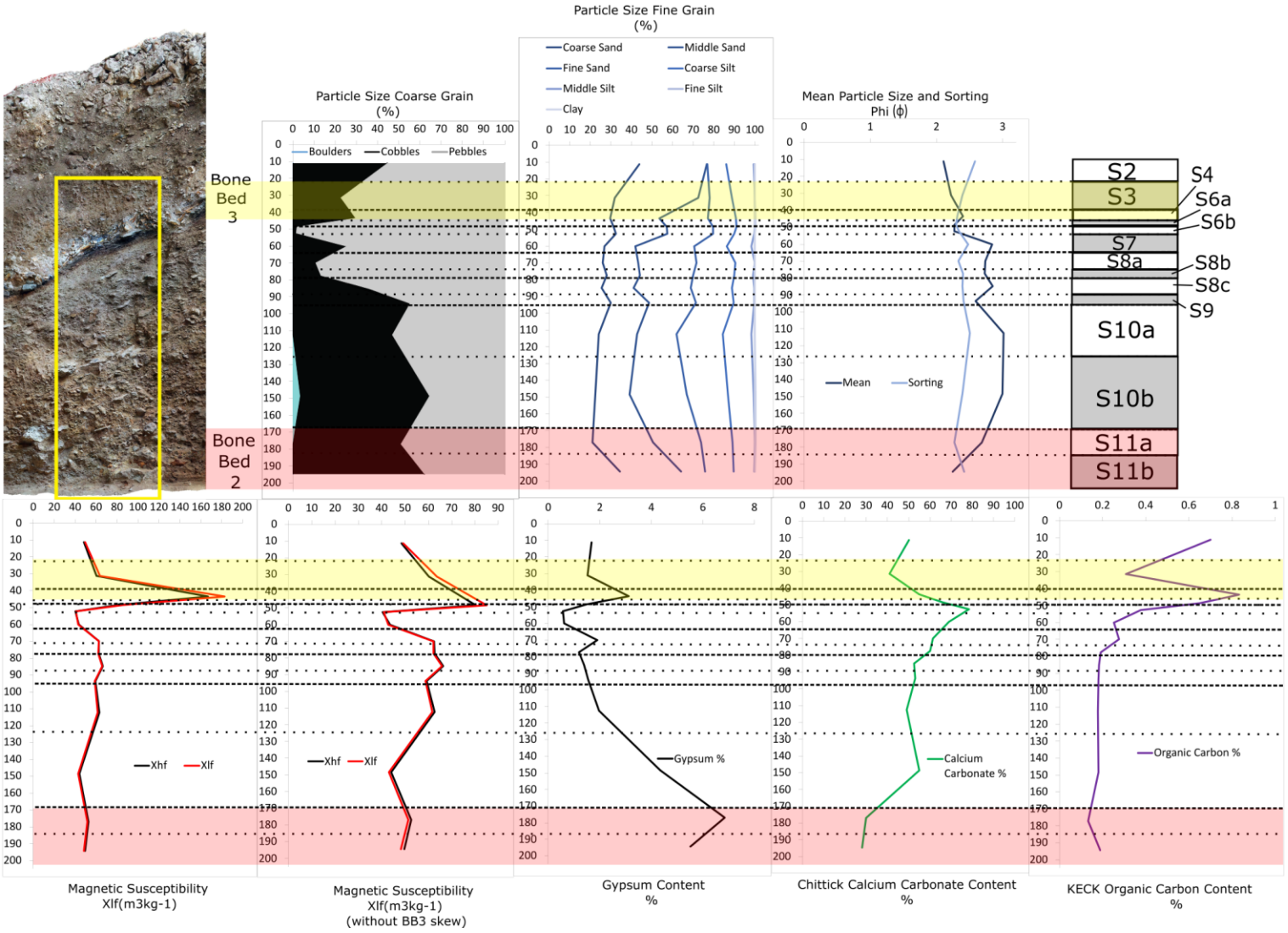

Figure 6.5. Laboratory results for CS02.

Table 6.5. Origin of Bone Bed 3 in CS02.

Analysis	Jump Drive*	Secondary Processing*	Column Sample 2
Stratigraphic	Bones intermixed with sediment and gravel in bone beds.	Minimum mixing with sediment and gravel.	Very poorly sorted (2.0-3.0φ) mix of bone, gravels, and little sediment. This portion of BB3 has eroded downslope and is thinner and more compressed.
	Not restricted to stratigraphic boundaries and not restricted to boundary orientation.	Discreet layer of bone that doesn't cross stratigraphic boundaries and bones that lie parallel to stratigraphic boundaries.	The bones and gravel do parallel the stratigraphic boundaries which are also more distinct and abrupt.
Particle Size	Fining upward sequence.	Predominately bone with little matrix and no fining upward sequence.	There is a fining upwards sequence within BB3 which is capped by increasing coarse materials associated with slope erosion and the accumulation of stratum 2 overtop of BB3.
Magnetic Susceptibility	Dramatic spike in values occurring in association with each individual event.	A smaller, less dramatic spike; only one spike in association with BB2.	Very dramatic spike (182 χlf) in stratum 4, the lower portion of BB3.
Organic Content	Dramatic spike in values occurring in association with each individual event.	A smaller, less dramatic spike; only one spike in association with BB2.	Very dramatic spike in stratum 4 (0.83%), which consists of the lower portion of BB3.
Carbonate Content	Decrease in bone beds due to exogenic deposition from drive event.	No difference across bone beds or natural strata due to continuous endogenic deposition.	BB3 shows a decreasing trend through strata 6a, 4, and 3 (66%, 55%, and 41% respectively) which supports the introduction of exogenic materials.
Gypsum Content	Increase in bone beds due to upland sources during drive event.	Consistent across natural and bone bed strata.	There is a spike in gypsum content (3.12%) in stratum 4 which also supports the introduction of outside materials.

* Analysis results contradicting expectations are grayed out.

Bone Bed 2 Results

Within CS02, Bone Bed 2 is only represented by Stratum 11, which is subdivided into strata 11a and 11b (Figure 6.4). While this is a narrow picture of Bone Bed 2, the analyses still lean towards supporting the hypothesis that this bone bed formed as the result of a bison drive event (Table 6.6). Unfortunately, a determination of the number of events cannot be made at this time due to this limitation.

Stratigraphically, Bone Bed 2 is very poorly sorted (2.0 φ) with no clear patterning to the orientation of bones or gravels (Table 6.6; Figure 6.5). Additionally, in 2019 when the column was extended into the floor, the observed lower boundaries of the Bone Bed 2 strata were not distinct or abrupt in nature. The particle size distribution shows an increase in size of both gravel and sediment clast material within Stratum 11a (Figure 6.5; Appendix A). This trend is mirrored in the mean particle size as well. Calcium carbonate increases substantially in Stratum 10b suggesting that the material within Bone Bed 2 is more exogenic in nature while the overlaying natural layers are more endogenic. Additionally, the gypsum content within Bone Bed 2 is much higher than the overlaying stratum which also supports an exogenic origin from outside the shelter.

The MS analysis shows a small spike within Stratum 11a (51 χlf) which decreases into Stratum 10b, the overlaying non-bone bed zone; but, without the lower Bone Bed 2 strata or underlying natural layers, it is difficult to discern any patterns for this analysis (Figure 6.5; Appendix A). This is true for the organic carbon content data as well. It remains stable across most of the column with only a small decrease in Stratum 11a. This may be due to the fact that Stratum 11a represents the very top of Bone Bed 2 and the more organically rich layer were not captured in this analysis.

Table 6.6. Origin of Bone Bed 2 in CS02.

Analysis	Jump Drive*	Secondary Processing*	Column Sample 2
Stratigraphic	Bones intermixed with sediment and gravel in bone beds	Minimum mixing with sediment and gravel	Very poorly sorted (2.0 φ) mix of bone, gravels, and sediment.
	Not restricted to stratigraphic boundaries and not restricted to boundary orientation	Discreet layer of bone that doesn't cross stratigraphic boundaries and bones that lie parallel to stratigraphic boundaries	The bones do not consistently parallel the stratigraphic boundaries. Additionally, there is no distinct or very abrupt lower boundary to the strata within BB2.
Particle Size	Fining upward sequence	Predominately bone with little matrix and no fining upward sequence	A clear fining upwards sequence of both coarse and fine clasts materials can be seen from stratum 11b into stratum 11a.
Magnetic Susceptibility	Dramatic spike in values occurring in association with each individual event	A smaller, less dramatic spike; only one spike in association with BB2	A small spike in MS (51 χlf) is seen in stratum 11a.
Organic Content	Dramatic spike in values occurring in association with each individual event	A smaller, less dramatic spike; only one spike in association with BB2	There is a slight decrease in organic content of stratum 11a (0.13%), but overall, it trends smoothly until BB3.
Carbonate Content	Decrease in bone beds due to exogenic deposition from drive event	No difference across bone beds or natural strata due to continuous endogenic deposition	Carbonate content is stable across strata 11b and 11a with a large spike occurring in stratum 10c of 55% (non-bone bed layer).
Gypsum Content	Increase in bone beds due to upland sources during drive event	Consistent across natural and bone bed strata	There is a single spike in gypsum in stratum 11a (6.8%) which suggests an increase in exogenic materials. This spike occurs at the upper portion of BB2 and then decreases with depth.

* Analysis results contradicting expectations are grayed out.

Column 6

Column Sample 6 is on the south side of the talus cone and along the western face of PS07 (Figure 6.6). This places CS06 near the apex of the cone and immediately south of CS01. While they share a similar location at the thickest vertical portion of the cone, PS07 looks very different. This is because PS07 is not cut as far into the talus cone and therefore the soils do not slope as dramatically south. They do trend down to the east along the major slope of the talus cone to the rear of the shelter.

Within CS06, only Bone Bed 2 was exposed and investigated for this thesis. This is also the portion of the cone, PS07, that encompasses the three fiercely debated Bone Bed 2 layers (Table 6.7; Figure 6.7). Stratum 11 is the upper most portion of Bone Bed 2 and is recognized as the upper unburned layer of the three debated Bone Bed 2 strata. Below Stratum 11 is Stratum 11c which is a thin, 5 to 6 cm, layer that occurs locally within and to the east of the column. This thin stratum may represent an eroded and redeposited portion of Stratum 11.

The center of Bone Bed 2 is encompassed by Stratum 12 which is an ashy layer of heavily burned bone and rocks and recognized as the middle, burned layer of the three Bone bed 2 strata (Table 6.7; Figure 6.7). This mass of burned materials lies atop Stratum 13 which is a thin, 5 to 10 cm, mass of colluvium with unburned bones. As Stratum 13 isn't seen across PS07, it may be a localized colluvial event. This along with its placement between strata 12 and 14, the lower and third recognized stratum of Bone Bed 2, has been used as an argument that multiple drive events are represented within this bone bed (Dibble and Lorrain 1968; Dibble 1970; Bement 1986; Bousman et al. 2004; Holliday 1997; Prewitt 2007; Turpin 2004).

Figure 6.6. Location of CS06 and CS07 within PS07, southern profile of talus cone.

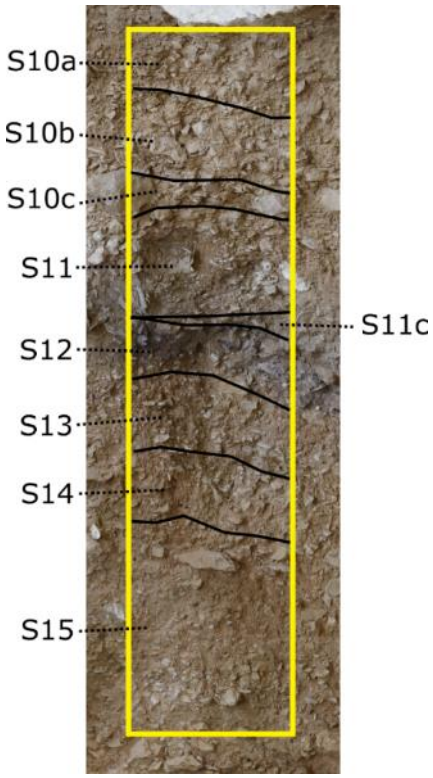

Figure 6.7. CS06 with strata designations.

Table 6.7. Summary of strata within CS06.

ASWT Designation	Dibble Designation	Notes*
S10a	Zone 2b	Colluvium with angular to subangular gravels and cobbles in silty matrix. Slightly bedded along talus cone contour.
S10b	Zone 2b	Colluvium with angular to subangular gravels and cobbles in loamy matrix. Similar to 10a with redder coloration and increased loam. In places, stratum 10b directly overlays stratum 11a.
S10c	Zone 2b	Very reddish silty loam base of stratum 10b seen discontinuously across talus profile.
S11	BB2	Massive poorly sorted colluvium with angular to subangular gravels and cobbles in a sandy loam. Upper portion of Bone Bed 2 – abundant unburned bison bone. Grades from gravel matrix in west to silty loam matrix in east.
S11c	BB2	Thin 5 to 6 cm zone locally observed east of column. Lens of small angular pebbles and gravel in silty matrix of slightly paler color. Possible redeposited portion of Bone Bed 2.
S12	BB2	Ashy deposit with heavily burned bones and rocks, roughly 12 to 20 cm thick.
S13	BB2	Thin layer of massive colluvium with occasional unburned bone fragments. May represent localized colluvial event which separates the main bone bed strata 12 and 14.
S14	Zone 1	Massive colluvium with occasional unburned bones and slight bedding. May represent an upslope facies of S14b seen to the east. Not recognized as Bone Bed 2 in Dibble's profile (Dibble 1964).
S15	Zone 1	Thick zone of tabular spalls with silty gray matrix and alternating lenses of reddish-brown matrix. Surface on which Bone Bed 2 lies. Correlates to strata 13 to 15 in CS01 which were thicker deposits of the alternating reddish and gray lenses and roof spalls.

*Derived from profile, column, and personal notes of Dr. Kilby, Dr. Hamilton, and Ashley Eyeington.

Bone Bed 2 Results

Within CS06, Bone Bed 2 represents a bison drive and likely multiple events, but the number of events could not be pinned down due to inconsistencies within the data as to which stratigraphic unit the drives occurred. The southern profile (PS07) has the thickest and most distinct portion of Bone Bed 2. Within CS06, Bone Bed 2 is represented by six strata: 11, 11c, 12, 13, 14, and 14b (Figure 6.8; Table 6.8). Stratigraphically, all six layers remain very poorly sorted (2.0 φ) with a high mean particle size (2.0-3.0 φ). Strata 11 and 11c both have abrupt boundaries and materials do not appear to cross those defined boundaries. While there are some horizontal trends along the slope of strata 11 and 11c, the bones and gravels within still have mixed orientations. Stratum 12 has a clear boundary and there was visual evidence of bones and gravels encroaching into Stratum 13. Conversely, Strata 13 and 14 have gradual boundaries and the materials within do not adhere to stratigraphic boundaries or orientation.

The PSA for both gravels and sediment show multiple fining upwards sequences (Figure 6.8; Appendix A). The gravel size distribution shows a peak in cobbles with Stratum 13 and fining upwards through Stratum 12, followed by another sequence in strata 11c and 11. This is mirrored by the mean particle size which shows higher particle size throughout strata 14b/14 and then peaking again in Stratum 11c. The sediment clast PSA also shows two fining upwards sequences, but these are restricted to the lower half of Bone Bed 2 with spikes occurring in strata 14b and 13.

MS, organic carbon content, and gypsum content all show a single distinct spike in values within Stratum 12 (Figure 6.8; Appendix A). All three analyses also increase in strata 14 or 14b as well, indicating a possible event within the lower portion of Bone Bed

2. The values for all three of these analyses in Stratum 12 are much higher than those previously seen for Bone Bed 2 in PS05. The peaks in value for MS and organic carbon occurring within strata 12 are unsurprising due to intense mass of burned bones and sediment which defines that stratum, but I find the spike in gypsum in Stratum 12 interesting.

My hypothesis is that gypsum will increase with the introduction of exogenic materials, specifically from upland sources. I would have expected gypsum content to peak in correlation with PSA, but this is not the case (Figure 6.8; Appendix A). It is possible the gypsum is percolating down the profile as a post depositional process. This is even more likely the case as gypsum dehydrates to anhydrite at temperatures as low as 200˚C (392˚F) and would not be present after the burning event that occurred within Bone Bed 2 (Bain 1990; Artieda et al. 2006). As such, the accumulation of gypsum within Stratum 12 must have occurred post-Bone Bed 2 deposition and burning.

The CCE analysis also shows some interesting trends (Figure 6.8; Appendix A). There are two peaks occurring in strata 14 and 12 within Bone Bed 2. While the associated decreases in strata 13 and 11 occur within 5 percent or so and are not dramatic, they do occur in conjunction with peaks and subsequent fining upwards sequences in particle size. As the shelter is carved from the Devil's River Formation, which is rich in calcium carbonate, these trends could be indicating an increase in spalling and rock fall from the shelter within strata 14 and 12.

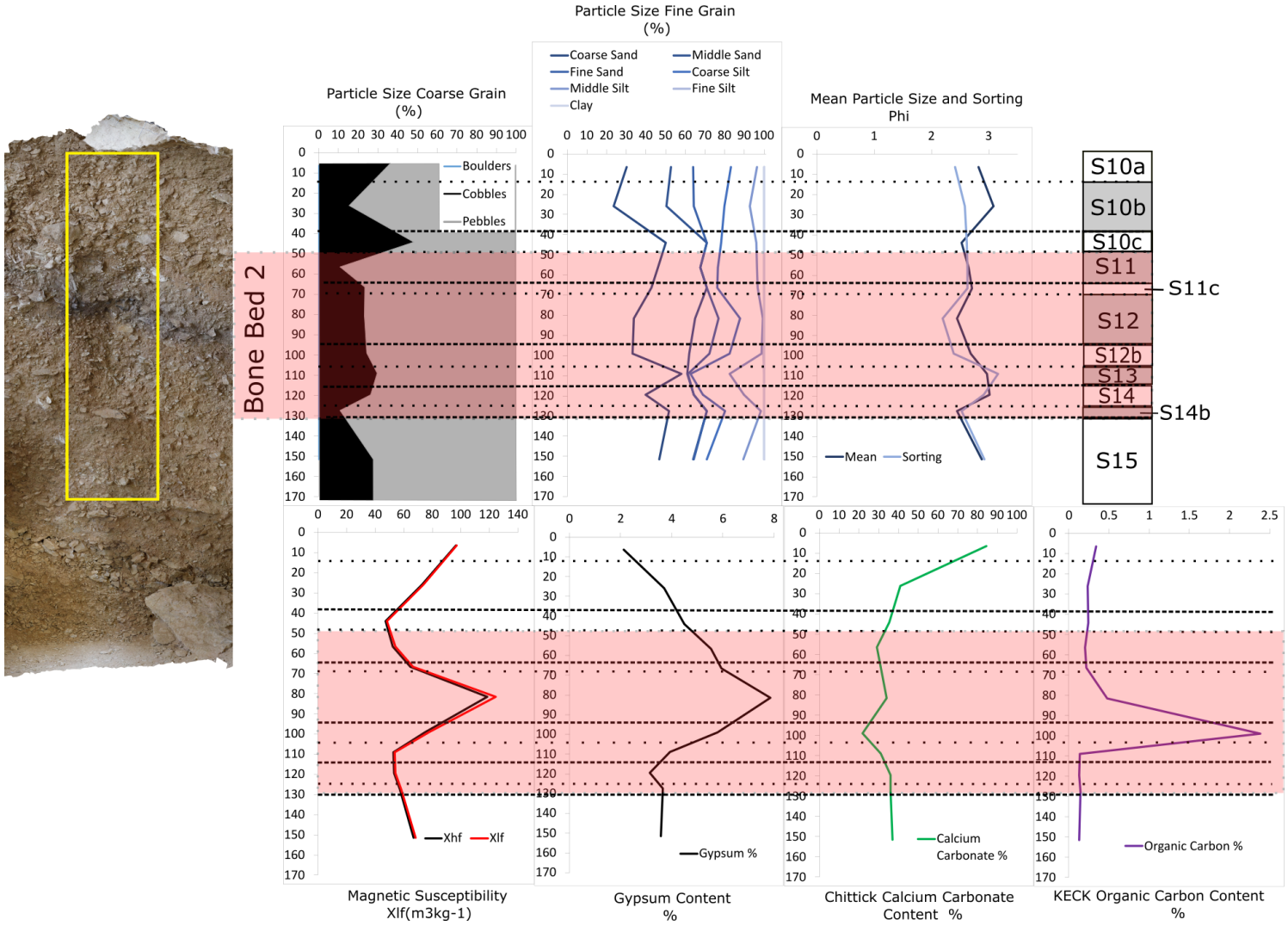

Figure 6.8. Laboratory results for CS06.

Table 6.8. Origin of Bone Bed 2 in CS06.

Analysis	Jump Drive*	Secondary Processing*	Column Sample 6
Stratigraphic	Bones intermixed with sediment and gravel in bone beds	Minimum mixing with sediment and gravel	Very poorly sorted (2.0 φ) mix of unburned bone, unburned gravels, and sediment.
	Not restricted to stratigraphic boundaries and not restricted to boundary orientation	Discreet layer of bone that doesn't cross stratigraphic boundaries and bones that lie parallel to stratigraphic boundaries	Six recognized strata. Bones and rocks do parallel the downslope trend within but predominately at the lower boundary of stratum 11 and somewhat at the base of stratum 12. Strata 13 and 14 have gradual boundaries and the materials within do not adhere to stratigraphic boundaries as well.
Particle Size	Fining upward sequence	Predominately bone with little matrix and no fining upward sequence	Coarse grain PSA shows two fining upwards sequences which is mirrored by the mean particle size. The sediment PSA also shows two fining upwards sequences, but the within different strata.
Magnetic Susceptibility	Dramatic spike in values occurring in association with each individual event	A smaller, less dramatic spike; only one spike in association with BB2	Single distinct increase (124 χlf) in stratum 12.
Organic Content	Dramatic spike in values occurring in association with each individual event	A smaller, less dramatic spike; only one spike in association with BB2	Single distinct increase (0.48%) in stratum 12.
Carbonate Content	Decrease in bone beds due to exogenic deposition from drive event	No difference across bone beds or natural strata due to continuous endogenic deposition	Carbonate remains stable from stratum 15 through BB2, but markedly increases above BB2 in strata 10c to 10a (35.5%, 41%, 84.5%, respectively). Additionally, there are two small decreases in carbonate content in strata 13 and 11 (31% and 29%, respectively).
Gypsum Content	Increase in bone beds due to upland sources during drive event	Consistent across natural and bone bed strata	Single distinct increase (7.8%) in gypsum in stratum 12.

* Analysis results contradicting expectations are grayed out.

Column 7

Column Sample 7, similar to CS02, is located on the eastern toe slope of the talus cone. As such, this column contains a condensed portion of Bone Bed 2 represented as strata 11, 12b, 14, and 14b (Figure 6.9; Table 6.9). Column Sample 7 has the most distinctive representation of Bone Bed 2 and the multiple strata represented within (Figure 6.9). It is also the portion of the southern profile which corresponds to Dibble's published profile and descriptions of BB2a, BB2b, BB2c (1964). This will be explored further in the next chapter, but briefly, Stratum 11 is the same layer as found in CS06, further upslope and to the west.

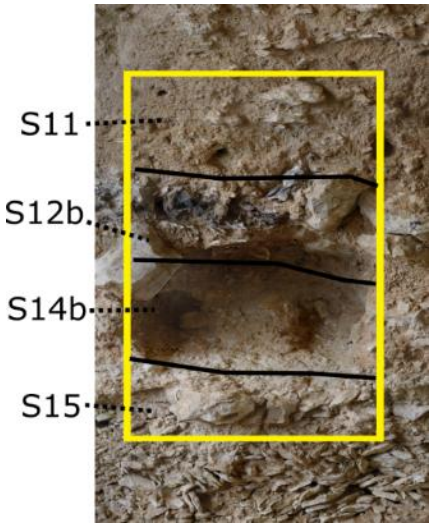

Figure 6.9. CS07 with strata designation.

Stratum 12b begins near the middle of PS07 and about a meter east of CS06. This stratum is similar to Stratum 12 but is the most heavily burned portion of Bone Bed 2. Due to the slope of the cone, it is possible that Stratum 12b is a downslope facies of Stratum 12. It is distinctive due to the high amount of oxidized matrix (7.5YR 6/6, reddish yellow) and reduced matrix (Gley2 6/10B, bluish gray) focused near the base of Stratum 12b. These burned lenses are similar to the oxidized and reduced zones seen below Bone Bed 3 in PS05 (S6a and S6b). Stratum 14 was subdivided during excavation

of the column into strata 14 and 14b. Stratum 14b is similar to its upslope facies Stratum 14 but is generally less rocky and contains more bone.

Table 6.9. Summary of strata within CS07.

ASWT Designation	Dibble Designation	Notes*
S11	BB2a	Massive poorly sorted colluvium with angular to subangular gravels and cobbles in a reddish sandy loam. Upper portion of Bone Bed 2 – abundant unburned bison bone.
S12b	BB2b	Ashy deposit with heavily burned and calcined bones and burned rocks, roughly 12 to 20 cm thick. Portions have been reduced to a blue gray particularly along the base of the layer.
S14	BB2c	Massive colluvium with occasional unburned bones and slight bedding.
S14b	BB2c	Reddish gritty loam that has become heavily reduced along its contact with stratum 12b. Unburned bone increases with depth.
S15	Zone 1	Thick zone of tabular spalls with silty gray matrix and alternating lenses of reddish-brown matrix. Surface on which Bone Bed 2 lies. Correlates to strata 13 to 15 in CS01 which were thicker deposits of the alternating reddish and gray lenses and roof spalls. Charcoal sample (FN60534)

*Derived from profile, column, and personal notes of Dr. Kilby, Dr. Hamilton, and Ashley Eyeington.

Bone Bed 2 Results

Within CS07, Bone Bed 2 represents one or two bison drive events, but further work is needed to firmly define the stratigraphic context of the number of events. Bone Bed 2 consists of multiple visually striking layers. Both strata 11 and 12b have abrupt lower boundaries with no cross horizonal inclusions. Conversely, strata 14 and 14b have more gradual lower boundaries and evidence of bones and gravels crossing stratigraphic limitations. These visually distinct layers have been used as the justification for the proposal of multiple bison drive events being represented within Bone Bed 2 (Dibble and Lorrain 1968; Dibble 1970; Bement 1986; Bousman et al. 2004; Holliday 1997; Prewitt 2007; Turpin 2004).

The gravel PSA shows two fining upwards sequences with peaks in strata 14b and 12b (Table 6.10; Figure 6.10). The lower sequence in Stratum 14b may be problematic as the cobble's values in the overlaying Stratum 14 is near zero percent (Appendix A). This cannot be the case based on visual observations of the column and in situ stratum. I believe this is the result of sampling bias or error. These strata were divided during excavation, and it may be that the cobble size materials were either left out of the Stratum 14 sample or grouped into the Stratum 14b bags. Either way, the sediment PSA shows a single fining upwards sequence with the highest value occurring in 14b and so, for the purpose of this thesis, we can assume there is a fining upwards sequence in the lower portion of Bone Bed 2 in CS07. This assumption will need to be confirmed via retesting in the future.

Results from MS, organic carbon content, and CCE all indicate one single spike in values (Appendix A). The highest MS values occur within both strata 12b and 14 (Table 6.10; Figure 6.10). The values in Stratum 12b are slightly higher, but it is minimal (78 χlf and 74 χlf, respectively), and as such, likely do not represent separate depositional events. The CCE value peaks in Stratum 15, below Bone Bed 2. This is what I would have expected as Stratum 15 is a massive zone of roof spalls and would have largely been deposited through endogenic processes. Gypsum, on the other hand, has two spikes in value occurring in strata 14b and 11 (Table 6.10; Appendix A).

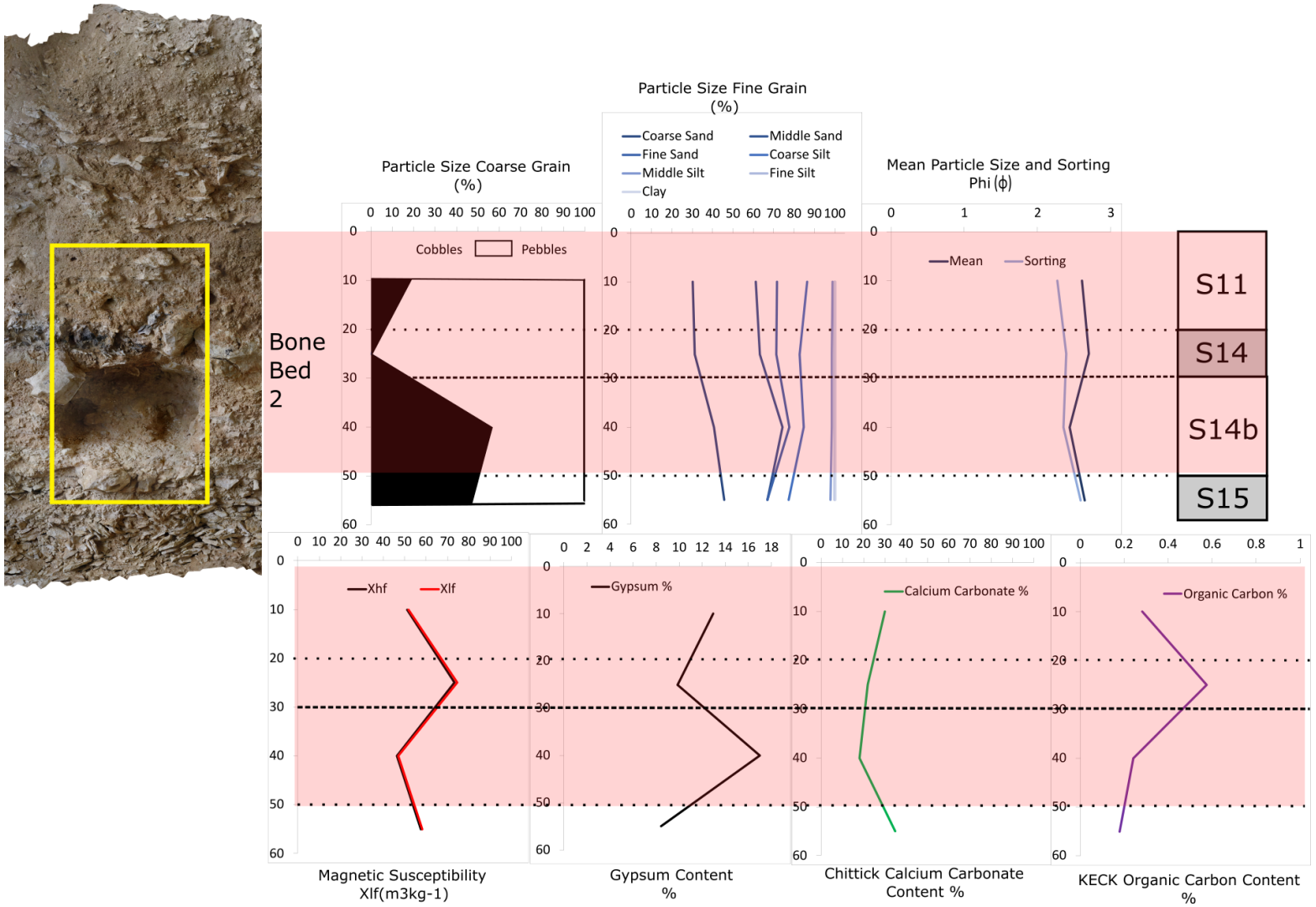

Figure 6.10. Laboratory results for CS07.

Table 6.10. Origin of Bone Bed 2 in CS07.

Analysis	Jump Drive*	Secondary Processing*	Column Sample 7
Stratigraphic	Bones intermixed with sediment and gravel in bone beds	Minimum mixing with sediment and gravel	Very poorly sorted mix of bone, gravels, and sediment.
	Not restricted to stratigraphic boundaries and not restricted to boundary orientation	Discreet layer of bone that doesn't cross stratigraphic boundaries and bones that lie parallel to stratigraphic boundaries	The bones do not consistently parallel the stratigraphic boundaries. Additionally, only strata 11 and 12 have abrupt boundaries with no trans horizonal mixing.
Particle Size	Fining upward sequence	Predominately bone with little matrix and no fining upward sequence	Two fining upwards sequences in the gravel PSA with peaks in 14b and 12b. One fining upwards sequence in sediment PSA with a spike occurring in 14b.
Magnetic Susceptibility	Dramatic spike in values occurring in association with each individual event	A smaller, less dramatic spike; only one spike in association with BB2	Highest values are in strata 12b and 14 (78 χlf and 74 χlf, respectively).
Organic Content	Dramatic spike in values occurring in association with each individual event	A smaller, less dramatic spike; only one spike in association with BB2	Spikes in stratum 12b (2.38%)
Carbonate Content	Decrease in bone beds due to exogenic deposition from drive event	No difference across bone beds or natural strata due to continuous endogenic deposition	Slightly decreasing down the BB2 profile before spiking in stratum 15 (35%).
Gypsum Content	Increase in bone beds due to upland sources during drive event	Consistent across natural and bone bed strata	Highest values is in stratum 14b (17%) which significantly decreases through stratum 12b before spiking again in stratum 11(13%).

* Analysis results contradicting expectations are grayed out.

Column 8

Column Sample 8 is located on the eastern most toe slope of the cone in PS08 (Figure 6.11). Due to its location within the talus cone, the identified layers within CS07 are largely downslope eroded representations of the strata previously discussed. Overall, the upper half of the column consists of strata 8 and 10, along with their various substrata, which are similar to their upslope facies. They do differ in that both matrix and gravel bedding were observed within PS08. This is because these deposits eroded downslope and therefore were subjected to post depositional processes which sorted the materials. In CS08, Bone Bed 2 is represented by strata 11 and 14b (Figure 6.12; Table 6.11). Both strata are reddish in color and include an abundance of bison bone. A few burned bones and rocks were observed, but no evidence of in situ burning was found in either stratum.

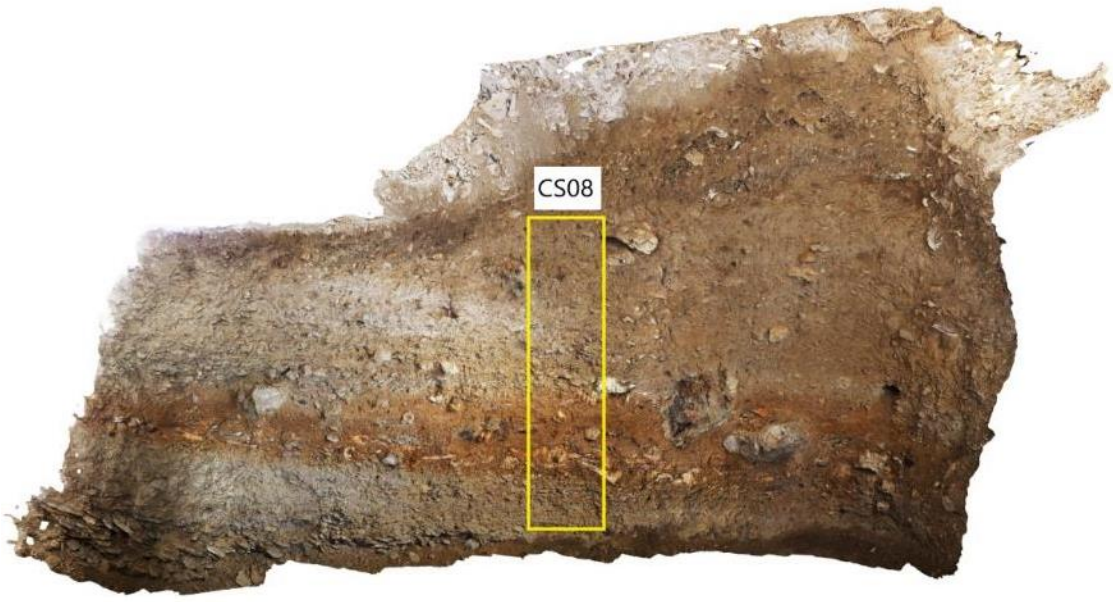

Figure 6.11. Location of CS08 within PS08, eastern profile of talus cone.

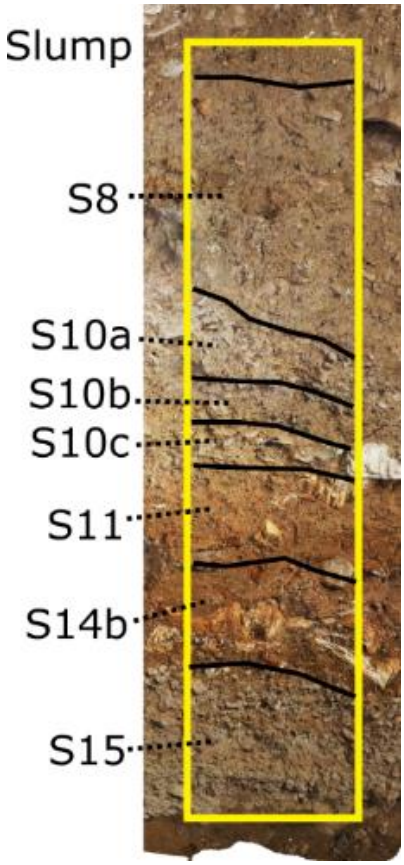

Figure 6.12. CS08 with strata designation.

Bone Bed 2 Results

As CS08 is located at the toe slope of the talus cone, the Bone Bed 2 strata within appear to have been deposited via erosion from higher upslope. This means they do not present a picture of what the initial depositional event looked like, but still may provide information via sedimentological and mineralogical data as to the nature of Bone Bed 2. Stratigraphically, strata 11 and 14b are both visually distinct and the inclusions of bone and gravel do generally follow stratigraphic orientations. There are materials that cross stratigraphic boundaries though, particularly within Bone Bed 2 and at the lower boundary of Stratum 14b (Table 6.12; Figure 6.13).

Table 6.11. Summary of strata within CS08.

ASWT Designation	Dibble Designation	Notes*
S8	Zone 2b	Moderately bedded colluvium which steeply slopes to the north. Distinct bedding noted in some portions is likely due to slope erosion. Was subdivided into 8a, 8b, and 8c in notes based on gravel size and sphericity.
S10a	Zone 2b	Colluvium with angular to subangular gravels and cobbles in pale gray silty matrix (10YR 7/2). Slightly bedded and steeply deeps to the north where it transitions into a denser gravel zone.
S10b	Zone 2b	Pebbles and gravels with slight bedding in reddish sandy loam (10YR 6/3). Similar to 10a with redder coloration and increased loam. Charcoal sample (FN60553)
S10c	Zone 2b	Bedded gravels with intermixed bone fragments in gray silt loam matrix (10YR 7/2).
S11	BB2	Occasional boulders, cobbles, and small gravels in fine reddish silt loam (7.5YR 5/6). Upper portion of Bone Bed 2 – abundant unburned bison bone. One burned boulder and burned bone identified but otherwise burning is not evident.
S14b	BB2	Highly variable layer of pebbles, cobbles, and a dense accumulation of unburned bison bones. Discontinuous lenses of pebbles and coarser grained sediment noted within the southern portion as well as along the lower boundary. Not recognized as Bone Bed 2 in Dibble's profile (Dibble 1964).
S15	Zone 1	Thick zone of tabular spalls with silty gray matrix and alternating lenses of reddish-brown matrix. Surface on which Bone Bed 2 lies.

The PSA shows a single fining upwards trend across Bone Bed 2 in both the gravel and sediment analyses (Table 6.12; Appendix A). This trend is also seen in the mean particle size data. Due to the limited context of Bone Bed 2 in this column, testing the hypothesis of number events is impossible within the scope of this thesis. Magnetic susceptibility decreases down the column, but spikes in Stratum 11.

Gypsum also spikes within Bone Bed 2, but within the lower component, Stratum 14b. The CCE data is much lower throughout Bone Bed 2 and increase substantially above it in the non-bone bed layers (Table 6.12; Appendix A). These analyses together suggest a change from exogenic to endogenic accumulation. The organic carbon

percentage also decreases in Stratum 11, which I would not have expected due to the high occurrence of bone and organic material.

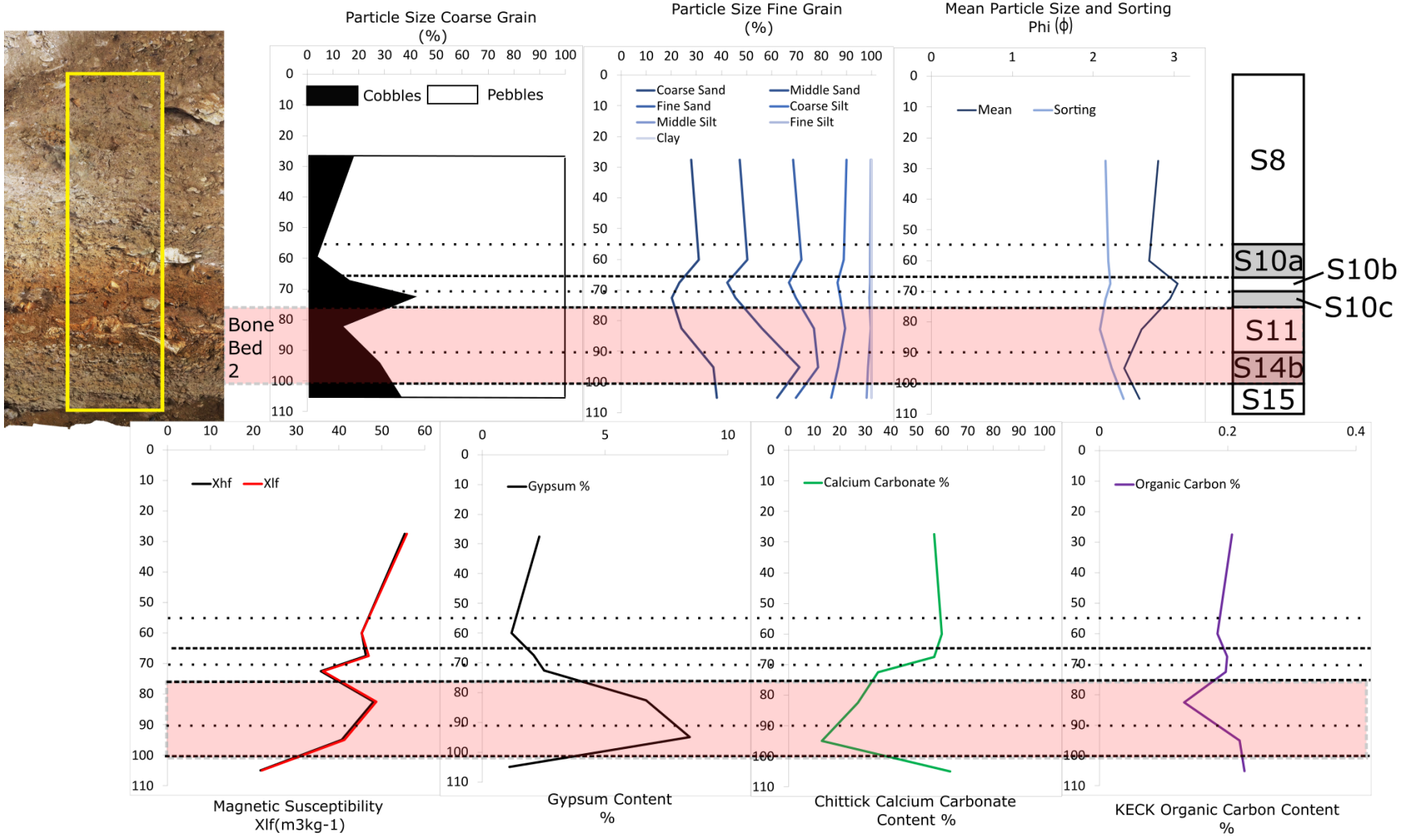

Figure 6.13. Laboratory results for CS08.

Table 6.12. Origin of Bone Bed 2 in CS08.

Analysis	Jump Drive*	Secondary Processing*	Column Sample 7
Stratigraphic	Bones intermixed with sediment and gravel in bone beds	Minimum mixing with sediment and gravel	Very poorly sorted mix of bone, gravels, and sediment.
	Not restricted to stratigraphic boundaries and not restricted to boundary orientation	Discreet layer of bone that doesn't cross stratigraphic boundaries and bones that lie parallel to stratigraphic boundaries	Bone and gravel do follow stratigraphic orientation but are not restricted by stratigraphic boundaries.
Particle Size	Fining upward sequence	Predominately bone with little matrix and no fining upward sequence	Single fining upwards sequence across BB2 strata 14b and 11.
Magnetic Susceptibility	Dramatic spike in values occurring in association with each individual event	A smaller, less dramatic spike; only one spike in association with BB2	Single spike in value within BB2 in stratum 11 (48 χlf).
Organic Content	Dramatic spike in values occurring in association with each individual event	A smaller, less dramatic spike; only one spike in association with BB2	Single spike in value within BB2 in stratum 14 (0.22%).
Carbonate Content	Decrease in bone beds due to exogenic deposition from drive event	No difference across bone beds or natural strata due to continuous endogenic deposition	Decreased values across BB2 with spikes occurring in the underlying and overlying non-bone bed strata.
Gypsum Content	Increase in bone beds due to upland sources during drive event	Consistent across natural and bone bed strata	Much higher values in BB2 with the highest value occurring in stratum 14b (8.4%)

* Analysis results contradicting expectations are grayed out.

Concluding Thoughts

Overall, the talus cone is a very dynamic and complex study subject. The position of the columns and the profile sections investigated present challenges in interpretation. Specifically, the slopes of all facies and amount of post depositional erosion have impacted each column differently (Figure 6.14.). As I was working through the results section, it became clear that my hypotheses were much too simplified to be applied universally across the cone.

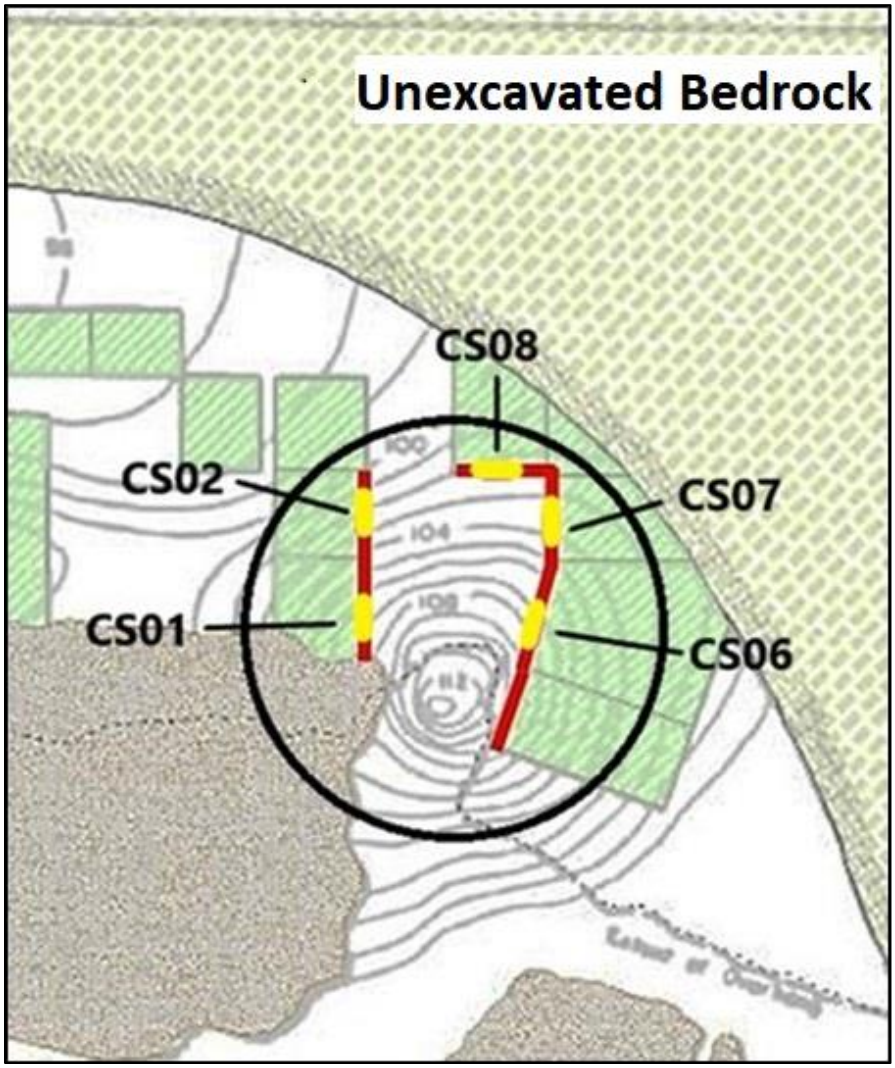

Figure 6.14. Close up of the topography of the talus cone in relation to the column samples (modified from Kilby et al. 2020).

After rethinking the orientation of the columns within the talus cone a few things have become clear. First, CS01 and CS06 are located the closest to the apex of the cone and as such should have the deposit most likely to represent the original drive event. They should also contain the thickest portion of the deposits. As such, we can assume that discrete events would be best persevered within those two columns as the remaining columns are located on the distal edges of the talus cone. Those deposits have been more thoroughly impacted by post depositional processes such as erosion and slope wash. While CS01 and CS06 would also inevitably have some disturbance from material and water washing through the notch, this deposition may have also helped bury and preserve the bone beds.

It also happens that these two columns have the most distinct representation of the two bone beds: CS01 has the most complete representation of Bone Bed 3 while CS06 has the most complete representation of Bone Bed 2. Even though CS07 has the most famous and controversial representation of Bone Bed 2, it is located further down slope and so has been impacted by erosion and slope wash which likely caused redistribution of the deposits. Though, I cannot definitively state why Bone Bed 2 in CS07 has such distinct stratigraphy, I believe it does have to do with the sloping nature of the cone. The lower unburned layer (Stratum 14) and middle burned layer (Stratum 12) may represent a single event, with a burned cap, which was covered by a later second drive event (Stratum 11). The distinct stratigraphy simply being a result of those two events eroding downslope from the apex of the cone creating a downslope facies of Bone Bed 2.

Despite the unusual morphology of the cone, a few things can also be said about the results from the five column samples (Table 6.13). Firstly, in the two columns (CS01

and CS02) that contained deposits from Bone Bed 3, all results point to a single bison drive event. While only two columns included Bone bed 3, this still suggests that it represents a valid comparison for what a single bison drive event should look like (Table 6.14.). Overall, all six analyses did fluctuate similarly in both Bone Bed 2 and Bone Bed 3, with the results of Bone Bed 3 occurring consistently within the same stratigraphic location. Though Bone Bed 2's results were not as clear as to the number of events, all five columns also suggest that Bone Bed 2 formed as the result of a bison drive event. This can most clearly be seen the stratigraphy and fining upwards sequences of PSA, but also in the correlating spikes in values in MS, gypsum content, calcium carbonate content, and organic carbon content.

Table 6.13. Final Results by Column.

Column Sample	**Jump Drive or Secondary Processing**	**Number of Events**
CS01	Bone Bed 2: Jump Drive Bone Bed 3: Jump Drive	Bone Bed 2: 1-2 events Bone Bed 3: 1 event
CS02	Bone Bed 2: Jump Drive Bone Bed 3: Jump Drive	Bone Bed 2: undetermined Bone Bed 3: 1 event
CS06	Bone Bed 2: Jump Drive	Bone Bed 2: 2 events
CS07	Bone Bed 2: Jump Drive	Bone Bed 2: 1-2 events
CS08	Bone Bed 2: Jump Drive	Bone Bed 2: undetermined

Finally, while no consistent trend could be found across the columns as to the number of events represented, three of the five columns do suggest the possibility of two depositional events. Drawing from zooarchaeological methods of minimum number of individuals, we can assume that the minimum number of events represented in Bone Bed 2 is two events (White 1953; Lyman 2018). This is particularly clear when we focus on CS01 and CS06, which has the highest potential to contain discrete events, but also when we look at the results of CS07 (Table 6.13).

Table 6.14. Attribute Comparison of Bone Bed 2 and Bone Bed 3.

Bone Bed	Stratigraphy	PSA	MS	Gypsum	Calcium Carbonate	Organic Carbon
Bone Bed 3	Multiple strata with mass mixing and elements crossing stratigraphic boundaries	Distinct fining upwards sequence	Distinct spike in value at base	Distinct spike in value at base	Decrease in value at base	Distinct spike in value at base
Bone Bed 2	Multiple strata with mass mixing and elements crossing stratigraphic boundaries	Distinct fining upwards sequences	Distinct fluctuations in value	Distinct fluctuations in value	Distinct fluctuations in value	Distinct fluctuations in value

A final thing to address is my hypotheses about exogenic and endogenic processes being discernable through gypsum and calcium carbonate percentages. What I first hypothesized was that gypsum would increase as external sediments did, due to the it being sourced from the uplands. What I didn't understand was that gypsum within the canyon may have a pedogenic origin through groundwater precipitation. After discussion with my committee member, Charles Frederick, I realized I missed the target here. What I should have focused on were decreases in calcium carbonate. We know that the Devil River has a high percentage of calcium carbonate, so where is the non-calcareous silt and sand coming from? Future questions on sediment sourcing for the talus cone could help address this.

In the next chapter, I break down the cone into four depositional zones: Bone Bed 3, Zone 2, Bone Bed 2, and Zone 1. The zones between and underlaying the two bone beds are derived from Dibble's original interpretations of the talus cone (Dibble and Lorrain 1968). The purpose is to reconstruct the depositional history of the cone as a

whole and to interpret the depositional units independently. This allows for a more cohesive interpretation of the bone beds within the talus cone.

VII. DISCUSSION AND INTERPRETATIONS

Before getting too far into the discussion of the results and subsequent interpretations, it is important to emphasize some of the underlying theories behind them. Specifically, the understanding of depositional processes in rockshelter environments and on slopes. When I began this project, it became clear that I wasn't going to find background literature on sites that look like the talus cone in Bonfire Shelter. There is a lot of information out there on rockshelters and talus slopes, but not on a talus cone which formed beneath an erosional wash on the edge of a large, and mostly enclosed, rockshelter. My interpretations following in the chapter largely draw on general rockshelter formation processes, post depositional processes specifically within shelters and on slopes (Donahue and Adovasio 1990; Farrand 2001; Goldberg and Macphail 2006; Laville 1976; Rapp and Hill 2006; Schiffer 1987; Waters 1992), and previous investigations in the canyon (Dibble and Lorrain 1968; Ferrell 2020; Kilby et al. 2020; Nielsen 2017; Pagona 2019; Ramsey 2020; Rodriguez 2015).

Depositional History of the Talus Cone

My discussion of the depositional history of the talus cone with interpretations derived from my field observations and laboratory analyses detailed in Chapters 4 through 6. This discussion is organized temporally, beginning with the oldest depositional unit, Zone 1, followed by Bone Bed 2, Zone 2, and finally, Bone Bed 3 (Figure 7.1). The zones below and between the two bone beds are derived from Dibble's original interpretations of the talus cone (Dibble and Lorrain 1968).

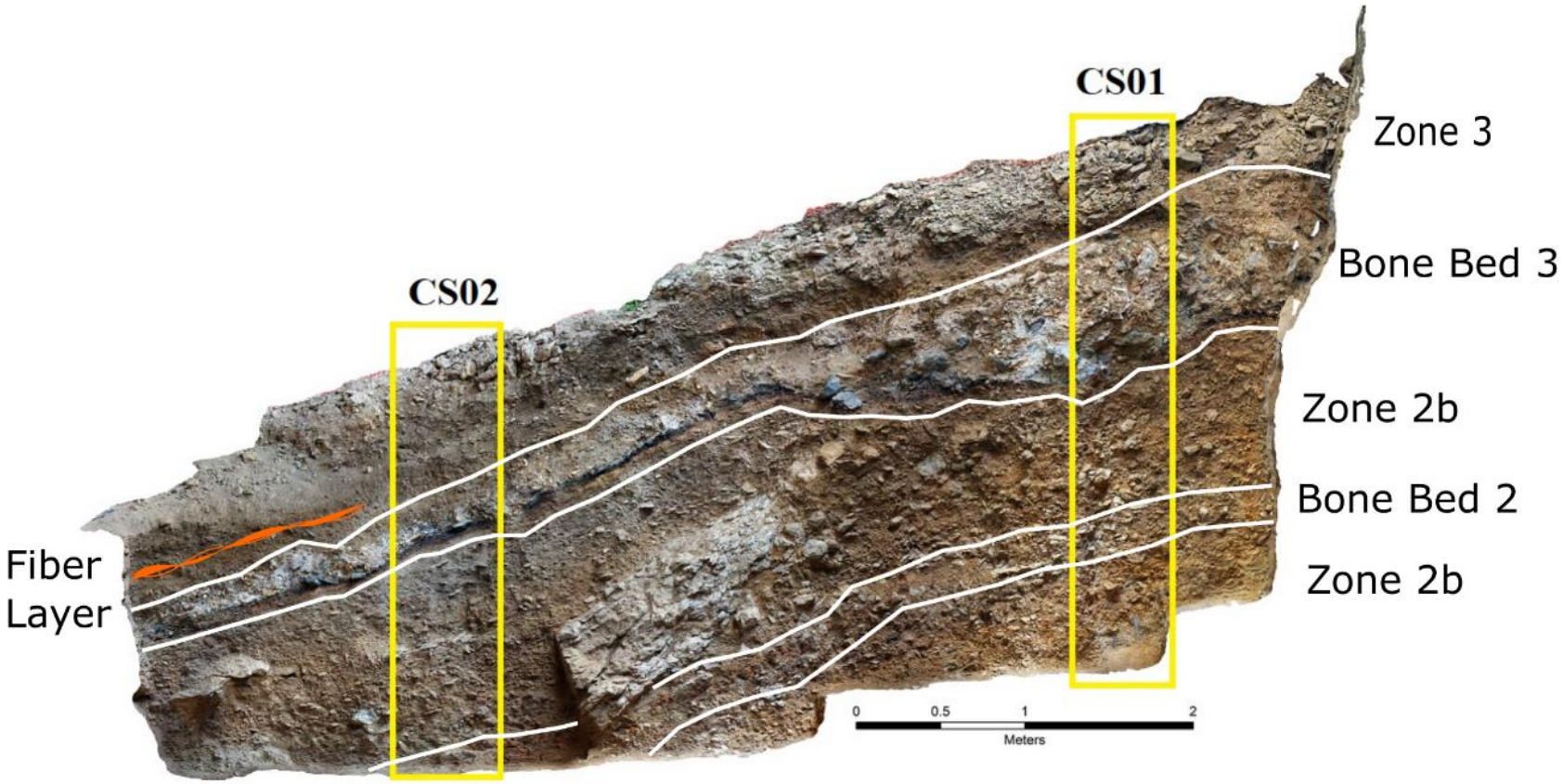

Figure 7.1. Southern profile of talus cone with zones identified by Dibble (modified from Dibble and Lorrain 1968:50).

Zone 1

Zone 1 is the lowermost unit and was documented both in the talus cone and shelter interior (Dibble and Lorrain 1968:24). It predominately consists of limestone spalls with clast supported light gray silt. During the more recent excavations done by ASWT, this zone was identified and classified as Stratum 15.

As part of the investigations presented in this thesis, Stratum 15 was sampled in CS01, CS06, CS07, and CS08 (Appendix A). Overall, the sampling for Stratum 15 was most fruitful on the southern and eastern side of the cone, as it steeply dips to the north and east and, as such, was not captured in CS02. From the laboratory analyses, there is one major trend within Zone 1; this is a decrease in the amount of gypsum with an increase in the CCE, seen in CS01, CS07, and CS08. As previously discussed, my hypothesis was that gypsum would increase with the introduction of exogenic materials while CCE would increase when endogenous processes were occurring. As Stratum 15 is a massive spall zone this suggests that the materials composing this layer originated from the Devils River Formation and inside the shelter interior. The remaining analyses showed inconsistent trends, such as MS which increased, decreased, and stayed the same depending on the sample. Even the PSA wasn't consistent. This is not necessarily surprising as the spalls vary in size and generally fall into the medium to very coarse pebble size (Wentworth 1922).

While only a minimal window into Zone 1 was available from this investigation, it does seem to support previous investigators' interpretations. During the original investigations by Dibble, he suggested that Zone 1 largely formed through mechanical weathering of the roof with some exogenous material being introduced from notch above

(Dibble and Lorrain 1968: 26-27). Additionally, he suggested that the mass amount and sharp angular nature of the spalls indicated that this Late Pleistocene zone was deposited during a wetter and colder period of time which was supported by later pollen and stratigraphic analyses (Cummings 1990; Robison 1997).

Bone Bed 2

Within the talus cone, Bone Bed 2 lies between Dibble's Zone 1 and Zone 2 (Dibble and Lorrain 1968). Dibble's initial interpretation of Bone Bed 2 included three stratigraphic units, Components A through C, within Bone Bed 2. From top to bottom, they consist of an upper unburned layer of bone and sandy silt sediment, a thin middle layer of carbon-stained silt and burned bone, and a lower layer of unburned bone and sandy silt similar to the upper layer (Dibble and Lorrain 1968:29). It is this very distinct layering that has been the most popular reason for justifying the hypothesis that multiple cultural events are represented.

In the talus cone, Bone Bed 2 is represented by strata 11, 12, 13, 14 and their various substrata. Overall, Bone Bed 2 does indeed appear to have formed as the result of a bison drive event. This can be seen in various analyses as spikes or decreases in values across all five column samples. Specifically, spikes in MS, gypsum, calcium carbonate, and organic carbon generally occurred once or twice in each column's represented portion of Bone Bed 2. This is similar to the single spike which occurred in those same analyses at the base of Bone Bed 3 in both CS01 and CS02. Also, fining upwards sequences in coarse and fine grain PSA were noted in all five representations of Bone Bed 2, as well as the two Bone Bed 3 samples of CS01 and CS02.

What is less clear is how many events are represented. The locations of the columns within the talus cone and subsequent depositional processes on the different areas of the cone, make it difficult to infer cross-cone depositional events. Sample size of two columns (CS02 and CS08) is too small (i.e., only a partial representation of Bone Bed 2) and cannot be used to determine number of events per the methods utilized in this thesis. The remaining three columns do suggest at least one event with a possibility of two total events. As discussed in the previous chapter, I conclude that a minimum number of two events are represented in Bone Bed 2. This is particularly clear in column CS06 which, based on its location in the cone, has the best-preserved representation of Bone Bed 2.

The issue being that the two potential events do not correlate between columns or sometimes even within a single column. For example, CS06 suggests that two drives may have occurred in strata 11 and 13 or possibly in strata 12 and 14b. In sum, the results of this thesis cannot definitively characterize the depositional events occurring in Bone Bed 2. It does provide a broad overview of the cone which can be used in the future for more refined hypotheses which should include running the fine PSA column samples collected in 2019 with a focus on the southern portion of the cone and specifically CS06. The lessons learned and future research suggestions are outlined in further detail in the concluding chapter.

Zone 2

Zone 2 lies between Bone Bed 2 and Bone Bed 3. Within the talus cone, it is described as talus debris which is tan to light gray silt intermixed with various sizes of limestone spalls (Dibble and Lorrain 1968:26). In contrast, Zone 2 within the shelter

interior was divided into two subzones: Zone 2a and Zone 2b. Dibble proposed that these two zones actually formed simultaneously due to the positioning of Bone Bed 2 in relation to the zones (Dibble and Lorrain 1968:29). Within the shelter interior Zone 2a underlies Bone Bed 2, while within the talus cone Bone Bed 2 is found within Zone 2b. This suggests that Zone 2a began to accumulate within the shelter interior while Zone 2b was accumulating on the talus cone. After Bone Bed 2 was deposited, both zones continued to accumulate resulting in Bone Bed 2 overlying and underlying portions of Zone 2a and 2b.

Based on stratigraphic designations provided in this thesis, Zone 2 encompasses strata 6, 7, 8, 9, 10, and their various substrata. Dibble noted that Zone 2 contained smaller, often more weathered spalls and an increase in silt from the underlying Zone 1 (1968: 27). He suggested that this zone was deposited during a warmer interval when less freeze-thaw was occurring and materials were predominately being deposited via alluvial mechanisms through the notch. This can be seen in some of the columns as increases in calcium carbonate specifically in the uppermost and lowermost portions of Zone 2. Additionally, the PSA data across the columns appears to be more dynamic throughout Zone 2 with increases in the silt content throughout the zone (CS01, CS02, and CS06). The bulk sampling of columns cannot provide more detail to the history of Zone 2, but does appear to confirm Dibble's initial interpretations. Finer samples could define specific depositional event within the zone that could then be tied to paleoenvironmental data from the region.

Bone Bed 3

Bone Bed 3 is the thickest and most obvious bone bed in the talus cone. It is generally centered at the apex of the cone and is predominantly exposed on the northern face of the cone. The portions of Bone Bed 3 on the southern and eastern portion of the cone lay on the current eroded surface and were not incorporated into columns on those faces. As noted by Dibble, this zone is a massive jumble of bone with little to no silt inclusions and has been heavily scorched and intensely burned (1968: 42). While no analysis, until this point, has been done on Bone Bed 3 by ASWT, little evidence has come to light that contradicts the interpretation that it represents one mass bison drive event. This was confirmed by my analyses.

In both CS01 and CS02 there are almost unanimous results that Bone Bed 3 is a bison drive and a single event. While there is little sediment, the layers are heavily mixed with no clear orientation to the bones or rocks. All laboratory analyses point to one clear spike in values and one clear fining upwards trend in PSA. Overall, my research has shown that Bone Bed 3 is a suitable representative of what a single bison drive would look like and makes a valuable comparison for other bone beds. This comes with the caveat that Bone Bed 3 is young, in relation to Bone Bed 2, and as such strong consideration of post depositional processes must be given. Nonetheless, it does provide a valid basis for hypothesizing and framing analyses for future research.

Rate of Accumulation

One of the things I had hoped to do across the cone was calculate the rate of accumulation across the four depositional units in the talus cone. The goal being to look at how the bone bed layers compare to the non-bone bed layers with the assumption that

bone beds formed as the result of a bison drive should have a higher rate of accumulation over a short period of time. The apex of the cone and CS01 and CS06 are presumed to be the best-preserved location of not only the bone beds, but the interlaying Zone 2. The north face of the cone and CS01 is the only location with Bone Bed 2, Zone 2, and Bone Bed 3 represented. As such, it was used to calculate the rate of accumulation for the cone (Table 7.1.).

First, I estimated the thickness of Bone Bed 2, Zone 2, and Bone Bed 3 from elevation data collected during the excavation of CS01. I then calculated the temporal span for each unit. For Bone Bed 3, an estimated span of 10 years was applied with the assumption that this bone bed is a single event and that material continued to be contributed for a time after the drive event. Bone Bed 2 was estimated to be 1,000 years to include both the Folsom and Plainview components. I then calculated the rate of accumulation which is the thickness of the accumulation in centimeters divided by the duration of accumulation in years for Bone Bed 2, Zone 2, and Bone Bed 3 (Table 7.1).

Table 7.1. Rate of Accumulation in CS01.

CS01 Zones	**Thickness**	**Temporal Span (years)**	**Rate (cm per year)**
Bone Bed 3	68	10*	6.8
Zone 2	70	9,000	0.008
Bone Bed 2	30	1,000	0.03

Bone Bed 3 is anomalously large due to being a single event, being comprised mostly of bone, and being less compressed. Unsurprisingly, Bone Bed 3 has a very high rate of sedimentation. A more interesting trend is the one seen in Bone Bed 2 and especially when you compare it with Zone 2. The rate of accumulation for Bone Bed 2 is

nearly an order of magnitude greater than Zone 2. This is true even when Bone Bed 2 was given an assumed temporal span of 1,000 years to include both events. Based on my calculations, Bone Bed 2 accumulated four times faster than Zone 2. A rate much faster than the overlaying natural deposits and suggesting that it is a bison drive event.

VIII. LESSONS LEARNED AND FUTURE WORK

Despite some of the drawbacks of my methods, I do feel like we have firmly addressed one of the research questions: Bone Bed 2 clearly fits the model of a bison drive event. Less definitive are the number of events represented within. While I cannot fully address that question, there are several columns that point to the possibility of multiple cultural events, and at a minimum there are two bison drive events represented within Bone Bed 2. I would recommend that a future analyst should run the fine samples collected in 2019 to compare and build a more refined depositional model.

This should be done on the south wall of the cone to address the question of Bone Bed 2. Ideally, both the corresponding samples for CS06 and CS07 would be run. This would not only aid in addressing the number of events represented but may also help us understand why the three stratigraphically distinct zones of Bone Bed 2 are only seen at the toe of the cone (CS07) and not as clearly within CS06. I believe that the deposits within CS07 represent downslope facies of the two bison drive events represented in Bone bed 2, but further analysis is needed to evaluate this hypothesis.

Next, the samples parallel to CS01 and CS02 should be analyzed. Looking at the northern face of the cone would better address questions on Bone Bed 3 as well as the intervening Zone 2. I think it would be valuable to interpret both units to build a fuller idea of what bone bed versus non-bone bed strata look like. Further analysis of Zone 2 would also be valuable in addressing questions about paleoenvironment. If different depositional units could be identified within Zone 2, then determinations of climatic conditions could be discerned.

When I began this thesis, I had grand ideas of presenting a much more thorough depositional model of the talus cone. What this thesis has actually done is lay the groundwork for future models. There are a number of things that could have been done differently to present a more precise picture of the talus cone and Bone Bed 2.

First of all, the sampling should have been finer. I wanted to come up with a full cross-cone picture and decided to run all five columns. This only provided a broad picture as many of strata samples had upwards of 20-plus gallons of dirt. Running one MS sample from thick strata was not sufficient to address questions on individual depositional events. This was slightly less of an issue with the finer strata within Bone Bed 2, yet how can I be sure that the one sample I pulled is representative of the entire stratum? I did assist in the collection of 10-cm samples in correlation with each column after I began analysis. The hope was to incorporate them as needed but running only the bulk samples proved to be cumbersome enough.

Additionally, I should have been more careful documenting and collected cobbles and boulders. I aided in the collection of three of the five columns, but this was before I had signed on for this project. The cumbersome nature of the larger rocks means there was certainly sampling biases occurring during collection. This is most evident in CS07 which has no cobbles for Stratum 14 (they were most likely lumped into Stratum 14b which was split during excavation).

Finally, now that we have analyses for all five columns, it is clear that not all columns are created equal. Some columns are better suited to address questions on Bone Bed 3 (CS01 and CS02) while others are better for Bone Bed 2 (CS06 and CS07). While I am glad to have provided data for the entirety of the cone, I should have focused on one

face of the talus cone (the south side) so I could more thoroughly address the research questions.

What this thesis does accomplish is to present a mass of data and some initial geoarchaeological interpretations on the bone beds and talus cone at Bonfire Shelter. As this the is the first attempt to analyze sediment samples from Bonfire with an emphasis on Bone Bed 2, it simply stands as a steppingstone for future research and hopefully a learning tool on how to better address the site. With the data presented here, a number of new questions can be asked, and further research done to better our understanding of Paleoindian lifeways in Texas.

While more research is warranted, my results coupled with the recent conclusions by James Ramsey (2020) have provided some new information on the Paleoindian component at Bonfire Shelter. This is particularly true of his determination that Bone Bed 2 appears to have accumulated as a result of a bison drive. We can now confidently say that bison drives have been occurring at the site since the Late Pleistocene. This changes our current understandings of Paleoindian subsistence methods as well as expands the previous accepted region understood to be utilized in bison drive hunting techniques.

Also, while I cannot say how many events are definitively represented within Bone Bed 2, we can now see there are at least two bison drive events. This coupled with the occurrence of both Plainview and Folsom technology at Bonfire suggests a continued tradition and knowledge of the landscape. Further work is needed to understand how these two cultural groups relate to the recognized bison drives, but there are two obvious options: groups were coming together and using Bonfire repeatedly through time, or the knowledge is being passed down through time between cultural groups.

APPENDIX SECTION

Appendix A.1. Raw Data Collected: LOI, Calcium Carbonate Content, Organic Carbon Content, Magnetic Susceptibility

Sample (Column No. - Strata No.)	Top Elevation of Sample (cmbs)	LOI			Chittick	KECK Lab	Magnetic Susceptibility		
		Gypsum %	Calcium Carbonate %	Organic Carbon %	Calcium Carbonate %	Organic Carbon %	Xhf	Xlf	Xfd
1-3	0	5.45	3.22	0.85	38.50	0.64	85.47	95.73	10.72
1-4	37	0.89	2.85	0.52	45.00	0.46	240.15	271.09	11.41
1-5	59	3.12	1.68	0.65	31.00	1.59	327.54	372.88	12.16
1-6	62	6.39	4.28	1.34	38.00	0.90	59.45	60.22	1.28
1-7	65	4.64	4.99	0.90	41.50	0.27	49.40	48.90	-1.03
1-8	70	2.60	6.38	0.71	43.00	0.21	46.05	45.78	-0.58
1-9	85	3.13	5.15	0.85	37.00	0.23	48.41	48.52	0.23
1-10	115	4.20	4.14	1.13	35.50	0.16	36.92	36.06	-2.38
1-11	162	7.13	3.08	1.01	29.00	0.12	53.60	53.17	-0.80
1-12	184	5.93	3.85	1.07	32.50	0.24	59.70	59.52	-0.31
1-13	198	6.41	3.84	0.99	30.00	0.14	46.60	46.32	-0.59
1-14	211	6.32	3.30	1.29	25.00	0.12	49.68	49.26	-0.86
1-15	226	4.81	5.04	0.88	40.00	0.11	54.53	54.23	-0.54
2-2	0	1.69	4.93	1.15	50.00	0.70	48.56	49.27	1.45
2-3	23	1.52	2.85	0.76	41.00	0.31	60.22	63.74	5.52
2-4	40	3.12	3.89	0.66	55.00	0.83	166.85	182.82	8.73
2-6a	47	1.49	5.87	0.60	66.00	0.65	80.33	85.17	5.69
2-6b	50	0.57	7.45	0.41	78.50	0.38	40.28	40.82	1.34
2-7	55	0.62	6.43	0.42	69.00	0.25	43.63	42.87	-1.78
2-8a	65	1.91	5.98	0.54	61.50	0.28	62.39	62.28	-0.17
2-8b	75	1.20	5.74	0.55	60.00	0.19	62.73	62.22	-0.80

Sample (Column No. - Strata No.)	Top Elevation of Sample (cmbs)	LOI			Chittick	KECK Lab	Magnetic Susceptibility		
		Gypsum %	Calcium Carbonate %	Organic Carbon %	Calcium Carbonate %	Organic Carbon %	Xhf	Xlf	Xfd
2-8c	80	1.40	5.33	0.71	52.50	0.18	66.49	65.89	-0.91
2-9	90	1.55	5.50	0.84	53.00	0.18	59.22	58.91	-0.52
2-10a	98	1.96	5.22	0.66	49.00	0.18	62.80	61.69	-1.80
2-10b	128	4.34	5.22	0.63	55.00	0.18	44.11	43.05	-2.45
2-11a	170	6.84	2.91	1.10	30.00	0.13	52.73	51.52	-2.35
2-11b	185	5.51	2.93	1.21	28.00	0.19	49.64	48.31	-2.76
6-10a	0	2.11	4.05	0.63	84.50	0.34	96.47	97.22	0.77
6-10b	13	3.68	4.33	0.88	41.00	0.23	72.71	73.62	1.23
6-10c	39	4.49	4.38	0.98	35.50	0.24	47.10	48.18	2.23
6-11	49	5.54	3.45	1.14	29.00	0.20	52.26	54.07	3.35
6-11c	64	5.95	3.41	0.99	31.00	0.21	64.63	66.25	2.44
6-12	69	7.84	3.31	0.91	34.00	0.48	118.65	124.31	4.56
6-12b	75	—	—	—	—	—	75.10	78.08	3.83
6-13	94	3.94	3.70	0.97	31.00	0.13	52.73	53.71	1.83
6-14	104	3.13	4.39	0.79	36.00	0.12	53.26	54.13	1.61
6-14b	115	3.63	4.23	0.83	36.00	0.14	57.44	58.45	1.73
6-15	120	3.57	4.08	0.80	37.00	0.12	67.14	68.28	1.68
7-11	0	12.94	3.29	1.06	30.00	0.28	51.10	51.79	1.34
7-12b	28	5.79	2.30	1.19	22.00	2.38	75.10	78.08	3.83
7-14	38	9.86	2.10	1.49	22.00	0.57	73.41	74.59	1.57
7-14b	48	16.97	1.81	1.37	18.00	0.24	46.30	46.94	1.36
7-15	63	8.42	4.09	0.87	35.00	0.18	57.58	58.32	1.26

Sample (Column No. - Strata No.)	Top Elevation of Sample (cmbs)	LOI			Chittick	KECK Lab	Magnetic Susceptibility		
		Gypsum %	Calcium Carbonate %	Organic Carbon %	Calcium Carbonate %	Organic Carbon %	Xhf	Xlf	Xfd
8-8	0	2.32	5.36	0.60	57.00	0.21	55.26	55.77	0.92
8-10a	55	1.20	6.32	0.61	60.00	0.18	45.21	45.21	0.00
8-10b	65	2.08	5.47	0.73	57.00	0.20	46.22	46.97	1.59
8-10c	70	2.52	4.53	0.89	35.00	0.20	35.67	36.29	1.72
8-11	75	6.66	3.33	1.00	27.00	0.13	48.03	48.60	1.18
8-14b	90	8.44	1.65	1.32	13.00	0.22	40.59	41.25	1.60
8-15	100	1.11	6.99	0.60	63.00	0.23	21.69	22.03	1.53

Appendix A.2. Raw Data Collected: Fine Grain Particle Size and Descriptive Statistics

		Percent Fine PSA (μm)							Descriptive Statistics			
Sample (Column No. -Strata No.)	**Top Elevation of Sample (cmbs)**	**Coarse Sand (2000-500)**	**Middle Sand (500-200)**	**Fine Sand (200-50)**	**Coarse Silt (55-20)**	**Middle Silt (20-5.0)**	**Fine Silt (5.0-2.0)**	**Clay (<2)**	**Mean**	**Sorting**	**Skewness**	**Kurtosis**
1-3	0	27.86	26.76	20.92	9.29	12.95	2.21	0.01	Fine Sand	Very Poorly Sorted	Fine Skewed	Mesokurtic
1-4	37	42.52	27.22	13.24	8.56	8.01	0.43	0.01	Medium Sand	Very Poorly Sorted	Very Fine Skewed	Mesokurtic
1-5	59	19	40.53	16.31	8.84	14.89	0.41	0.02	Fine Sand	Very Poorly Sorted	Very Fine Skewed	Mesokurtic
1-6	62	31.48	25.81	21.64	10.21	10.26	0.59	0.01	Fine Sand	Very Poorly Sorted	Fine Skewed	Mesokurtic
1-7	65	41	23.13	11.63	11.28	11.34	1.61	0.01	Fine Sand	Very Poorly Sorted	Very Fine Skewed	Platykurtic
1-8	70	51.89	16.96	8.67	8.08	12.16	2.23	0.01	Medium Sand	Very Poorly Sorted	Very Fine Skewed	Platykurtic
1-9	85	39.99	20.3	10.96	15.71	11.67	1.36	0.01	Fine Sand	Very Poorly Sorted	Very Fine Skewed	Platykurtic
1-10	115	28.26	26.98	17.25	9.58	14.89	3.03	0.01	Fine Sand	Very Poorly Sorted	Very Fine Skewed	Platykurtic

		Percent Fine PSA (µm)							Descriptive Statistics			
Sample (Column No. -Strata No.)	**Top Elevation of Sample (cmbs)**	**Coarse Sand (2000-500)**	**Middle Sand (500-200)**	**Fine Sand (200-50)**	**Coarse Silt (55-20)**	**Middle Silt (20-5.0)**	**Fine Silt (5.0-2.0)**	**Clay (<2)**	**Mean**	**Sorting**	**Skewness**	**Kurtosis**
1-11	162	30.5	31.79	5.64	9.6	18.7	3.77	0.01	Fine Sand	Very Poorly Sorted	Very Fine Skewed	Platykurtic
1-12	184	34.74	32.35	1.17	9.19	18.92	3.6	0.03	Fine Sand	Very Poorly Sorted	Very Fine Skewed	Platykurtic
1-13	198	25.68	33.97	10.99	12.77	14.39	2.18	0.02	Fine Sand	Very Poorly Sorted	Very Fine Skewed	Platykurtic
1-14	211	28.05	35.76	6.33	13.19	14.41	2.25	0.01	Fine Sand	Very Poorly Sorted	Very Fine Skewed	Platykurtic
1-15	226	42.41	27.31	2.04	10.71	15.54	1.96	0.02	Fine Sand	Very Poorly Sorted	Very Fine Skewed	Platykurtic
2-2	0	43.93	32.76	0.06	9.31	13.32	0.6	0.02	Fine Sand	Very Poorly Sorted	Very Fine Skewed	Very Leptokurtic
2-3	23	31.79	40.56	5.67	10.93	10.86	0.18	0.01	Fine Sand	Very Poorly Sorted	Very Fine Skewed	Leptokurtic
2-4	40	29.49	24.08	23.65	13.66	9.09	0.03	0	Fine Sand	Very Poorly Sorted	Fine Skewed	Platykurtic
2-6a	47	31.27	26	22.26	11.61	8.73	0.13	0	Fine Sand	Very Poorly Sorted	Fine Skewed	Platykurtic

		Percent Fine PSA (µm)							Descriptive Statistics			
Sample (Column No. -Strata No.)	**Top Elevation of Sample (cmbs)**	**Coarse Sand (2000-500)**	**Middle Sand (500-200)**	**Fine Sand (200-50)**	**Coarse Silt (55-20)**	**Middle Silt (20-5.0)**	**Fine Silt (5.0-2.0)**	**Clay (<2)**	**Mean**	**Sorting**	**Skewness**	**Kurtosis**
2-6b	50	32.35	25.02	22.31	10.21	9.85	0.25	0.01	Fine Sand	Very Poorly Sorted	Fine Skewed	Mesokurtic
2-7	55	26.78	15.14	28.59	15.93	11.95	1.59	0.02	Fine Sand	Very Poorly Sorted	Symmetrical	Platykurtic
2-8a	65	25.89	17.46	28.27	18.85	9.41	0.02	0.02	Fine Sand	Very Poorly Sorted	Symmetrical	Platykurtic
2-8b	75	27.95	16.25	25.78	19.85	9.41	0.74	0.02	Fine Sand	Very Poorly Sorted	Symmetrical	Platykurtic
2-8c	80	25.55	15.54	27.67	20.01	10.75	0.45	0.03	Fine Sand	Very Poorly Sorted	Symmetrical	Platykurtic
2-9	90	29.91	18.58	22.85	18.26	10	0.39	0.01	Fine Sand	Very Poorly Sorted	Fine Skewed	Platykurtic
2-10a	98	24.17	18.5	19.12	22.49	13.92	1.78	0.02	Very Fine Sand	Very Poorly Sorted	Symmetrical	Platykurtic
2-10b	128	22.45	16.71	27.81	19.99	12.34	0.7	0	Fine Sand	Very Poorly Sorted	Symmetrical	Platykurtic
2-11a	170	20.87	29.5	23.32	15.35	10.81	0.15	0	Fine Sand	Very Poorly Sorted	Fine Skewed	Mesokurtic

		Percent Fine PSA (µm)							Descriptive Statistics			
Sample (Column No. -Strata No.)	**Top Elevation of Sample (cmbs)**	**Coarse Sand (2000-500)**	**Middle Sand (500-200)**	**Fine Sand (200-50)**	**Coarse Silt (55-20)**	**Middle Silt (20-5.0)**	**Fine Silt (5.0-2.0)**	**Clay (<2)**	**Mean**	**Sorting**	**Skewness**	**Kurtosis**
2-11b	185	34.24	29.77	11.88	13.73	10.02	0.34	0.02	Fine Sand	Very Poorly Sorted	Very Fine Skewed	Platykurtic
6-10a	0	30.14	22.7	11.3	19.04	13.28	3.54	0	Fine Sand	Very Poorly Sorted	Very Fine Skewed	Platykurtic
6-10b	13	23.47	27.09	13.72	15.6	13.04	7.06	0.02	Very Fine Sand	Very Poorly Sorted	Very Fine Skewed	Platykurtic
6-10c	39	50.24	20.61	0.08	7.39	17.91	3.77	0	Fine Sand	Very Poorly Sorted	Very Fine Skewed	Very Platykurtic
6-11	49	46.24	21.46	0.05	8.99	19.73	3.52	0.01	Fine Sand	Very Poorly Sorted	Very Fine Skewed	Very Platykurtic
6-11c	64	42.93	28.01	0.11	5.21	20.42	3.31	0.01	Fine Sand	Very Poorly Sorted	Very Fine Skewed	Very Platykurtic
6-12	69	33.88	31.28	11.71	11.05	11.61	0.46	0.01	Fine Sand	Very Poorly Sorted	Very Fine Skewed	Platykurtic
6-12b	75	—	—	—	—	—	—	—	Fine Sand	Very Poorly Sorted	Very Fine Skewed	Platykurtic
6-13	94	57.98	3.18	0.07	1.42	19.89	17.45	0.01	Fine Sand	Very Poorly Sorted	Very Fine Skewed	Very Platykurtic

		Percent Fine PSA (µm)							Descriptive Statistics			
Sample (Column No. -Strata No.)	**Top Elevation of Sample (cmbs)**	**Coarse Sand (2000-500)**	**Middle Sand (500-200)**	**Fine Sand (200-50)**	**Coarse Silt (55-20)**	**Middle Silt (20-5.0)**	**Fine Silt (5.0-2.0)**	**Clay (<2)**	**Mean**	**Sorting**	**Skewness**	**Kurtosis**
6-14	104	39.85	24.51	0.16	4.32	21.03	10.14	0	Very Fine Sand	Very Poorly Sorted	Very Fine Skewed	Very Platykurtic
6-14b	115	51.65	19.37	0.09	9	18.37	1.52	0	Fine Sand	Very Poorly Sorted	Very Fine Skewed	Very Platykurtic
6-15	120	46.79	17.38	0.08	6.79	18.41	10.53	0.01	Fine Sand	Very Poorly Sorted	Very Fine Skewed	Very Platykurtic
7-11	0	30.09	31.14	10.18	14.94	12.33	1.31	0.01	Fine Sand	Very Poorly Sorted	Very Fine Skewed	Platykurtic
7-12b	28	33.11	28.99	10.25	10.28	16.17	1	0.02	Fine Sand	Very Poorly Sorted	Very Fine Skewed	Platykurtic
7-14	38	31.14	32.1	8.13	11.32	15.95	1.35	0.01	Fine Sand	Very Poorly Sorted	Very Fine Skewed	Leptokurtic
7-14b	48	40.43	33.72	3.36	7.09	13.91	1.48	0.01	Fine Sand	Very Poorly Sorted	Very Fine Skewed	Very Platykurtic
7-15	63	45.76	21.02	0.08	10.35	20.67	2.11	0.01	Fine Sand	Very Poorly Sorted	Fine Skewed	Platykurtic
8-8	0	27.96	19.43	21.44	21.19	9.88	0.08	0.01	Fine Sand	Very Poorly Sorted	Very Fine Skewed	Platykurtic

		Percent Fine PSA (µm)							Descriptive Statistics			
Sample (Column No. -Strata No.)	**Top Elevation of Sample (cmbs)**	**Coarse Sand (2000-500)**	**Middle Sand (500-200)**	**Fine Sand (200-50)**	**Coarse Silt (55-20)**	**Middle Silt (20-5.0)**	**Fine Silt (5.0-2.0)**	**Clay (<2)**	**Mean**	**Sorting**	**Skewness**	**Kurtosis**
8-10a	55	30.9	19.56	21.47	17.1	10.56	0.4	0.01	Very Fine Sand	Very Poorly Sorted	Fine Skewed	Platykurtic
8-10b	65	23.08	19.26	24.63	19.61	13.04	0.37	0.01	Fine Sand	Very Poorly Sorted	Fine Skewed	Platykurtic
8-10c	70	20.05	25.53	24.17	17.85	11.7	0.69	0.01	Fine Sand	Very Poorly Sorted	Very Fine Skewed	Platykurtic
8-11	75	24.1	32.08	20.89	12.51	10.16	0.24	0.01	Fine Sand	Very Poorly Sorted	Very Fine Skewed	Mesokurtic
8-14b	90	36.91	34.32	7.33	8.26	11.89	1.28	0.01	Fine Sand	Very Poorly Sorted	Very Fine Skewed	Platykurtic
8-15	100	38.28	24.04	7.56	14.17	14.15	1.79	0.01	Fine Sand	Very Poorly Sorted	Very Fine Skewed	Platykurtic

Appendix A.3. Raw Data Collected: Coarse Grain Particle Size

		Percent Coarse PSA								
Sample (Column No. - Strata No.)	**Top Elevation of Sample (cmbs)**	**Boulder**	**Cobbles 3**	**Cobbles 2**	**Cobbles 1**	**Very Coarse Pebble**	**Coarse Pebble**	**Medium Pebble**	**Fine Pebble**	**Very Fine Pebble**
1-3	0	0.00	0.00	4.30	12.60	4.60	2.20	7.90	8.10	60.30
1-4	37	0.00	21.88	26.83	16.26	18.51	3.50	3.55	1.25	8.21
1-5	59	0.00	0.00	0.00	44.71	12.59	0.00	12.76	7.89	22.04
1-6	62	0.00	0.00	3.86	8.30	22.22	15.46	20.42	14.99	14.76
1-7	65	0.00	0.00	5.28	13.12	23.64	13.06	20.58	13.65	10.67
1-8	70	0.00	8.28	4.58	10.36	17.95	16.76	18.21	12.88	10.98
1-9	85	0.00	8.09	7.57	16.70	21.47	14.27	16.05	8.68	7.16
1-10	115	0.00	8.68	23.90	21.12	26.98	5.69	7.49	3.66	2.48
1-11	162	0.00	9.07	20.45	16.81	18.44	11.22	13.36	5.76	4.88
1-12	184	0.00	7.16	13.89	15.86	27.37	10.47	13.40	6.09	5.76
1-13	198	0.00	0.00	11.33	20.51	25.64	15.90	14.40	6.97	5.24
1-14	211	0.00	4.74	17.82	22.25	21.35	13.94	10.50	5.09	4.31
1-15	226	0.00	0.00	3.42	11.40	28.44	16.38	20.78	11.53	8.05
2-2	0	0.00	23.38	9.84	11.21	15.36	10.47	12.61	9.31	7.82
2-3	23	0.00	0.00	2.83	19.89	11.26	4.58	11.04	7.38	43.02
2-4	40	0.00	9.31	15.46	5.00	4.76	6.49	19.59	20.91	18.49
2-6a	47	0.00	0.00	1.93	0.00	3.99	11.73	24.02	32.09	26.25
2-6b	50	0.00	0.00	0.00	1.74	4.01	9.12	19.23	30.57	35.34
2-7	55	0.00	0.00	12.15	13.40	20.59	7.85	20.37	14.82	10.81
2-8a	65	0.00	0.00	7.07	3.71	9.58	13.04	30.87	19.63	16.10
2-8b	75	0.00	0.00	2.75	10.57	22.16	12.92	23.15	15.98	12.47
2-8c	80	0.00	2.97	16.07	16.90	22.16	14.55	14.72	7.46	5.17
2-9	90	0.00	5.31	28.82	21.20	19.29	4.68	9.42	6.78	4.52
2-10a	98	0.00	11.23	17.55	18.23	26.81	7.15	8.13	4.82	6.08
2-10b	128	3.68	12.21	26.13	22.54	18.69	2.79	5.49	4.80	3.67
2-11a	170	0.00	12.07	29.08	9.78	11.03	4.42	11.37	9.16	13.08
2-11b	185	0.00	8.17	38.29	15.68	16.40	0.86	5.57	6.60	8.44

		Percent Coarse PSA								
Sample (Column No. - Strata No.)	**Top Elevation of Sample (cmbs)**	**Boulder**	**Cobbles 3**	**Cobbles 2**	**Cobbles 1**	**Very Coarse Pebble**	**Coarse Pebble**	**Medium Pebble**	**Fine Pebble**	**Very Fine Pebble**
6-10a	0	0.00	22.36	0.00	12.83	24.87	9.07	15.03	8.68	7.16
6-10b	13	0.00	3.18	5.52	6.66	13.83	18.54	29.34	13.00	9.93
6-10c	39	0.00	13.57	19.48	15.08	20.63	7.02	13.47	5.88	4.88
6-11	49	0.00	0.00	0.00	10.78	11.63	18.10	27.15	18.50	13.83
6-11c	64	0.00	13.42	1.54	8.60	13.13	21.49	20.76	10.32	10.74
6-12	69	0.00	0.00	9.48	13.77	18.39	16.43	19.58	11.93	10.42
6-12b	75	—	—	—	—	—	—	—	—	—
6-13	94	0.00	0.00	0.00	24.48	14.90	0.00	5.28	8.12	47.22
6-14	104	0.00	8.47	8.14	12.96	8.16	15.23	22.59	12.62	11.83
6-14b	115	0.00	0.00	6.70	19.81	18.94	15.22	22.78	9.21	7.34
6-15	120	0.00	3.86	0.00	7.00	20.35	22.57	25.36	11.52	9.33
7-11	0	0.00	9.53	10.36	7.84	14.31	22.97	20.42	7.69	6.88
7-12b	28	0.00	0.00	9.53	8.73	7.30	16.41	24.55	15.12	18.35
7-14	38	0.00	0.00	0.00	0.00	6.30	13.82	10.88	21.75	47.25
7-14b	48	0.00	19.34	24.70	10.58	6.31	6.48	3.51	4.50	24.58
7-15	63	0.00	3.96	21.93	19.50	12.15	6.90	11.79	10.40	13.36
8-8	0	0.00	0.00	2.33	13.98	11.17	17.93	20.30	19.75	14.54
8-10a	55	0.00	0.00	0.00	3.05	5.46	24.87	23.05	25.80	17.78
8-10b	65	0.00	0.00	12.28	3.03	5.94	13.79	20.47	23.07	21.42
8-10c	70	0.00	18.67	8.32	13.54	6.17	3.84	16.68	16.76	16.03
8-11	75	0.00	0.00	9.52	2.68	4.62	4.73	14.08	44.44	19.93
8-14b	90	0.00	0.00	18.90	8.10	4.44	2.85	12.53	14.81	38.38
8-15	100	0.00	18.25	7.89	8.38	14.37	13.03	19.27	11.91	6.89

Appendix A.4 Raw Data Collected: Carbon-Nitrogen Isotopic Results

		Isotopic Results		Carbonates Removed			Original Sample	
Sample (Column No. -Strata No.)	**Top Elevation of Sample (cmbs)**	**$d^{15}N$ vs. Air**	**$d^{13}C$ VPDB**	**N%**	**C%**	**C/N**	**N%**	**C%**
1-3	0	10.74	-23.39	0.13	1.07	8.25	0.08	0.64
1-4	37	12.76	-22.97	0.14	1.21	8.57	0.08	0.70
1-5	59	11.36	-25.64	0.08	0.86	10.52	0.04	0.46
1-6	62	13.79	-23.41	0.07	0.54	7.97	0.04	0.31
1-7	65	21.85	-20.04	0.24	1.47	6.04	0.14	0.83
1-8	70	21.23	-20.48	0.21	1.16	5.48	0.12	0.65
1-9	85	21.58	-20.58	0.15	0.69	4.54	0.08	0.38
1-10	115	14.61	-21.93	0.07	0.45	6.58	0.04	0.25
1-11	162	18.01	-21.54	0.44	2.70	6.08	0.26	1.59
1-12	184	12.38	-22.02	0.07	0.47	7.03	0.04	0.28
1-13	198	14.84	-20.47	0.26	1.38	5.28	0.17	0.90
1-14	211	11.17	-22.76	0.05	0.33	6.77	0.03	0.19
1-15	226	10.96	-22.84	0.09	0.42	4.49	0.06	0.27
2-2	0	10.36	-22.75	0.05	0.30	6.11	0.03	0.18
2-3	23	9.20	-23.34	0.08	0.36	4.61	0.05	0.21
2-4	40	9.80	-23.18	0.05	0.30	6.24	0.03	0.18
2-6a	47	9.07	-24.13	0.08	0.37	4.96	0.05	0.23
2-6b	50	9.54	-22.97	0.05	0.29	5.84	0.03	0.18
2-7	55	10.11	-23.93	0.07	0.25	3.51	0.05	0.16
2-8a	65	10.65	-22.87	0.05	0.30	6.22	0.03	0.18
2-8b	75	7.28	-25.19	0.04	0.17	3.89	0.03	0.12
2-8c	80	12.75	-22.70	0.06	0.20	3.43	0.04	0.13
2-9	90	16.83	-20.17	0.07	0.29	4.00	0.05	0.19
2-10a	98	16.08	-20.71	0.08	0.38	4.59	0.05	0.24
2-10b	128	12.75	-22.75	0.06	0.21	3.80	0.04	0.14

		Isotopic Results		Carbonates Removed			Original Sample	
Sample (Column No. -Strata No.)	**Top Elevation of Sample (cmbs)**	**$d^{15}N$ vs. Air**	**$d^{13}C$ VPDB**	**N%**	**C%**	**C/N**	**N%**	**C%**
2-11a	170	10.03	-23.76	0.05	0.18	3.65	0.03	0.12
2-11b	185	7.63	-24.90	0.03	0.17	5.07	0.02	0.11
6-10a	0	11.63	-23.27	0.10	0.54	5.58	0.06	0.34
6-10b	13	10.46	-23.88	0.08	0.36	4.45	0.05	0.23
6-10c	39	10.67	-23.60	0.09	0.38	4.29	0.06	0.24
6-11	49	11.10	-23.83	0.08	0.31	3.90	0.05	0.20
6-11c	64	13.89	-22.40	0.09	0.33	3.70	0.06	0.21
6-12	69	18.80	-19.02	0.21	0.72	3.40	0.14	0.48
6-12b	75	—	—	—	—	—	—	—
6-13	94	11.82	-24.52	0.06	0.20	3.32	0.04	0.13
6-14	104	8.60	-24.86	0.04	0.20	4.57	0.03	0.12
6-14b	115	9.14	-24.97	0.05	0.22	4.54	0.03	0.14
6-15	120	8.75	-24.88	0.04	0.18	4.79	0.03	0.12
7-11	0	16.70	-19.94	0.09	0.43	4.89	0.06	0.28
7-12b	28	16.69	-13.38	0.70	3.52	5.03	0.47	2.38
7-14	38	17.28	-16.84	0.18	0.87	4.88	0.12	0.57
7-14b	48	17.56	-21.08	0.08	0.35	4.29	0.06	0.24
7-15	63	13.44	-24.51	0.05	0.29	5.71	0.03	0.18
8-8	0	13.02	-22.73	0.06	0.36	6.25	0.03	0.21
8-10a	55	12.17	-23.35	0.05	0.32	6.02	0.03	0.18
8-10b	65	11.20	-23.27	0.05	0.34	6.97	0.03	0.20
8-10c	70	12.42	-23.23	0.05	0.33	6.61	0.03	0.20
8-11	75	14.31	-22.61	0.05	0.20	4.09	0.03	0.13
8-14b	90	16.85	-20.61	0.07	0.34	4.77	0.05	0.22
8-15	100	13.07	-24.79	0.05	0.40	8.70	0.03	0.23

REFERENCES CITED

Allen, Bruce D.
2005 Ice Age Lakes in New Mexico. *New Mexico Museum of Natural History and Science Bulletin No. 28.*

Alley, Richard B.
2000 The Younger Dryas cold interval as viewed from central Greenland. *Quaternary Science Reviews* 19:213-226.

Amick, Daniel S.
2017 Evolving Views on the Pleistocene Colonization of North America. Article. *Quaternary International* 431:125-151.

Antevs, E.
1935 The Occurrence of Flints and Extinct Animals in Pluvial Deposits near Clovis, New Mexico, Part II: Age of Clovis Lake Beds. *Proceedings, Philadelphia Academy of Natural Sciences* 87:304–311.

Bain, Roger J.
1990 Diagenetic, Nonevaporative Origin for Gypsum. *Geology* 18(5):447-450.

Baker, Tony
2017 "The Belen Point." In *Plainview: The Enigmatic Paleoindian Artifact Style of the Great Plains*, edited by Vance T Holliday, Eileen Johnson, and Ruthann Knudson, 174–88. Salt Lake City, UT: The University of Utah Press.

Basham, Matt G.
2015 Subsistence Strategies and Landscape Use in the Canyon Edge Zone: Eagle Nest Canyon, Langtry, Texas. Master's thesis, Department of Anthropology Texas State University, San Marcos, Texas.

Bement, Leland C.
1986 *Excavations of the Late Pleistocene Deposits of Bonfire Shelter, Val Verde County, Texas*. Texas Archeological Survey Archeology Series 1, University of Texas, Austin.

2007 Bonfire Shelter: A Jumping off Point for Comments for Byerly et al. *American Antiquity* 72(2):366-372.

2016 Folsom Bison Hunters on the Southern High Plains of North America. In *Stones, Bones, and Profiles: Exploring Archaeological Context, Early American Hunter-Gatherers, and Bison,* edited by Marcel Kornfeld and Bruce B Huckell, 291–311. Boulder: University Press of Colorado.

Bement, Leland C, and Kent J Buehler
1994 Preliminary Results from the Certain Site: A Late Archaic Bison Kill in Western Oklahoma. *Plains Anthropologist* 39 (148): 173–83.

Binford, Lewis R.
1978 *Nunamiut Ethnoarchaeology.* Academic Press Inc., New York.

Black, Stephen L.
2001 Bonfire Exhibit. On Texas Beyond History, https://www.texasbeyondhistory.net/bonfire/, accessed March 2019.

2013 Archaeologist of the Lower Pecos Canyonlands. In *Painters in Prehistory: Archaeology and Art of the Lower Pecos Canyonlands,* edited by Harry J. Shafer. Trinity University Press, San Antonio.

2017 Introduction to Ancient Southwest Texas (ASWT) Investigations. In *Lower Pecos Canyonlands Academy Guidebook,* edited by Ken Lawrence, pp. 7-9. Texas Archeological Society.

Black, Stephen L. and J. Philip Dering
2008 Lower Pecos Canyonlands. On Texas Beyond History, www.texasbeyondhistory.et/pecos/, accessed March 2019.

Black, S.L. and Thorns, A.V.,
2014 Hunter-gatherer earth ovens in the archaeological record: fundamental concepts. *American Antiquity*, 79(2), pp.204-226.

Bousman, C. B., B. W. Baker, and A. C. Kerr
2004 Paleoindian Archeology in Texas. In *The Prehistory of Texas*. Edited by Timothy K. Pertulla, pp. 15–97. Texas A&M University Press, College Station.

Bousman, C. Britt, and David O. Brown
1998 Setting the Stage: Previous Paleoclimatic Research in Texas and Surrounding Areas. *Plains Anthropologist.* 43(164):105–110.

Boyd, Carolyn E., Amanda M. Castañeda, and Charles W. Koenig
2012 Reassessment of Red Linear Pictographs in the Lower Pecos of Texas. *American Antiquity*.

Bryant, V.M., and Larson, D.L.
1968 Pollen Analysis of the Devil's Mouth Site, Val Verde County, Texas. In: *Sorrow, W., The Devil's Mouth Site: The Third Season*. Papers of the Texas Archaeological Salvage Project, 14:57–70

Bryant Jr, Vaughn M
1969 Late Full-Glacial and Post-Glacial Pollen Analysis of Texas Sediments. Ph.D. Dissertation, Texas: The University of Texas, Austin

1977a A 16,000-year Pollen Record of Vegetation Change in central Texas. *Palynology* 1:143-155.

1977b Preliminary Pollen Analysis of Hinds Cave. In: *Shafer, H.J. and Bryant, V.M. (eds.), Archaeological and Botanical Studies at Hinds Cave, Val Verde County, Texas*. Texas A&M University Anthropology Laboratory Special Series, 1:70–80.

Bryant, V. M., Jr., and R. G. Holloway
1985 A Late Quaternary Paleoenvironmental Record of Texas: An Overview of the Pollen Evidence. In: *Pollen Records of Late Quaternary North American Sediments*, edited by V. M. Bryant and R. G. Holloway, pp. 39-70. American Association of Stratigraphic Palynologist Foundation, Dallas.

Buchanan, Briggs, J. David Kilby, Marcus J. Hamilton, Jason M. LaBelle, Kelton A. Meyer, and Jacob Holland-Lulewicz
2021 Bayesian Revisions of the Folsom Age Range Using IntCal20. *PaleoAmerican* 7(2):133-144.

Bureau of Economic Geology (BEG)
1977 Del Rio Sheet (scale 1:250,000). Geologic Atlas of Texas. Bureau of Economic Geology, The University of Texas at Austin, Austin, Texas.

Bush, Leslie L., and J. Kevin Hanselka
2017 Plants and Plant Remains at Eagle Nest Canyon. In *Lower Pecos Canyonlands Academy Guidebook*, edited by Ken Lawrence, pp. 23-30. Texas Archeological Society.

Byerly, Ryan M., Judith R. Cooper, David J. Meltzer, Matthew E. Hill, and Jason M. LaBelle
2005 On Bonfire Shelter (Texas) as a Paleoindian Bison Jump: An Assessment Using GIS and Zooarchaeology. *American Antiquity* 70(4):595-629.

2007a A Further Assessment of Paleoindian Site-Use at Bonfire Shelter. *American Antiquity* 72(2):373-381.

Byerly, Ryan M., Judith R. Cooper, David J. Meltzer, and Jim Theler
2007b Exploring Paleoindian Site-Use at Bonfire Shelter (41VV218). *Bulletin of the Texas Archaeological Society*.

Carlson, Kristen, and Leland Bement
2013a Organization of Bison Hunting at the Pleistocene/Holocene Transition on the Plains of North America. *Quaternary International* 297: 93–99.

Castañeda, Amanda M.
2015 The Hole Story: Understanding Ground Stone Bedrock Feature Variation in the Lower Pecos Canyonlands. Master's thesis, Department of Anthropology, Texas State University, San Marcos, Texas.

Chadderdon, Mary Frances
1983 Baker Cave, Val Verde County, Texas: The 1976 excavations. Center for Archaeological Research, University of Texas at San Antonio, San Antonio, TX.

Cohen, K.M., S.C. Finney, P.L Gibbard, and J.X. Fan
2020 The ICS International Chronostratigraphic Chart. Episodes 36: 199-204, https://stratigraphy.org/ICSchart/ChronostratChart2020-03.pdf, accessed February 2020.

Cordova, C. E. & Johnson, W. C.
2019 Supplemental material. *An 18 ka to Present Pollen- and Phytolith-Based Vegetation Reconstruction from Hall's Cave, South-Central Texas, USA.*

Cotter, J.L.
1937 The Occurrence of Flints and Extinct Animals in Pluvial Deposits near Clovis, New Mexico, Part IV: Report on Excavation at the Gravel Pit, 1936. *Proceedings, Philadelphia Academy of Natural Sciences* 90:2-16.

1938 The Occurrence of Flints and Extinct Animals in Pluvial Deposits near Clovis, New Mexico, Part IV: Report on Field Season 1937. *Proceedings, Philadelphia Academy of Natural Sciences* 90:113–117.

Crowther, J., and P. Barker
1995 Magnetic Susceptibility: Distinguishing Anthropogenic Effects from the Natural. *Archaeological Prospection* 2:207–215.

Dalan, Rinita A.
1996 Soil Magnetism, An Approach for Examining Archaeological Landscapes. *Geophysical Research Letters* 23(2):185–188.

2006 Magnetic Susceptibility. In *Remote Sensing in Archaeology: An Explicitly North American Perspective*. J. Johnson, M. Giardano, and K. Kvamme (editors), pp. 161–203. University of Alabama Press, Tuscaloosa, Alabama.

2008 A Review of the Role of Magnetic Susceptibility in Archaeologeophysical Studies in the USA: Recent Developments and Prospects. *Archaeological Prospection* 15:1–31.

Dalan, Rinita A., and Subir K. Banerjee
1998 Solving Archaeological Problems Using Techniques of Soil Magnetism. *Geoarchaeology* 13:3–36.

Dalan, R. A., and B. W. Bevan
2002 Geophysical Indicators of Culturally Embraced Soils and Sediments. *Geoarchaeology: An International Journal* 17 (8): 779–810.

Davenport, J. Walker
1938 Archaeological Exploration of Eagle Cave, Langtry Texas. Papers of the Witte Memorial Museum. The Witte Museum, San Antonio, TX.

Dearing, J. A.
1999a Magnetic Susceptibility. In *Environmental Magnetism: A Practical Guide*. J. Walden, F. Oldfield, and J. Smith (editors), pp. 35–62. Technical Guide No. 6. Quaternary Research Association, London.

1999b Environmental Magnetic Susceptibility Using the Bartington MS2 System. Available at http://www.gmw.com/magnetic_properties/MS2_support.html. Accessed February 2020.

Dering, J.P.
1979 Pollen and Plant Macrofossil Vegetation Records Recovered from Hinds Cave, Val Verde County, Texas. Master's thesis, Department of Anthropology, Texas A&M University, College Station.

2002 Amistad National Recreation Area: Archeological Survey and Cultural Resources Inventory. In *Intermountain Cultural Resources Management Anthropology Projects.* No. 68. National Park Service, Santa Fe, NM.

2007 Assessment of Botanical and Faunal Assemblages from Paleoindian and Early Archaic Components on the Periphery of the Southern Plains. *Bulletin of the Texas Archeological Society* 78:177-195.

Dibble, D. S.
1967 *Excavations at Arenosa Shelter, 1955-66*. Submitted to National Park Service, Austin, Texas.

Dibble, D.S., and D. Lorrain
1968 Bonfire Shelter: A Stratified Bison Kill Site, Val Verde County, Texas. Miscellaneous Papers 1. Austin: Texas Memorial Museum, University of Texas at Austin.

Donahue, Jack, and James M. Adovasio
1990 Evolution of Sandstone Rockshelters in Eastern North America; A Geoarchaeological Perspective. In Archaeological Geology of North America, edited by Norman P. Lasca, and Jack Donahue. *Geological Society of America* (4):231-251.

Durner, Wolfgang, Sascha C. Iden, and Georg von Unold
2017 The Integral Suspension Pressure Method (ISP) for Precise Particle-Size Analysis by Gravitational Sedimentation. *Water Resources Research*, 53:33-48.

Farrand, William R.
2001 Sediments and Stratigraphy in Rockshelters and Caves: A Personal Perspective on Principles and Pragmatics. Article. *Geoarchaeology* 16(5):537-557.

Farrell, Sean P.
2020 New Excavations of Late Pleistocene Deposits at Bonfire Shelter: A Geoarchaeological Approach to Determining the Origins of Bone Bed 1. Master's thesis, Department of Anthropology, Texas State University, San Marcos, Texas.

Folk, Robert L.
1980 Petrology of Sedimentary Rocks. Hemphill Publishing Company, Austin, Texas.

Frederick, Charles
2010 Geoarchaeological Investigations. In Archaeological Data Recovery on Three Sites Along the San Antonio River, Bexar County, Texas, by Antonio E. Padilla and David L. Nickels, pp. 449–462. Ecological Communications, Corporation, Austin, Texas.

2012 Site Formation Processes and Implications for Archeology in the South Fork of the San Gabriel. In *The Siren Site (41WM1126) and the Long Transition from Archaic to Late Prehistoric Lifeways on the Eastern Edwards Plateau*, Williamson County, Texas, by Steve Carpenter, Kevin A. Miller, Brett Houk, Mary Jo Galindo, Charles Frederick, John Lowe, Ken Lawrence, Kevin Hanselka, and Abby Peyton, pp. 8-1–8-24. SWCA Environmental Consultants, Austin, Texas.

2017 Landscapes and Uplands. *In Texas Archeological Society Lower Pecos Canyonlands Academy Guidebook*. Texas Archeological Society Academy, 2017.

Freeman, Val, L.
1961 Contact of Boquillas Flags and Austin Chalk in Val Verde and Terrell Counties, Texas. *AAPG Bulletin* (45):105-107.

Frison, George C.
1991a *Prehistoric Hunters of the High Plains*. Second Edition. San Diego, California: Academic Press.

1991b. "The Archeological Record for the Northwestern Plains and Mountains." In *Prehistoric Hunters of the High Plains*, Second, 15–137. San Diego, California: Academic Press.

2004. *Survival by Hunting*. Berkeley, California: University of California Press.

Gale, Stephen J., Peter G. Hoare
1991 *Petrographic Methods for the Study of Unlithified Rocks*. Halsted Press, an Imprint of John Wiley & Sons, Inc., New York.

Goldberg, P., Richard I. Macphail
2013 *Practical and Theoretical Geoarchaeology*. John Wiley & Sons, Inc., New York.

Graham, John Allen, and William A. Davis
1958 *Appraisal of the Archeological Resources of Diablo Reservoir, Val Verde County, Texas*. Archeological Salvage Field Office, Austin, TX. Submitted to US National Park Service.

Hall, Grant D., and Stephen L. Black
2010 Chronological Bibliography of Lower Pecos Archaeology. *Bulletin of the Texas Archeological Society* 81:205-226.

Harbor, Ryan Lee
2011 Facies Characterization and Stratigraphic Architecture of Organic-Rich Mudrocks, Upper Cretaceous Eagle Ford Formation, South Texas. Master's thesis, Department of Geological Sciences, University of Texas, Austin.

Heiri, Oliver, André F. Lotter, and Gerry Lemcke
2001 Loss on Ignition as a Method for Estimating Organic and Carbonate Content in Sediments: Reproducibility and Comparability of Results. *Journal of Paleolimnology* 25(1):101-110.

Hester, T R.
1983 Late Paleoindian Occupations at Baker Cave, Southwestern Texas. *Bulletin of the Texas Archeological Society* 53:101–120.

Hevly, R.H.
1966 A Preliminary Pollen Analysis of Bonfire Shelter. In: Story, D.A., and Bryant, V.M. Jr., (eds.) *A Preliminary Study of Paleoecology of the Amistad Reservoir Area*. Report submitted to the National Science Foundation, Department of Anthropology, University of Texas at Austin: 165–178.

Holliday, Vance T.
1995 *Stratigraphy and Paleoenvironments of Late Quaternary Valley Fills on the Southern High Plains*. Geological Society of America, Memoir 186.

1997 *Paleoindian Geoarchaeology of the Southern High Plains*. University of Texas Press.

Holliday, Vance T, Eileen Johnson, and Ruthann Knudson, eds.
2017 *Plainview: The Enigmatic Paleoindian Artifact Style of the Great Plains*. Salt Lake City, UT: The University of Utah Press.

Howard, E.B.
1935a The Occurrence of Flints and Extinct Animals in Pluvial Deposits near Clovis, New Mexico, Part I: Introduction. *Proceedings, Philadelphia Academy of Natural Sciences* 87:299–303.

1935b Evidence of Early Man in North America. *The Museum Journal* 42-2-3, University of Pennsylvania Museum.

Johnson, L., Jr.
1964 The Devil's Mouth Site: A Stratified Campsite at Amistad Reservoir, Val Verde County, Texas. Archeology Series 6. Department of Anthropology, The University of Texas at Austin.

Jones, R. S., and J. J. Leffler
2003 Phase I and II Archaeological Investigations on Camp Mabry, Travis County, Texas, Archaeological Studies Report No. 2. Center for Archaeological Studies, Texas State University-San Marcos, Texas.

Jurgens, Christopher J.
2005 Zooarcheology and Bone Technology from Arenosa Shelter (41VV99), Lower Pecos Region, Texas. Unpublished Ph.D. Dissertation. Department of Anthropology. The University of Texas at Austin.

Kelly, Robert L
2013 *The Lifeways of Hunter-Gatherers: The Foraging Spectrum*. Cambridge University Press.

Kilby, David, and Marcus Hamilton
2018 New Investigations at Bonfire Shelter: A Consideration of Bison Jumps and Their Implications for Paleoindian Social Organization. Paper presented at the 83rd Annual Meeting of the Society for American Archaeology Washington, D.C.

Kilby, David J., Sean P. Farrell, and Marcus J. Hamilton
2020 New Investigations at Bonfire Shelter, Texas Examine Controversial Bison Jumps and Bone Beds. *Plains Anthropologist* 66(257):34-57.

Kochel, Craig R.
1988 Extending Stream Records with Slackwater Paleoflood Hydrology: Examples from West Texas. In *Flood Geomorphology*, edited by Victor R. Baker, Craig R. Kochel, and Peter C. Patton. Wiley Interscience Publications, New York, New York.

Koenig, Charles W.
2012 Burned Rock Middens, Settlement Patterns, and Bias in the Lower Pecos Canyonlands of Texas. Master's thesis, Department of Anthropology, Texas State University, San Marcos, Texas.

Koenig, Charles W., and Stephen L. Black
2015 *Eagle Nest Canyon 2016: Eagle Cave Investigations*. Ancient Southwest Texas Project, Texas State University.

Koenig, Charles W., J. David Kilby, Christopher J. Jurgens, Lorena Becerra-Valdivia, Christopher W. Ringstaff, J. Kevin Hanselka, Leslie L. Bush, Charles D. Frederick, Stephen L. Black, Amanda M. Castaneda, Ken L. Lawrence, Madeline E. Mackie, and Jim I. Mead
2021 *A Newly Identified Younger Dryas Component in Eagle Cave, Texas*. American Antiquity.

Koenig, Charles, Mark D. Willis, and Stephen L. Black
2017 Beyond the Square Hole: Application of Structure from Motion Photogrammetry to Archaeological Excavation. *Advances in Archaeological* Practice 5 (1): 54-70.

Kornfeld, Marcel, George C. Frison, and Mary Lou Larson
2010 *Prehistoric Hunter-Gatherers of the High Plains and Rockies*. Third Edition. Left Coast Press, Walnut Creek, CA.

Krumbein, W.C., and L.L. Sloss
1963 *Stratigraphy and Sedimentation*. Freeman, San Francisco, Calif., 2nd ed.

Laville, Henri, Jean Philippe Rigaud, and James Sackett
1980 *Rock Shelters of the Périgord: Geological Stratigraphy and Archaeological Succession*. Studies in Archaeology. Academic Press, New York, NY.

Lawrence, Ken, and Charles Frederick
2012 Geomorphology-Geoarchaeology: Site Formation and Chronostratigraphy. In *Data Recovery Investigations on the Eastern Side of the Siren Site (41WM1126), Williamson County, Texas*. A. Peyton, S. Carpenter, J. D. Lowe, and K. Lawrence. SWCA Cultural Resource Report No. 12-236. SWCA Environmental Consultants, Austin.

Lock, B.E., and B. Wawak
2010 Eagle Ford (Boquillas) Formation and Associated Strata in Val Verde County, Texas. In *South Texas Geological Society Guidebook 2010-1*. South Texas Geological Society, San Antonio, TX.

Lundelius, E. L.
1984 *A Late Pleistocene Mammalian Fauna from Cueva Quebrada, Val Verde County, Texas*. Special Publications of the Carnegie Museum of Natural History. University of Texas at Austin. Geology Foundation.

Machette, M.N.
1986 Calcium and Magnesium Carbonates, in M.J. Singer and P. Janitzky, Eds., *Field and Laboratory Procedures Used in a Soil Chronosequence Study*, pp. 30-33. U.S. Geological Survey Bulletin 1848.

Mauldin, R. P., and A. L. Figueroa
2006 Data Recovery Excavations at 41PR44, Fort Wolters, Parker County, Texas, Archaeological Report, No. 369, Center for Archaeological Research, University of Texas at San Antonio, San Antonio, Texas.

Martin, George C.
1933 Archaeological Exploration of the Shumla Caves. Big Bend Basket Maker Papers 3, Bulletin 3. In *Bulletin of the Witte Memorial Museum*. Southwest Texas Archaeological Society, San Antonio, TX.

McAndrews, J.H., and Larson, D.A.
1966 Pollen Analysis of Eagle Cave. In: Story, D.A., and Bryant, V.M.m Jr., (eds.) *A Preliminary Study of Paleoecology of the Amistad Reservoir Area*. Report submitted to the National Science Foundation, Department of Anthropology, University of Texas at Austin: 178–184.

McLane, Michael
1995 *Sedimentology*. Oxford University Press, New York.

Meltzer, David J., Ryan Byerly, and Judith Cooper
2007 An Alternative Interpretation of Paleoindian Site Use at Bonfire Shelter. *Bulletin of the Texas Archaeological Soci*ety 78:159–160.

National Park Service (NPS)
2019 Great Plains Province, https://www.nps.gov/articles/greatplainsprovince.htm, accessed March 2019.

2021 National Historic Landmarks, https://www.nps.gov/subjects/nationalhistoriclandmarks/search.htm, accessed January 2021.

Natural Resources Conservation Service (NRCS)
2019 Web Soil Survey. U.S. Department of Agriculture, http://websoilsurvey.nrcs.usda.gov, accessed November 2019.

Nielsen, Christina
2017 A Microstratigraphic Approach to Evaluating Site Formation Processes at Eagle Cave (41VV167). Master's thesis, Department of Anthropology, Texas State University, San Marcos, Texas.

Omernik, J.M. and G.E. Griffith
2014 Ecoregions of the conterminous United States: evolution of a hierarchical spatial framework. *Environmental Management* 54(6):1249-1266.

Omran, El-Sayed E.
2016 A Simple Model for Rapid Gypsum Determination in Arid Soils. *Modeling Earth Systems and Environment*, 2(4):1–12.

Pagano, Victoria C.
2019 Stories in the Sand: Excavation and Analysis of the Sayles Adobe Terrace (41VV2239) in Eagle Nest Canyon, Langtry, Texas. Master's thesis, Department of Anthropology, Texas State University, San Marcos, Texas.

Parson, Mark L.
1956 *1963 Test Excavations at Fate Bell Shelter, Amistad Reservoir, Val Verde County, Texas*. Miscellaneous Papers 4, Austin: Texas Archeological Salvage Project.

Patton, P., and D.S. Dibble
1982 Archeologic and Geomorphic Evidence from the Paleohydraulic Record of the Pecos River in West Texas. *American Journal of Science* 282: 97-121.

Pearce, James Edwin, and A. T. Jackson
1933 A Prehistoric Rockshelter in Val Verde County, Texas. Bureau of Research in the Social Sciences Study No. 6, Anthropological Papers, Vol. 1, No. 3. The University of Texas at Austin, Austin, TX.

Potzger, J.E., and B.C. Thrap
1943 Pollen Record of Canadian Spruce and Fir from Texas Bog. *Science* 98:584.

1947 Pollen Profile from a Texas Bog. *Ecology* 28:274-280.

Prewitt, Elton R.
2007 To Jump or to Drag: Reflections on Bonfire Shelter." *Bulletin of the Texas Archeological Society* 78: 149–58.

Rachel, David M., Kate Zeigler, Rober Dello-Russo, and Christian Solfsburg
2021 Lake levels and trackways: An alternate model to explain the timing of human-megafauna trackways intersections, Tularosa Basin, New Mexico. *Quaternary Science Advances* 3.

Ramsey, James O.
2020 Bonfire Shelter: A Zooarchaeological Reevaluation of Bone Bed 2. Master's thesis, Department of Anthropology, Texas State University, San Marcos, Texas.

Rapp, George (Rip) Jr., and Christopher L. Hill
2006 *Geoarchaeology: The Earth-Science Approach to Archaeological Interpretations.* Yale Press University.

Robinson, David G.
1997 Stratigraphic Analysis of Bonfire Shelter, Southwest Texas: Pilot Studies of Depositional Processes and Paleoclimate. *Plains Anthropologist* 42 (159): 33–43.

Rodriguez, D.P.
2015 Patterns in the Use of the Rockshelters of Eagle Nest Canyon, Langtry Texas. Master's thesis, Department of Anthropology, Texas State University, San Marcos, Texas.

Rosenmeier, Abbot
2005 Loss on Ignition (LOI) Procedures. In *Geology 3931: Paleoenvironmental Analysis - Laboratory Standard Operating Procedures*. University of Pittsburgh, Department of Geology and Environmental Science, Pittsburgh, PA.

Ross, Richard E.
1965 *The Archaeology of Eagle Cave*. Papers of the Texas Archeological Salvage Project, No. 7, Austin, Texas.

Saunders, J.W.
1986 The Economy of Hinds Cave. PhD. Dissertations, Department of Anthropology, Southern Methodist University, Dallas.

Sayles, E. B.
1935 *An Archaeological Survey of Texas*. Medallion Papers. Book, Globe, AZ.

Seersholm, F.V, D.J. Werndly, A. Grealy, M. Bunce, T. Johnson, A. Linderholm, E.M. Keenan Early, E.L. Lundelius, B. Winsborough, G.E. Farr, R. Toomey, A.J. Hansen, B. Shapiro, M.R. Waters, G. McDonald, and T.W. Stafford
2020 Rapid range shifts and megafaunal extinctions associated with late Pleistocene climate change, *Nature Communications*, 11(1).

Sellards, E.H.
1938 Artifacts Associated with Fossil Elephant. *Geological Society of America Bulletin* 49:999-1010.

1952 *Early Man in America*. University of Texas Press, Austin.

1955 Fossil Bison and Associated Artifacts from Milnesand, New Mexico, *American Antiquity* 20:336-344.

Sellards, E.H., and G.L. Evans
1960 The Paleo-Indian Cultural Succession in the Central High Plains of Texas and New Mexico. In: *Men and Cultures*, edited by Anthony F.C. Wallace. University of Pennsylvania Press, Philadelphia.

Sellards, E.H., G.L. Evans. And G.E. Meade
1947 Fossil Bison and Associated Artifacts from Plainview, Texas. *Geological Society of America Bulletin* 58:927–954.

Setzler, Frank M.
1932 Cave Burials in Southwestern Texas. In *Explorations and Fieldwork of the Smithsonian Institution*, Publication 3235, edited by The Smithsonian Institution, pp. 35-37. The Lord of Baltimore Press, Baltimore, MD.

Schiffer, Michael B.
1987 *Formation Processes in the Archaeological Record*. University of New Mexico, Albuquerque, NM.

Shafer, H. J
1986 *Ancient Texans: Rock Art and Lifeways along the Lower Pecos*. Texas Monthly Press, Austin.

Shafer, Harry J., and Vaughn M. Bryant Jr.
1977 Archeological and Botanical Studies at Hinds Cave, Val Verde County, Texas. Special Series, No 1. Submitted to Texas A&M University, Anthropology Laboratory, College Station, TX.

Schulte, E. E. and B. G. Hopkins
1996 Estimation of Soil Organic Matter by Weight Loss–On–Ignition. In *Soil Organic Matter: Analysis and Interpretation*. F.R. Magdoff, M.A. Tabatabai, and E.A. Hanlon (editors), pp. 21–31. Soil Science Society of America, Special Publication No. 46. Madison, Wisconsin.

Schumacher, Brian A.
2002 *Methods for the Determination of Total Organic Carbon (TOC) in Soils and Sediments*. U.S. Environmental Protection Agency, Ecological Risk Assessment Support Center, Las Vegas, NV.

Sorrow, William M.
1968 The Devil's Mouth Site: The Third Season, 1967: Test Excavations at the Nopal Terrace Site, Val Verde County, Texas, Spring 1967. *Papers of the Archeological Salvage Project* 15. University of Texas. Austin, Texas.

Stein, Julie K.
2001 Archaeological Sediments in Cultural Environments. In *Sediments in Archaeological Contexts*, edited by Julie K. Stein and William R. Farrand, pp.1–28. The University of Utah Press, Salt Lake City.

Stock, Janet A.
1983 *The Prehistoric Diet of Hinds Cave, Val Verde County, Texas*. Department of Anthropology, Texas A&M University. College Station, Texas

Stock, C., and F.D. Bode
1937 The Occurrence of Flints and Extinct Animals in Pluvial Deposits near Clovis, New Mexico, Part III: Geology and Vertebrate Paleontology of the Quaternary near Clovis, New Mexico. Proceedings, Philadelphia Academy of Natural Sciences 88:219–241.

Storer, D. A.
2005 The Chemistry of Soil Analysis. Terrific Science Press, Middleton, OH.

Texas Historical Commission (THC)
2019 Texas Archeological Sites Atlas restricted database. https://atlas.thc.state.tx.us/, accessed April 2019.

Turpin, Solveig A.
1982 Seminole Canyon: The Art and the Archeology. Texas Archeological Survey Research Report No. 83. Texas Archeological Survey, University of Texas at Austin, Austin, TX.

1994 Lower Pecos Prehistory: The View from the Caves. In *The Caves and Karst of Texas*, edited by W.R. Elliott and G. Veni, pp. 69-84. National Speleological Society, Hunstville, Alabama.

2004 The Lower Pecos River Region of Texas and Northern Mexico. In *The Prehistory of Texas*, edited by T.K. Pertulla, pp. 266-280. Texas A&M University Press, College Station.

Turpin, Solveig A., and Leland C. Bement
1988 The Site and Its Setting. *Plains Anthropologist* 33(122):1-18.

U.S. Geological Survey (USGS)
2021 Texas geologic map data. Available at: https://txpub.usgs.gov/txgeology/. Accessed September 2021.

Veni, G.
1994 Hydrogeology and evolution of caves and karst in the southwestern Edwards Plateau, Texas. Pp. 13-30, in *The Caves and Karst of Texas* (W. R. Elliott and G. Veni, eds.). National Speleological Society, Huntsville, Alabama.

Waters, Michael R.
1992 *Principles of Geoarchaeology: A North American Perspective*. University of Arizona Press, Tucson, AZ.

Wendorf, F., and J.J. Hester
1975 *Late Pleistocene Environments on the Southern High Plains*. Publications of the Fort Burgwin Research Center No. 9. Taos.

Wentworth, Chaster K.
1922 A Scale of Grade and Class Terms for Clastic Sediments. *The Journal of Geology* 3-(5):377-392.

Wermund, E.G.
2019 "Physiographic Map of Texas 1996," Bureau of Economic Geology, http://legacy.lib.utexas.edu/geo/fieldguides/physiography_print.html, accessed May 2019.

Wiewel, Adam S., and Kenneth L. Kvamme
2014 Magnetic Investigations of Nomadic Group Encampments at Fort Clark State Historic Site, North Dakota. *Plains Anthropologist* 59(231):261–278.

Williams-Dean, Glenna J.
1978 Ethnobotany and Cultural Ecology of Prehistoric Man in Southwest Texas, Unpublished Ph.D. Dissertation, Department of Anthropology, Texas A&M University. College Station, Texas

Wyckoff, Don G, and Walter W Dalquest
1997 From Whence They Came: The Paleontology of Southern Plains Bison. *Plains Anthropologist* 42 (159): 5–32.

Zedeño, Maria Nieves, Jess A M Ballenger, and John R Murray
2014 Landscape Engineering and Organizational Complexity Among Late Prehistoric Bison Hunters of the Northwest Plains. *Current Anthropology* 55: 23–58.